2010-08-04

Determining the Function of Nuclear Bmp4

Trina Jane Loos
Brigham Young University - Provo

Determining the function of nuclear Bmp4

Trina J. Loos

A dissertation submitted to the faculty of
Brigham Young University
in partial fulfillment of the requirements for the degree of

Doctor of Philosophy

Laura C. Bridgewater, Chair
Joel S. Griffitts
Chin-Yo Lin
Michael R. Stark
Barry M. Willardson

Department of Microbiology and Molecular Biology

Brigham Young University

December 2010

ABSTRACT

Determining the function of nuclear Bmp4

Trina J. Loos

Department of Microbiology and Molecular Biology

Doctor of Philosophy

Bone morphogenetic protein 4 (Bmp4) is a well known growth factor that regulates gene expression through the SMAD signaling pathway. Bmp4 is involved in many developmental processes and has been identified as an important factor in several cancers, including melanoma, ovarian cancer, and colon cancer. Madoz-Gurpide et al. recently observed Bmp4 in the nuclei of a minor percentage of cells in colon cancer tissues. In addition, our lab has recently discovered a nuclear variant of Bmp2 (nBmp2), the TGF-β family member most closely related to Bmp4. These observations led us to hypothesize that a nuclear variant of Bmp4 (nBmp4) also exists. The results of chapter one report the existence of a nuclear variant of Bmp4. nBmp4 is translated from an alternative start codon downstream of the signal peptide sequence which allows a bipartite nuclear localization signal to direct translocation of nBmp4 to the nucleus. Chapter 2 and 3 further report that nBmp4 interacts with several subunits in the SCF E3 ubiquitin ligase, namely two Regulator of Cullins (ROC) proteins, five Cullin proteins, and two F-box proteins. Due to the known role of the SCF E3 ubiquitin ligase in regulating the cell cycle, the effect of nBmp4 on cell cycle progression was analyzed and the results show that nBmp4 affects the cell cycle by causing cells to accumulate in G0/G1. The association of nBmp4 and the SCF E3 ubiquitin ligase components and the affect that nBmp4 has on the cell cycle suggest that nBmp4 functions in the nucleus by inhibiting the SCF E3 ubiquitin ligase from ubiquitinating target proteins that are involved in regulating cell cycle progression. Finally, the initial stages in the generation of an nBmp4 over-expression mouse are described. The results of this research clearly change the traditional paradigm that Bmp4 performs all of its functions via extracellular signaling and introduce the existence of a nuclear variant that is involved in cell cycle regulation.

Keywords: nuclear localization signal, Bmp4, SCF E3 ubiquitin ligase, cell cycle, ROC1, ROC2

ACKNOWLEDGEMENTS

There are so many people that I would like to acknowledge for their help throughout the last four years. I am extremely grateful for the advice and guidance of my advisor, Dr. Laura Bridgewater. I am also grateful for the continued support from each of my committee members. I also received tremendous help from Dr. Jeffery Barrow and Jubal Stewart in preparation to generate the nBmp4 over-expression mouse. Sen Wu, Yuanyuan Wu, and Hideaki Tomita at the University of Utah were extremely helpful in troubleshooting the Southern blots and performing the Long Range PCR. I am also grateful for the friendship and help from so many fellow students, namely Amy Gray, Rebecca Plimpton, Jaime Mayo, Jenny Felin, and Alyson Howlett. I also want to recognize Ryan Cordner for his work on the ROC sequential deletion analyses in yeast.

I am especially grateful for my husband Steve and his incredible support. He has spent long hours in the lab keeping me company. I am grateful for his patience through the stressful times that I've had during the last two years. I am also very grateful for my family and their support and listening ears during these intense years of graduate school.

Finally, I am very grateful for the support of the Microbiology and Molecular Biology Department here at BYU, and especially for Elaine Rotz and all the work that she does for all of the graduate students here. I couldn't have made it through without the support of the department and also the support of the BYU Cancer Research Center from their summer fellowships.

Table of Contents

List of Figures

List of Tables

Abbreviations

Bmp2	Bone Morphogenetic Protein 2
Bmp4	Bone Morphogenetic Protein 4
BSA	Bovine serum albumin
cNLS	Classical Nuclear Localization Signal
CUL1	Cullin 1
DMSO	Dimethyl Sulfoxide
EDTA	Ethylenediaminetetraacetic Acid
FGF-2	Fibroblast Growth Factor 2
FGF-3	Fibroblast Growth Factor 3 (INT-2)
GFP	Green Fluorescent Protein
HEK 293T	Human embryonic kidney cells
HRP	Horseradish Peroxidase
IFN	Interferon
LiAc	Lithium Acetate
MMLV	Moloney Murine Leukemia Virus
nBmp2	Nuclear Bone Morphogenetic Protein 2
nBmp4	Nuclear Bone Morphogenetic Protein 4
NLS	Nuclear Localization Signal
p27	cyclin-dependent kinase inhibitor 1B (p27, Kip1)
PBS	Phosphate Buffered Saline
PCR	Polymerase Chain Reaction
PFA	Paraformaldehyde
PMSF	Phenylmethanesulfonyl fluoride
PTHrP	PTH-related peptide
QDO	Quadruple Dropout
ROC1	Regulator of Cullins 1, also known as Rbx1
ROC2	Regulator of Cullins 2, also known as Rnf7
SDS	Sodium dodecyl sulfate
SSC	Buffer used in Southern blot
SKP1	S-phase kinase-associated protein 1
SKP2	S-phase kinase-associated protein 2 (p45, Fbl1)
TAE	Tris, Acetic Acid, and EDTA buffer
TGF-β	Transforming growth factor beta
UAS	Upstream activation sequence
YPD medium	Yeast extract, peptone, and dextrose medium

Chapter 1: Nuclear Localization of Bmp4

Summary

Bone morphogenetic protein 4 (Bmp4) is a well known growth factor that regulates gene expression through the Smad signaling pathway. Bmp4 is involved in many developmental processes and has been identified as an important factor in several cancers, including melanoma, ovarian cancer, and colon cancer. Surprisingly, Madoz-Gurpide et al. observed Bmp4 in the nuclei of a minor percentage of cells in colon cancer tissues.[1] In addition, our lab has recently discovered a nuclear variant of Bmp2 (nBmp2), the TGF-β family member most closely related to Bmp4.[2] These observations led us to hypothesize that a nuclear variant of Bmp4 (nBmp4) also exists. The results in this chapter show that indeed there is a nuclear form of Bmp4. It is translated from an alternative start codon downstream of the signal peptide sequence, which allows a bipartite nuclear localization signal to direct translocation of nBmp4 to the nucleus. These findings suggest that Bmp4 functions not only as an extracellular signaling factor, but as a nuclear protein as well.

Introduction

The transforming growth factor beta (TGF-β) superfamily is responsible for a number of developmental pathways that promote differentiation and proliferation. There are several subfamilies of proteins included in the TGF-β superfamily, including bone morphogenetic proteins (BMPs), growth and differentiation factors, and Nodals[3]. There are approximately twenty BMP family members. The BMP family can be divided into subgroups, one of them consisting of Bmp2 and Bmp4 which are 80% identical in the C-terminal mature peptides.[4]

Bmp4 is an important growth factor that regulates gene expression. It is synthesized as a preproprotein, which is cleaved while in the secretory pathway after the Arg-X-Lys-Arg sequence by either Furin or proprotein convertase 6.[5] The C-terminal end dimerizes to form the mature growth factor before it is secreted, where it functions via the Smad signaling pathway[6, 7]. In this pathway, BMPs interact with their cognate receptors at the cell membrane which are made of two type I and two type II serine/threonine kinase receptors.[8] The receptors become activated and in turn activate receptor Smads (R-Smads: Smad1, Smad5, and Smad8) by phosphorylation.[6] Two activated R-Smads are then able to interact with the common Smad, Smad4, and as a heteromeric complex they are translocated to the nucleus. This heteromeric complex acts as a transcription factor to regulate gene transcription.[9] The Smad signaling pathway is subject to regulation at several different levels. For example, the activation of R-Smads is regulated by inhibitory Smads (Smad-6 and Smad-7). Additionally, R-Smads are subject to degradation by ubiquitination mediated by the HECT domain E3 ligases Smad ubiquitin regulatory factor 1 (Smurf1) and Smurf2.[9, 10]

Bmp4 was first identified as a protein that is highly similar to Bmp2, a protein that is sufficient to induce cartilage formation.[11] Bmp4 was actually originally named Bmp2B. Bmp4, along with other Bmp family members, is sufficient to induce bone formation in vivo.[4] In fact, Bmp2 and Bmp4 stimulate chemotactic migration of mesenchymal progenitor cells (MPCs) which suggests a functional role for these growth factors in attracting MPCs for bone development or remodeling.[12] Among its many roles, Bmp4 induces bone formation[13] and is involved in forebrain development,[14] inner ear development,[15] and mesoderm formation[16]. Bmp4 is also involved in bone fracture healing,[17] in regulating left-right asymmetry and heart laterality,[18] and in promoting self renewal in stem cells.[19]

Bmp4 is essential early in development, as evidenced by the fact that Bmp4 knockout mice die early in development. Although the phenotypes varied from mouse to mouse, most died between embryonic day 6.5 and 9.5.[16, 20, 21] Bmp4 is also highly involved in cell survival. Bmp4 can increase proliferation in adult hematopoietic stem cells.[7] On the other hand, exposure of human glioblastoma cells to Bmp4 causes a reduction in proliferation but does not cause apoptosis.[22] Similarly, mature Bmp4 induces senescence in A549 lung cancer cells which was correlated with an increased susceptibility to apoptosis.[23] In the developing limb bud, secreted Bmp4 causes cell death.[24] Therefore, the roles that Bmp4 plays in cell survival are pleiotropic.

There are two different promoters in the human Bmp4 gene which give rise to three different transcripts.[25] These promoters are regulated in a cell type- and differentiation-dependent manner. In fact, Van Den Winjgaard et. al. note that the presence of multiple promoters and transcripts suggests that the regulation of Bmp4 is complex and could be regulated by different stimuli.[25]

Among its many functions, Bmp4 has also been identified as an important factor in several cancers, including melanoma,[26] ovarian cancer,[27, 28] and colon cancer.[29] Bmp4 is known to have tumor suppressive activities, though some tissues are resistant to the growth suppression.[30] Interestingly, Madoz-Gurpide et al. observed Bmp4 in the nuclei of a minor percentage of cells in colon cancer tissues[1].

Recently, the Bridgewater lab identified Bmp2, a protein that is closely related to Bmp4, as a possible transcriptional regulator for the *Col11a2* gene. This potential novel function of Bmp2 was discovered through yeast-one hybrid assays as well as through DNA affinity chromatography in combination with mass spectrometry. Subsequent detailed analyses of Bmp2 revealed that a nuclear form of Bmp2 (which was named nBmp2) is translated from an

alternative start codon that allows it to bypass the secretory pathway. It is then translocated to the nucleus via a bipartite nuclear localization signal (NLS)[2, 31]. Research is underway to determine the function of nBmp2.

Due to the observation of Bmp4 in the nuclei of cancer tissues and the recent discovery of nBmp2, we hypothesize that a nuclear variant of Bmp4 also exists. Because Bmp4 is such a well studied *secretory* protein, the discovery of an alternative *nuclear* form of Bmp4 is extremely significant. The results of this research will change the traditional paradigm that Bmp4 performs all of its functions via extracellular signaling. Because Bmp4 plays a role in so many different processes, it seems logical that another variant of the protein could be responsible for some of these roles.

Proteins are transported to the nucleus in several ways, including the classical nuclear import pathway.[32] In the classical pathway, importin α interacts with a protein containing a classical nuclear localization signal (cNLS). A cNLS consists of one (monopartite) or two (bipartite) clusters of basic amino acids that are separated by ten intervening amino acids.[33, 34] Importin α also binds to importin β and together these proteins translocate the cargo protein into the nucleus through the nuclear pore complex.[35, 36] The energy for nuclear transport in the classical nuclear import pathway is provided by a small GTPase, Ran.[37] Ran cycles between two states: being bound to GTP in the nucleus and being bound to GDP in the cytoplasm.[38-41] The import complexes bind to cargo proteins in the cytoplasm in the absence of RanGTP. Then when the complex arrives in the nucleus, it binds to RanGTP and releases the cargo proteins in the nucleus.[32]

In order to determine if an NLS is functional within the classical nuclear import pathway, four criteria must be met.[32, 42] First, the NLS must be necessary for nuclear translocation. This

can be determined by replacing the basic amino acids with alanine and then determining if the nuclear localization of the protein of interest has been hindered. Second, the NLS must be sufficient to target an unrelated protein to the nucleus. Usually this is accomplished by preparing a fusion construct containing the putative NLS and green fluorescent protein (GFP), transfecting the construct into cells, and analyzing the localization patterns of GFP. Third, the protein of interest must interact with importin through the putative NLS. Finally, in order to determine which import pathway is being utilized, the import pathway must be disabled and this must disrupt the nuclear localization of the protein of interest. Through these criteria, it may be determined if a protein is being localized to the nucleus through a putative nuclear localization signal. We will simply use the first two criteria because the particular nuclear import pathway is not pertinent to the present study of a nuclear variant of Bmp4.

Experimental Procedures

Cell culture

Rat chondrosarcoma (RCS), 10T1/2, Balb3T3, MDA-MB-231, MDA-MB-435S, HepG2, HT-29, and MCF-7 cells were cultured in Dulbecco's Modified Eagle Medium High Glucose (Gibco, Invitrogen, Carlsbad, CA) supplemented with 2 mM L-Glutamine, 100 units/ml penicillin, 100 µg/ml Streptomycin, and 10% fetal bovine serum. Cells were subcultured regularly.

Immunocytochemistry

50,000 RCS, 10T1/2, Balb3T3, MDA-MB-231, MDA-MB-435S, HepG2, HT-29, or MCF-7 cells were seeded in Lab-Tek II Chamber slides (ISC Bioexpress, Kaysville, UT). 48 hours later, cells were washed three times with 1x PBS and fixed with 4%

paraformaldehyde/PBS for 30 minutes at room temperature. Cells were then washed 3 times with 1x PBS for 5 minutes each time. Then cells were permeabilized using permeabilization solution (1% BSA, 0.3% Triton X-100 in 1x PBS) for 40 minutes at room temperature. The cells were incubated with primary antibody solution (1:50 goat anti-Bmp4, 0.1% BSA + 0.3% Triton X-100) for two hours at room temperature and then overnight at 4^{o}C in a humid chamber (MBL International, Woburn, MA, Cat. No. JM-5674-100). The following day, the cells were washed with 1x PBS three times and then incubated with secondary antibody (0.1% BSA, 0.3% Triton X-100, 1:333 Alexa Fluor 488 donkey anti-goat) for 30 minutes at room temperature (Invitrogen, Carlsbad, CA). Cells were once again washed three times with 1x PBS, nuclei were counterstained with 1 µM TO-PRO-3 iodide (Invitrogen, Carlsbad, CA) for 10 minutes at room temperature, washed three times with 1x PBS, and mounted with Fluoromount G (SouthernBiotech, Birmingham, AL). After the Fluoromout-G dried, cells were visualized using an Olympus IX81 laser confocal microscope using excitation wavelengths of 488 nm and 633 nm.

Nuclear Extraction

In order to analyze nuclear proteins separate from cytoplasmic proteins, MCF-7 cells were grown to approximately 70% confluence. The media was then aspirated and the cells were rinsed twice with 1x PBS. The cells were collected by scraping and centrifuged for 5 minutes at 2000 rpm and 4^{o}C. The CelLytic^{TM} NuCLEAR^{TM} Extraction Kit (Sigma Aldrich, St. Louis, MO) was then used according to the manufacturer's instructions to separate nuclear from cytoplasmic proteins. Briefly, cells were incubated in lysis buffer for 15 minutes on ice. Cells were then pelleted by centrifuging at 2000 rpm for 5 minutes in the fridge. The pellets were then resuspended in lysis buffer and expelled through 27 gauge needles 5 times. The lysis was

verified using Trypan Blue Stain 0.4% (Invitrogen, Carlsbad, CA). The lysates were then centrifuged for 20 minutes at 4^{o}C and 8500 rpm. The supernatant was retained as the cytoplasmic fraction. Finally, the pellet was incubated with rotation in extraction buffer for 30 minutes at 4^{o}C, centrifuged for 5 minutes at 12,000 rpm and 4^{o}C, and the supernatant was retained as the nuclear fraction.

Western blot analysis

Equal mass samples (30 µg) were separated using 10 % Tris-Glycine-SDS PAGE and then transferred to nitrocellulose membranes. Membranes were probed with rabbit anti-BMP4 (Abcam, Cat. No. ab39973, Cambridge, MA) at a 1:400 dilution overnight at 4^{o}C. Membranes were further probed with donkey anti-rabbit horseradish peroxidase (HRP) conjugated secondary antibodies (Santa Cruz Biotechnology® Inc, Santa Cruz, CA). Finally, membranes were developed using Immobilon^{TM} Western Chemiluminescent HRP Substrate (Millipore, Billerica, MA) and visualized with autoradiography using Blue Basic Autorad Film (ISC Bioexpress, Kaysville, UT).

Construction of GFP/NLS fusion constructs

The Bmp4 preproprotein sequence was analyzed using an online prediction website (Psort II, http://psort.nibb.ac.jp/) in order to locate putative nuclear localization signals (NLSs). Figure 1.1 shows the mouse preproprotein sequence with four putative NLSs.

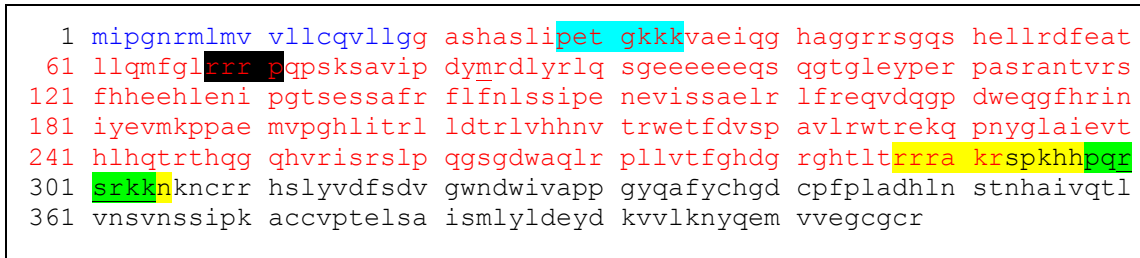

Figure 1.1 Psort II predicts four NLSs in the mouse Bmp4 preproprotein sequence. The mouse Bmp4 preproprotein sequence was obtained from the National Center for Biotechnology Information (Accession NM_007554). The signal peptide is indicated in blue, the propeptide in red, and the mature peptide in black. Psort II [http://psort.nibb.ac.jp/] was used to analyze the amino acid sequence, which predicted four NLSs. These NLSs were named NLS A (blue highlight), NLS B (black highlight), NLS C (yellow highlight, which continues through NLS D), and NLS D (green highlight). These predicted NLSs were subsequently prepared in GFP fusion constructs in order to test the functionality of each predicted signal.

DNA oligos were synthesized at Invitrogen (Carlsbad, CA) in order to prepare GFP fusion constructs with each NLS (see Table 1.1). Each oligo is designed with 5' overhang of GGCC. The oligos were resuspended in 50 µL TE buffer and incubated for 2 minutes at room temperature. The oligos were then vortexed for 30 seconds and centrifuged briefly. Oligos were prepared for electrophoresis by mixing 25 µL primer and 25 µL formamide with 1 µL 1% bromophenol blue. Each tube was then heated to 90^{o}C for 3 minutes. The oligos were loaded onto a polyacrylamide gel (30 ml 30% acrylamide solution, 31.5 g urea, 7.5 ml 10X TBE, 13.5 ml H_2O) and electrophoresed at 400 V until the samples were $^{2}/_{3}$ down the gel. The gel was stained with ethidium bromide, and the oligo bands were excised, crushed, and incubated in 5 ml TE overnight.

To finish preparing the oligos, they were concentrated using 3 cycles of liquid-liquid extraction with sec-butanol at a 1:1 ratio. Finally, the oligos were ethanol precipitated, washed, and resuspended in 30 µL TE.

Table 1.1 Oligos for GFP/NLS fusion protein expression plasmid construction. Oligos were synthesized at Invitrogen (Carlsbad, CA). These oligos were subsequently annealed and ligated into pCMV/*myc*/ER/GFP in frame with GFP in order to prepare GFP/NLS fusion protein expression plasmids.

NLSAsense	GGCCCCTGAGACCGGGAAGAAAAAATA
NLSAantisense	GGCCTATTTTTTCTTCCCGGTCTCAGG
NLSBsense	GGCCCGCCGCCGTCCGTA
NLSBantisense	GGCCTACGGACGGCGGCG
NLSCsense	GGCCCGCAGGAGGGCCAAACGTAGTCCCAAGCATCACCCACAGCGGTCCAG GAAGAAGAATTA
NLSCantisense	GGCCTAATTCTTCTTCCTGGACCGCTGTGGGTGATGCTTGGGACTACGTTTGG CCCTCCTGCG
NLSDsense	GGCCCCACAGCGGTCCAGGAAGAAGTA
NLSDantisense	GGCCTACTTCTTCCTGGACCGCTGTGG

Once the oligos were purified, equimolar portions of complementary pairs of oligos were annealed by boiling for 10 minutes and incubating at room temperature for 3 hours in the dark to create double stranded NLS sequences. Simultaneously, the GFP fusion protein expression plasmid pCMV/*myc*/ER/GFP was digested with *Not* I at 37^{o}C and dephosphorylated with calf intestinal alkaline phosphatase (Promega, Madison, WI) for 30 minutes at 37^{o}C. As noted above, each NLS sequence was flanked with a 5' GGCC. These ends were phosphorylated with T4 kinase in preparation to ligate the NLS sequences into the GFP fusion protein expression plasmid. Finally, each double stranded NLS sequence was ligated into the GFP vector and transformed into *E. coli* cells. Plasmids from the resulting colonies were purified using the Qiaprep® Spin Miniprep Kit following the manufacturer's protocol (Qiagen, Valencia, CA). All plasmids were sequenced by the BYU Sequencing Center to verify the correct insertion of the NLS sequence and that the NLS was in frame with the N-terminal GFP sequence.

Construction of Bmp4/GFP constructs

Murine Bmp4 cDNA was amplified from pSP72 (a kind gift from Dr. Ronald Koenig at the University of Michigan, Ann Arbor, MI) using the Bmp4cDNA primers shown in Table 1.2. It was then subcloned into pcDNA3.1/CT-GFP-TOPO using the GFP Fusion TOPO® TA

Expression Kit (Invitrogen, Carlsbad, CA) according to the manufacturer's protocol to prepare wtBmp4/GFP. ATG1 and ATG83 were mutated to A**A**G to generate the ATG1mtBmp4/GFP and ATG83mtBmp4/GFP fusion expression plasmids using the QuikChange II Site-Directed Mutagenesis Kit (Stratagene, La Jolla, CA) according to the manufacturer's protocol and the primers listed in Table 1.2. Additionally, NLSmtBmp4/GFP was prepared by mutating the putative NLSC (R**RR**AKRSPKHHPQRS**RKK**NK) to R**AA**AKRSPKHHPQRS**AAV**NK using two rounds of QuikChange II Site-Directed Mutagenesis and the primers listed in Table 1.2. All primers were synthesized by Invitrogen (Carlsbad, CA). All plasmids were verified by DNA sequencing performed in the BYU DNA Sequencing Center.

Table 1.2 Mutagenesis primers for preparation of mutant Bmp4/GFP fusion protein expression plasmids. Oligos were synthesized at Invitrogen (Carlsbad, CA). The mutated nucleotides are bolded and underlined. These primers were utilized in QuikChange II Site-Directed Mutagenesis in order to prepare plasmids that had a mutated conventional start codon, alternative start codon, or bipartite nuclear localization signal (which was mutated in two steps). Primers for the original PCR to insert Bmp4 into the pCMV/*myc*/ER/GFP (Invitrogen, Carlsbad, CA) plasmid are also included.

Bmp4cDNAprimer1	ATGGACTGTTATTATGCCTTGTTTT
Bmp4cDNAprimer2	GGCGGCATCCACACCCCTCTACC
Fmutstartcodon	GTTTTCTGTCAAGACACCA**A**GATTCCTGGTAACCG
Rmutstartcodon	CGGTTACCAGGAATC**T**TGGTGTCTTGACAGAAAAC
Fmutaltstartcodon	GTCATTCCGGATTACA**A**GAGGGACCTTTACC
Rmutaltstartcodon	GGTAAAGGTCCCTC**T**TGTAATCCGGAATGAC
FNLSmutround1	GGCCATACCTTGACCCGC**GCGGC**GGCCAAACGTAGTCCC
RNLSmutround1	GGGACTACGTTTGGCC**GCCGC**GCGGGTCAAGGTATGGCC
FNLSmutround2	GCATCACCCACAGCGGTCC**GCGGCGGT**GAATAAGAACTGCCGTCG
RNLSmutround2	CGACGGCAGTTCTTATTC**ACCGCCGC**GGACCGCTGTGGGTGATGC

Transient transfections, fixation of cells, and confocal microscopy

70,000 RCS cells were seeded into Lab-Tek II Chamber slides (ISC Bioexpress, Kaysville, UT) 18-24 hours prior to transfection. Cells were then transfected with 0.5 µg of GFP/NLSA, GFP/NLSB, GFP/NLSC, GFP/NLSD, wtBmp4/GFP, ATG1mtBmp4/GFP, ATG83mtBmp4/GFP, or NLSmtBmp4/GFP using the TransIT® -Jurkat Transfection Reagent according to the manufacturer's protocol (Mirus, Madison, WI). The media was changed after 24

hours. 48 hours after transfection, cells were washed three times with 1x PBS and fixed with 4% paraformaldehyde/PBS for 30 minutes at room temperature. Cells were then washed with 1x PBS three times and the nuclei were counterstained with 1 μM TO-PRO-3 iodide (Invitrogen, Carlsbad, CA) for 10 minutes. Finally, cells were washed with PBS three more times and slides were mounted with Fluoromount-G (SouthernBiotech, Birmingham, AL). After the Fluoromout-G dried, cells were visualized using an Olympus IX81 laser confocal microscope using excitation wavelengths of 488 nm and 633 nm. In order to quantify the percent of cells with Bmp4 localized to the nucleus, cells that expressed GFP were identified, counted, and categorized as nuclear or cytoplasmic.

Results

It has been shown that a nuclear variant of Bmp2 is localized to the nuclei of many tissue culture cell lines.[2] In order to determine if Bmp4 is also localized to the nucleus, we prepared a Bmp4/GFP fusion protein expression plasmid and transfected it into rat chondrosarcoma (RCS) cells. The cells were subsequently fixed and incubated with a nuclear stain in order to determine if the GFP was being localized to the nucleus. The results show that Bmp4 did, in fact, localize GFP to the nucleus.[2] As transient transfections do not always accurately reflect what is happening in the cell, we next looked at the endogenous localization of Bmp4. Rat chondrosarcoma (RCS) cells, 10T1/2, and Balb3T3 fibroblasts, MDA-MB-231, MDA-MB-435S and MCF-7 breast cancer cells, HepG2 liver cancer cells, and HT-29 colon cancer cells were seeded in chamber slides and allowed to grow for 48 hours. The cells were then fixed, probed with anti-Bmp4 antibodies, counterstained with a nuclear stain and analyzed by confocal fluorescence microscopy. The results show that endogenous Bmp4 is directed to the nucleus in each cell line, with the highest levels of nuclear localization appearing to be in the MCF-7 breast

cancer cell line (Figure 1.2.A). Western blots of nuclear and cytoplasmic extracts were immunoblotted to verify nuclear localization of Bmp4 (Figure 1.2.B).

(A)

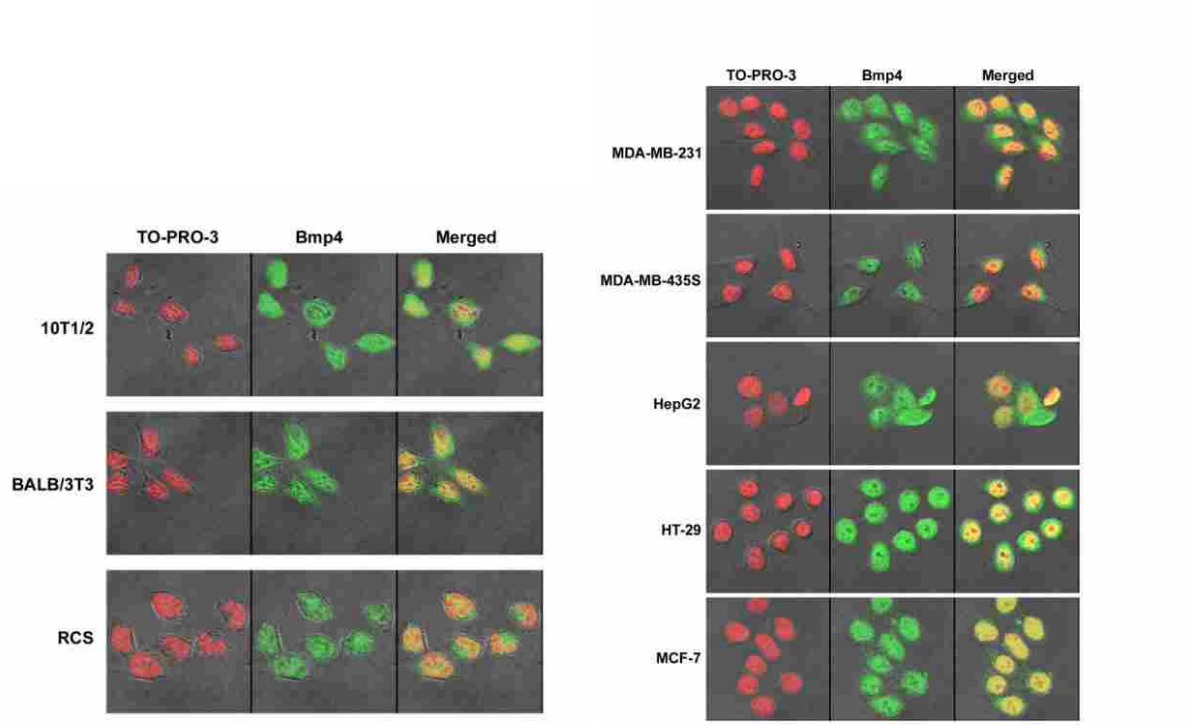

(B)

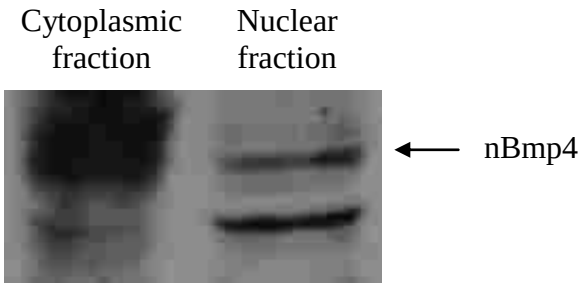

Figure 1.2 Endogenous Bmp4 is localized to the nucleus in cultured cells. (A) Non-transfected cells were stained using an anti-Bmp4 primary antibody and a FITC-labeled secondary antibody and examined via laser confocal microscopy. Nuclei were visualized by staining with TO-PRO-3 Iodide (red). Bmp4 antibody staining is indicated with green. Human cancer cell lines are shown in the right panel while 10T1/2 and BALB/3T3 fibroblast cells and rat chondrosarcoma (RCS) cells are shown in the left panel. The merged views clearly show that Bmp4 is located in the nucleus. **(B)** Nuclear and cytoplasmic extracts from MCF-7 cells were analyzed by immunoblotting with an anti-BMP4 antibody.

To delineate how Bmp4 is being localized to the nucleus, Psort II, an online computer program,[43] was used to predict nuclear localization signals (NLSs) in the Bmp4 amino acid sequence. Three small NLSs were predicted as well as a bipartite NLS (Figure 1.3.A). To test the functionality of the predicted NLS sequences, we produced fusion plasmids with each NLS sequence inserted in frame after to the 3' end of GFP. These constructs were then separately transfected into RCS cells. The cells were fixed and incubated with a nuclear stain in order to determine if the NLS was capable of directing GFP to the nucleus. When these fusion constructs were transfected into RCS cells, only one of the predicted NLSs, the bipartite NLS, was found to direct GFP to the nucleus (Figure 1.3.B). This suggests that the bipartite NLS is the functional signal that directs Bmp4 to the nucleus. Interestingly, the bipartite NLS overlaps the cleavage site for the mature form of secretory Bmp4 (wild type amino acid sequence RRRAKR|SPKHHPQRSRKKN with the normal cut site indicated by a bar). This NLS sequence would normally be cleaved while Bmp4 is being shuttled through the secretory pathway. This result suggests that there is a nuclear variant of Bmp4 that is an uncleaved proprotein, as protein processing would cleave and thus inactivate the bipartite NLS.

As protein processing would inactivate the predicted bipartite NLS, another mechanism must be responsible for producing a nuclear variant of Bmp4. Recently, the Bridgewater lab discovered that nBmp2 is translated from an alternative start codon.[2] This downstream start codon omits the signal peptide; thus the nuclear variant of Bmp2 is not processed through the secretory pathway and the bipartite NLS remains intact. From these findings, we decided to look for an analogous alternative start codon in Bmp4. NetStart 1.0 Prediction Server[44] was used to predict potential alternative start codons within Bmp4 cDNA. One of the high scoring potential

start codons was downstream from the signal peptide but upstream from the mature peptide, which is similar to the start codon utilized to produce nBmp2.

(A)

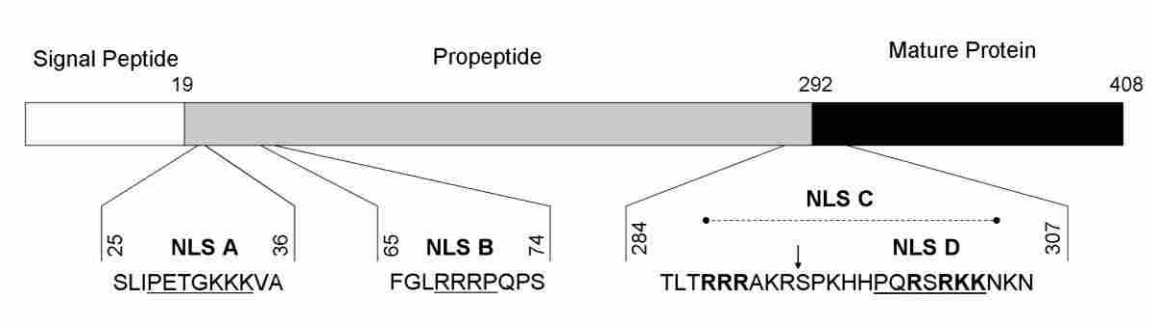

(B)

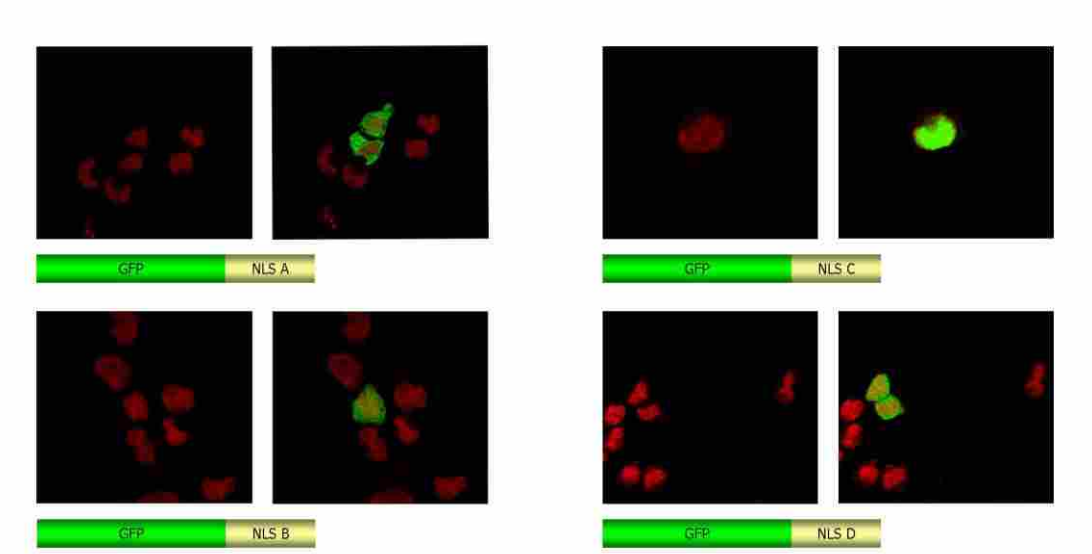

Figure 1.3 The Bmp4 preproprotein contains four predicted nuclear localization signals (NLSs), but only the bipartite NLS directs nuclear localization of GFP. (A) PSORT II[43] was used to analyze the mouse Bmp4 amino acid sequence. Four NLSs were predicted as shown. The arrow indicates the site of proteolytic cleavage to produce secretory Bmp4. (B). Four fusion constructs were built, transfected into RCS cells, and cells were examined via laser confocal microscopy to test the functionality of the predicted NLSs. NLSs A, B and D did not direct nuclear localization of GFP. NLS C localized GFP to the nucleus. The nuclei were stained with TO-PRO-3 Iodide (red) while the GFP is indicated with green.

To analyze the functionality of this alternative start codon in Bmp4, site-directed mutagenesis was used to change the potential alternative start codon (ATG) in the Bmp4/GFP fusion plasmid to A**A**G. In addition, we performed site-directed mutagenesis to change the conventional start codon from ATG to A**A**G, in order to force utilization of downstream alternative start codons. These plasmids were transfected into RCS cells and the number of GFP-expressing cells that displayed accumulation of GFP in the nucleus (indicating nuclear localization of Bmp4) was counted (see Table 1.3). 29% of cells transfected with wild type Bmp4 (wtBmp4/GFP) displayed GFP localized to the nucleus. This number was significantly decreased to 16% of transfected cells showing nuclear localization of GFP when the alternative start codon (ATG83mtBmp4/GFP) was mutated. Remarkably, 80% of the transfected cells contained nuclear Bmp4 when the conventional start codon was mutated (ATG1mtBmp4/GFP). Together, these results indicate that a significant amount of the time, Bmp4 is being localized to the nucleus when transfected into tissue culture cells and that this nuclear localization is probably due to other variants of Bmp4 rather than the full length protein. These results also indicate that a nuclear variant of Bmp4 is translated from the alternative start codon 83 (hereafter denoted nBmp4) since the amount of cells with nuclear localized GFP is significantly decreased when the production of this protein was hindered. Because the percent of cells with GFP in the nucleus did not decrease to 0% when the alternative start codon 83 was mutated, these findings also suggest that other alternative start codons may be used to generate other nuclear variants of Bmp4. However, the functional role of these other variants has not been elucidated.

Finally, in order to test the functionality of the bipartite NLS in the context of the entire Bmp4 gene, site-directed mutagenesis was used to prepare a plasmid in which the bipartite NLS was mutated. Several of the basic amino acids that are necessary for nuclear localization were

replaced with neutral amino acids (R**RR**AKRSPKHHPQRS**RKK**NK changed to R**AA**AKRSPKHHPQRS**AAV**N). This plasmid was also transfected into RCS cells and the number of GFP-expressing cells that had an accumulation of GFP in the nucleus (indicating nuclear localization of Bmp4) was counted. As seen in Table 1.3, mutating the bipartite NLS (NLSmtBmp4/GFP) severely decreased the amount cells with GFP localized to the nucleus. This result indicates that Bmp4 utilizes the bipartite NLS for localization to the nucleus.

Table 1.3 Nuclear localization of Bmp4 is contingent upon the alternative start codon and bipartite NLS. Bmp4 cDNA was cloned into pCMV/*myc*/ER/GFP to make a Bmp4/GFP fusion protein expression plasmid. The conventional start codon and predicted alternative start codon were mutated to AAG in order to force utilization of other start codons. Finally, another construct was prepared in which the important basic amino acids in the bipartite NLS were mutated to be alanines. These plasmids were transfected into RCS cells and the nuclear accumulation of the GFP fusion proteins was quantified.

Constructs used in transfection:	% of cells with nuclear localization ± S.E.
wtBmp4/GFP	**29 ± 6**
ATG1mtBmp4/GFP	**80 ± 14**
ATG83mtBmp4/GFP	**16 ± 3**
NLSmtBmp4/GFP	**3 ± 1**

Discussion

Proteins in the bone morphogenetic protein family have been studied for over two decades as secreted growth factors. However, the presence of nuclear variants has never been addressed. This study has clearly shown that there is a nuclear variant of Bmp4 (nBmp4). As shown by immunocytochemistry, the nuclear localization of Bmp4 is not isolated to one specific type of cells. In fact, Bmp4 was seen in the nuclei of every cell line that was examined. We have

determined that a prominent nuclear variant of Bmp4 is translated from ATG 83, as shown by the nearly 50% decrease in nuclear localization when ATG 83 was mutated and thus inactivated. Because the nuclear localization was not completely eliminated, this result also indicates that there may be other variants of Bmp4 that are localized to the nucleus. However, no other variants have been examined in this study. Finally, we have shown that a bipartite nuclear localization signal is responsible for localizing Bmp4 to the nucleus. This was clearly shown by the nearly complete abolishment of Bmp4 nuclear localization by mutating and thus inactivating the bipartite NLS.

The present study also suggests that Bmp4 and nBmp4 can be translated from the same transcript, assuming that the transfected constructs only produce one transcript. However, the possible contributions of alternative transcripts or splice variants to produce the two Bmp4 variants *in vivo* have not been analyzed.

The presence of other variants of Bmp4 is not unprecedented. It is interesting to note that the original discoverer of Bmp2 and Bmp4, John Wozney, noted that the transfection of BMP cDNA constructs yields the full length size and multiple smaller molecular weight forms of BMPs.[11] This indicates that other variants of the BMPs have been observed previously. Additionally, Oida et. al. identified an alternative transcript of Bmp4 in human placenta that excluded the first eight amino acids.[45] From these observations, it should not be a surprise that a smaller molecular weight variant of Bmp4 has been identified and further characterized.

The methods used here to analyze the nuclear localization of a protein are not innovative. As described in the introduction, a nuclear localization signal needs to be analyzed to determine its functionality through demonstrating its ability to localize GFP to the nucleus as well as its

ability to localize the full length protein to the nucleus. As an example, RAC3 was analyzed in the same manner to determine that its bipartite nuclear localization signal was functional.[46]

The phenomenon of two forms of a protein originating from the same transcript is not novel. In 1995, Patterson et. al. identified a protein, adenosine deaminase acting on RNA 1 (ADAR1) in which two forms of the protein are transcribed from the same transcript.[47] One form of ADAR1 is 150 kDa and is interferon (IFN)-inducible. The other form of ADAR1 is 110 kDa, is constitutively active, and is exclusively found in the nucleus.

Many of the genes that are seen to have multiple variants utilize internal ribosomal entry sites (IRESs) to generate different variants. Interestingly, many of the genes that have been determined to contain IRESs are involved in the growth of cells.[48] For instance, the human c-myc gene encodes two proteins, one that is translated from an upstream non-AUG start codon and another from the normal AUG start codon.[49] These two proteins, denoted c-Myc1 and c-Myc2, respectively, are transcription factors that have both similar and distinct DNA targets. [50, 51] Translation of these myc variants can occur through the conventional cap-dependent scanning mechanism or through the use of an internal ribosomal entry site.[52]

Members of the fibroblast growth factor family also generate multiple forms of the protein from a single transcript. For instance, fibroblast growth factor 2 (FGF-2) is translated from multiple initiation sites. FGF-2 has four initiation codons, three CUG start codons that are upstream of the conventional AUG start codon and one AUG start codon.[53, 54] Interestingly, the proteins that are translated from the three CUG start codons are all found predominantly in the nucleus due to the inclusion of an NLS that is located upstream of the conventional AUG start codon.[55, 56] FGF-3 was also found to have an alternative form that is translated from an upstream non-AUG initiation codon.[57] Similarly, this alternative form of FGF-3 is also localized

specifically to the nucleus while the form of FGF-3 that is translated from the conventional start codon is found predominantly in the secretory pathway.

Although the above examples are all of upstream alternative start codons, there is an example of a downstream alternative start codon. Nuclear variants of PTH-related peptide (PTHrP) proteins are translated from an alternative downstream start codon and localized to the nucleus through a nuclear localization signal that interacts with importin β1.[58, 59] This phenomenon was identified through the observation that nuclear PTHrP proteins were smaller than the full length PTHrP protein but larger than the mature form. Therefore, nuclear variants of PTHrP are very similar to nuclear BMP variants in that they are translated from downstream start codons, maintain part of the preproprotein, and are sent to the nucleus instead of through the secretory pathway.

To summarize the results of this chapter, the diagram shown in Figure 1.4 illustrates the pathway by which nBmp4 is produced and localized to the nucleus. nBmp4 is translated from an alternative start codon downstream from the signal peptide sequence. Without the N-terminal signal peptide, the protein is translated in the cytoplasm rather than the endoplasmic reticulum and thus avoids protein processing and secretion. Instead, the intact bipartite NLS directs translocation to the nucleus. The presence of nBmp4 is an exciting discovery. The finding that there are nuclear variants of Bmp2 and Bmp4 suggests that these are conserved variants. It also suggests that these proteins play important roles in the nuclei of cells.

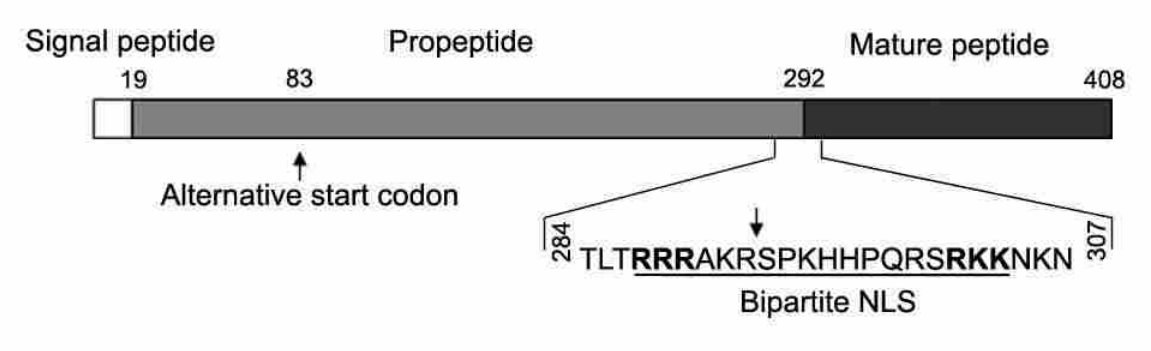

Figure 1.4 Summary of results concerning the production of nBmp4. nBmp4 is translated from an alternative start codon downstream from the signal peptide. Without this N-terminal signal, the protein is translated in the cytoplasm and thus avoids proteolytic cleavage (indicated by the arrow). The bipartite NLS is, therefore, not cleaved and directs nBmp4 to the nucleus.

Chapter 2: Identifying nBmp4 binding partners

Summary

As shown in chapter one, there is a novel family of nuclear bone morphogenetic proteins. This discovery has changed the traditional paradigm that bone morphogenetic proteins function solely through their actions as growth factors. The role that these nuclear bone morphogenetic proteins play in the nucleus is a crucial question to answer. This chapter attempts to uncover the nuclear function of nBmp4 by performing a yeast two-hybrid screen to identify potential binding partners of nBmp4. From the yeast two-hybrid screen, the two most frequently encountered binding partners were Regulator of Cullins 1 and 2 (ROC1 and ROC2), which are components of SCF E3 ubiquitin ligase complexes. Through the known roles of the identified binding partners, the data suggest that nBmp4 plays a role in protein degradation, cell cycle control, and apoptosis.

Introduction

As nuclear Bmp4 is a novel protein, there is no literature on the function of nBmp4. Therefore, we set out to determine the function of this novel protein. There are several ways by which the function of a protein may be delineated. For instance, siRNA can be used to knock down the protein of interest in a cell line and then the phenotype may be characterized. However, because Bmp4 and nBmp4 are presumably transcribed from the same transcript, we did not have the option to knock down the transcript with siRNA since this would eliminate both the secretory and nuclear variants of Bmp4. Eliminating both variants of Bmp4 would introduce lurking variables and interfere with identifying the separable function of nuclear Bmp4.

Another method used to uncover the function of a protein of interest is to determine its binding partners and thereby delineate the function of the protein of interest through the known functions of the identified interacting proteins. This may be accomplished through

immunoprecipitation followed by mass spectrometric analysis of the co-immunoprecipitated proteins. Alternatively, a yeast two-hybrid (Y2H) screen may be performed in which the protein of interest is used as a bait protein and a library of "prey" proteins are screened to identify positive interactions. Both of these techniques are useful in the identification of previously unknown interacting proteins. According to Mukherjee et. al., the Y2H is very popular because it is inexpensive, *in vivo*, and has the potential to screen a large number of protein-protein interactions in parallel.[60]

As described by Chien et. al., the Y2H system is a method to identify proteins that interact with a protein of interest.[61] In this system, the ability of the DNA binding domain and activation domain of some transcription factors to remain functional after being separated is exploited.[60] Accordingly, cDNA encoding the protein of interest is inserted into a plasmid encoding the DNA binding domain (BD) of Gal4 to create a Gal4BD fusion protein expression plasmid and is called the "bait". Similarly, cDNA fragments are ligated into copies of a vector containing the sequence coding for the activation domain (AD) of Gal4 to create a library encoding Gal4AD fusion "prey" proteins. The plasmids are then either co-transformed into yeast or transformed separately into two haploid strains of mating yeast and then the yeast cells are mated. Interactions between the bait and prey proteins are identified by their ability to activate reporter genes that contain the Gal4 binding site called the upstream activation sequence (UAS). The activation of transcription is caused by the AD and BD of Gal4 coming in close proximity to one another due to the interaction of the bait and prey. Therefore, the two domains of the Gal4 transcription factor can work together as an active transcription factor. The Y2H screen via yeast mating strategy is summarized in Figure 2.1.[60] The yeast two-hybrid technique was first used by

Fields and Song in 1989[62] and has since been exploited by many scientists in order to identify proteins that interact with their gene of interest and to verify protein-protein interactions.

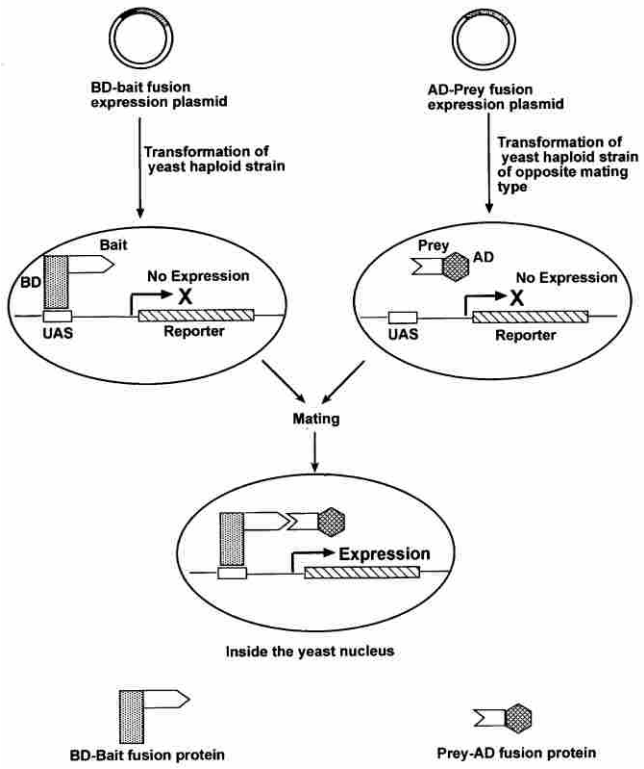

Figure 2.1 Schematic of yeast two-hybrid strategy via yeast mating. The protein of interest is encoded in a Gal4BD fusion protein expression vector while a cDNA library is ligated into a Gal4AD fusion protein expression plasmid. The vectors are transformed separately into two haploid strains of yeast that are opposite mating types and then the yeast are mated. Positive interactions are identified easily due to their ability to activate transcription of a reporter gene that contains the Gal4 binding site (upstream activation sequence, UAS). Figure from Mukherjee et al.[60]

There are many advantages to the Y2H system. As mentioned above, the Y2H is inexpensive, *in vivo*, and has the ability to screen a large number of interactions.[60] Additionally, the Y2H technique does not require the use of highly specific antibodies like the immunoprecipitation followed by mass spectrometry technique requires. Another advantage of the Y2H system is the immediate identification and availability of at least a partial cDNA clone encoding the binding partner, which can be used in subsequent experiments. The Y2H technique also allows identification of weak and transient interactions that might otherwise be difficult to

identify.[63] Finally, interactions obtained through an Y2H screen may provide clues about the function of the bait protein if the functions of the identified interacting proteins have been well studied.[60]

In order to validate the yeast two-hybrid assay, several tests must be done. For instance, the bait protein must first be tested for transcriptional activation of the reporter genes. If the bait protein can activate transcription of the reporter genes on its own then the Y2H assay cannot be used with the full length bait protein to identify binding partners. Additionally, Y2H data must be validated by co-immunoprecipitation experiments in tissue culture to verify the interaction and minimize false positive results.

Due to the various functions of Bmp4 and the recent discovery of its nuclear variant, nBmp4, we hypothesize that nBmp4 is a functional nuclear protein and that it may be responsible for some of the roles that Bmp4 has been determined to play. In order to delineate the function of nBmp4, we propose the use of the yeast two-hybrid screen to identify binding partners, which may suggest a functional role for nBmp4.

Experimental Procedures

Preparation of an MCF-7 cDNA library

A cDNA library was prepared from MCF-7 breast cancer cells for use in a yeast two-hybrid screen. First, RNA was extracted from MCF-7 breast cancer cells (passage 17) using the RNeasy Mini Kit (Qiagen, Valencia CA) according to manufacturer's protocol. A cDNA library was then constructed using the Matchmaker™ Library Construction Kit (Clontech, Mountain View, CA) according to the manufacturer's protocol. Briefly, the MCF-7 RNA was reverse transcribed using a Mokoney Murine Luekemia Virus (MMLV) Reverse Transcriptase and an oligo(dT) primer to make the first strand cDNA. The first strand cDNA was then amplified using

20 cycles of long distance PCR to make a double stranded cDNA library. The double stranded cDNA library was purified using a CHROMA SPIN^{TM} TE-400 column followed by ethanol precipitation and resuspension in 20 µL H_2O.

The MCF-7 cDNA library was inserted into pGADT7-Rec in order to create a Gal4 activating domain (AD) fusion library. This was accomplished by co-transformation of the cDNA library and *Sma*I-linearized pGADT7-Rec into AH109 yeast to promote *in vivo* homologous recombination using the Matchmaker^{TM} Library Construction and Screening Kit (Clontech, Mountain View, CA). Competent AH109 yeast cells were prepared using the lithium acetate method. Then 20 µL of MCF-7 cDNA library was transferred to a 15-ml conical tube along with 6 µL pGADT7-Rec and 20 µL Herring Testes Carrier DNA (previously denatured through two cycles of boiling for 5 minutes and cooling on ice for 5 minutes). 600 µL of competent AH109 cells were then added and the sample was mixed well by vortexing. Subsequently, 2.5 ml PEG/LiAc solution (40% polyethylene glycol 3350, 1x TE (10 mM Tris-HCl pH 8.0, 1 mM EDTA), 0.1 M lithium acetate) was added, the sample was mixed, and then it was incubated at 30^{o}C for 45 minutes with mixing every 15 minutes. After the 45 minute incubation, 160 µL DMSO was added and the sample was incubated at 42^{o}C for 20 minutes with mixing every 10 minutes. Cells were pelleted by centrifuging at 700 x g for 5 minutes, resuspended in 3 ml YPD Plus Liquid Medium (Clontech, Mountain View, CA), and incubated at 30^{o}C with shaking for 90 minutes. Finally, cells were pelleted by centrifuging at 700 x g for 5 minutes, resuspended in 30 ml 0.9% NaCl and spread on approximately 200 150-mm SD/-Leu plates. Transformed cells were allows to grow for 6 days at 30^{o}C.

In order to pool the selected transformants of the Gal4AD/MCF-7 cDNA library, the ~200 SD/-Leu plates were chilled for 3-4 hours at 4^{o}C. Then 5 ml freezing medium (YPD

medium (20 g/L peptone, 10 g/L yeast extract, 20 g/L dextrose) with 25% (v/v) glycerol) was added to each plate and the cells were collected into the medium. Even though approximately 50 plates didn't have any growth, this step took two days because of the large number of plates. Plates were stored in the fridge overnight during this time. Once all the cells were collected, the cDNA library was aliquoted into 500-600 1-ml aliquots and frozen at -80^{o}C. One aliquot was also used to spread 1:100, 1:1,000, and 1:10,000 dilutions onto SD/-Leu plates in order to determine the library titer.

Prepare nBmp4 bait

The yeast two-hybrid bait, Gal4BD/nBmp4, was prepared by PCR amplifying nBmp4 from Bmp4 cDNA (starting at ATG83) using the following primers:
5' AAAAAAGAATTCATGAGGGACCTTTACCGGCTCC 3' and
5' AAAAAAGGATCCATCAGCGGCATCCACACCCC 3'. The nBmp4 amplicon was ligated into pGBKT7 using the *EcoR*I and *BamH*I sites and a 5:1 insert:vector ratio.

The Gal4BD/nBmp4 bait was then tested for transcriptional activation. This was accomplished by transforming either pGBKT7 (empty Gal4BD vector) or Gal4BD/nBmp4 into AH109 and Y187 yeast strains using the small-scale lithium acetate yeast transformation procedure from the Yeast Protocols Handbook (Clontech, Mountain View, CA). The yeast transformants were plated on the following plates: SD media minus Trp (SD/-Trp), SD media minus Trp and His (SD/-Trp/-His), and SD media minus Ade and Trp (SD/-Ade/-Trp). The yeast transformants were then allowed to grow at 30^{o}C for 5 days. If the bait protein is inactive, it will grow on SD/-Trp plates but not on SD/-Ade/-Trp or SD/-His/-Trp plates. If the bait is active, it will grow on all plates. However, if there is leaky His expression then the transformants may grow on SD/-His/-Trp plates but not SD/-Ade/-Trp plates. This was the case with our bait

protein. To overcome the leaky His expression, SD/-Ade/-His/-Leu/-Trp (QDO) plates were used to screen the MCF-7 cDNA library for interactions with the Gal4BD/nBmp4 bait protein.

The Gal4BD/nBmp4 bait was also tested for toxicity. Specifically, 2 mm colonies from both the Gal4BD/nBmp4 and empty vector (pGBKT7) transformations into both AH109 and Y187 yeast were tested by growing them overnight in 50 ml SD/-Trp media with 20 µg/ml kanamycin at 30^{o}C with shaking at 250-270 rpm. Approximately 23 hours later, the absorbance at 600 nm was measured. The bait is determined to be nontoxic if absorbance is greater than 0.8. The absorbance of the bait and empty vector were both much greater than 0.8; therefore, Gal4BD/nBmp4 is nontoxic.

Yeast two-hybrid screen and analysis

After the toxicity and autoactivation of the bait protein were tested, the Gal4BD/nBmp4 bait protein was used to screen the MCF-7 library according to the Matchmaker^{TM} Library Construction and Screening Kit (Clontech, Mountain View, CA). The detailed protocol is as follows. The 50 ml culture containing Y187[Gal4BD/nBmp4] was centrifuged for 5 minutes at 600 x g. The supernatant was discarded and the cell pellet was resuspended in 4 ml SD/-Trp. Meanwhile, 10 tubes of AH109[MCF-7 library] were thawed at room temperature and concentrated by centrifuging at 600 x g for 30 seconds and resuspending in a total volume of 1.5-2 ml. The Y187[Gal4BD/nBmp4] culture was then combined with the AH109[MCF-7 library] and 45 ml 2x YPDA media (1x YPDA contains 20 g/L peptone, 10 g/L yeast extract, 20 g/L dextrose, 30 mg/L adenine hemisulfate) with 50 µg/ml kanamycin was added. The mating yeast were incubated at 30^{o}C with gentle agitation (~50 rpm) for 26 hours. The mating yeast were then centrifuged for 10 minutes at room temperature and 1000 x g. Meanwhile, the flask used for mating was washed twice with 50 ml 0.5x YPDA media with 50 µg/ml kanamycin. The cell

pellets were then resuspended in the 2 washes and centrifuged again at 1000 x g for 10 minutes at room temperature. Finally, the cell pellet was resuspended in 10 ml 0.5x YPDA media with 50 µg/ml kanamycin and plated on ~60 150-mm QDO plates. A small aliquot was also used to plate 1:10, 1:100, 1:1,000, and 1:10,000 dilution plates in order to determine the mating efficiency. The plated yeast were incubated at 30^{o}C for 5 days. The resulting colonies contained interacting bait and prey plasmids. The Gal4AD/prey clones were then identified through PCR amplification using the Matchmaker^{TM} AD LD-Insert Screening Amplimer Set (Cat. No. 630433) and the Advantage 2 PCR Polymerase Kit (both from Clontech, Mountain View, CA). The PCR amplicons were then sequenced at the BYU sequencing center using the T7 primer.

nBmp4 sequential deletion plasmid construction

Sequential deletion plasmids were prepared by dividing nBmp4 into 5 segments and preparing plasmids that had segments sequentially deleted from the N-terminus and from the C-terminus as shown in Figure 2.1. The corresponding fragments were amplified from the Gal4BD/nBmp4 plasmid using the primers given in Table 2.1. The primers were designed to contain *EcoR*I restriction sites included in the forward primers and *BamH*I restriction sites included in the reverse primers along with leading nucleotides to facilitate restriction digestion. The PCR amplicons were digested with *EcoR*I and *BamH*I, purified, and then ligated into pGBKT7 in frame with the GAL4 DNA binding domain. All primers were synthesized at Invitrogen (Carlsbad, CA). All plasmids were verified by DNA sequencing performed in the BYU DNA Sequencing Center.

Table 2.1 Primers for preparation of sequential deletion Gal4BD/nBmp4 fusion protein expression plasmids. All primers were synthesized at Invitrogen (Carlsbad, CA). These primers were used to PCR amplify fragments of nBmp4. The forward primers (denoted by an F) contain leading nucleotides to improve digestion by restriction enzymes and an *EcoR*I site. Likewise, the reverse primers (denoted by an R) contain leading nucleotides and a *BamH*I site. The PCR products were subsequently digested and ligated into pGBKT7 to create Gal4BD/nBmp4 fragment constructs.

1F	AAAAAAGAATTCCATCTGGAGAACATCCCAGGGAC
2F	AAAAAAGAATTCGAGGTTATGAAGCCCCCAGCAGAAAT
3F	AAAAAAGAATTCCAAGGGAGTGGAGATTGGGCCC
4F	AAAAAAGAATTCCGCCATTCACTATACGTGGACTTCA
FullLengthR	AAAAAAGGATCCATCAGCGGCATCCACACCCC
FullLengthF	AAAAAAGAATTCATGAGGGACCTTTACCGGCTCC
5R	AAAAAAGGATCCACGGCAGTTCTTATTCTTCTTCCTGGAC
6R	AAAAAAGGATCCAGGTAACGATCGGCTGATTCTGACG
7R	AAAAAAGGATCCATAAATGTTTATACGGTGGAAGCCCTGTTCC
8R	AAAAAAGGATCCTTCTTCGTGATGGAAACTCCTCACAGTG

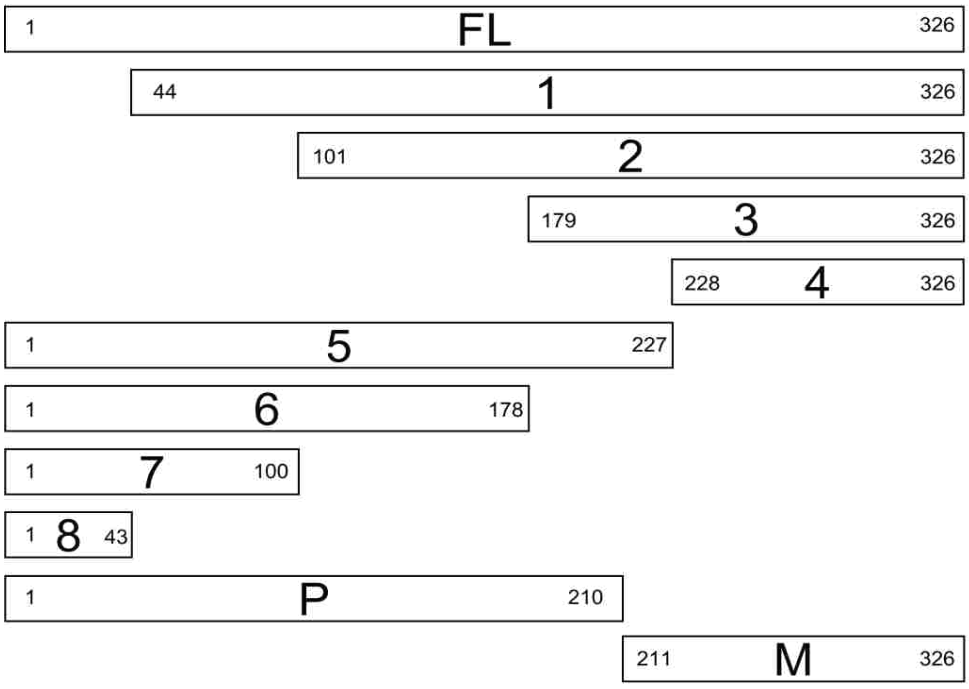

Figure 2.2 nBmp4 sequential deletion constructs. Segments of the GAL4BD/nBmp4 cDNA expression plasmid were sequentially deleted from the N- and C-termini as shown in order to delineate the domains within nBmp4 that interact with ROC1 and ROC2. Note that the amino acids are numbered starting with the alternative initiating methionine as amino acid 1.

ROC1 and ROC2 sequential deletion plasmid construction

The sequential deletion plasmids of GAL4AD/ROC1 and GAL4AD/ROC2 detailed in Figure 2.2 were prepared in order to determine the binding domains within ROC1 and ROC2 that interact with nBmp4. These plasmids were prepared by deleting various domains using the QuikChange® II Site-Directed Mutagenesis kit (Stratagene, La Jolla, CA) and the primers listed in Table 2.2. All plasmids were verified by DNA sequencing performed in the BYU DNA Sequencing Center. Note that the ROC1 cDNA construct retrieved from the yeast two-hybrid screen is a transcript variant missing exon 4. This transcript variant results in a truncated RING finger and an alternative C-terminus.

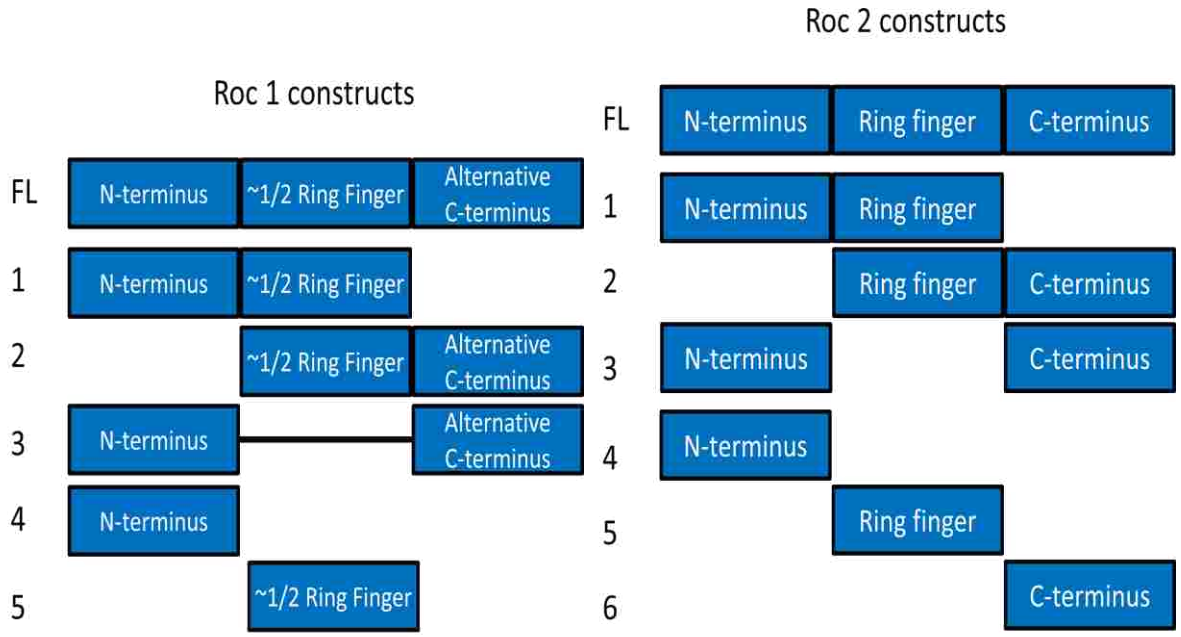

Figure 2.3 ROC1 and ROC2 sequential deletion constructs. Segments of the GAL4AD/ROC1 and GAL4AD/ROC2 expression plasmids were deleted as shown in order to delineate the domains within ROC1 and ROC2 that interact with nBmp4. Note that the ROC1 construct retrieved from the yeast two-hybrid screen is a transcript variant missing exon 4 which results in a truncated RING finger and alternative C-terminus.

Table 2.2 Primers for preparation of sequential deletion GAL4AD/ROC1 and GAL4AD/ROC2 fusion protein expression plasmids. All primers were synthesized at Invitrogen (Carlsbad, CA) and used in site-directed mutagenesis.

ROC1 Primers	
Delete N-term forward	CCGTGTGTTTCCAAATGTGCCATCTGCAGG
Delete N-term reverse	CCTGCAGATGGCACATTTGGAAACACACGG
Delete RING forward	GATATTGTGGTTGATAACGTATGGGCACTAGGAAAAG
Delete RING reverse	CTTTTCCTAGTGCCCATACGTTATCAACCACAATATC
Delete RING/C-term forward	GGGCCTGGGATATTGTGGTTGATAACTAATTGTTTTGTTATTC ATTTAATG
Delete RING/C-term Reverse	CATTAAATGAATAACAAAACAATTAGTTATCAACCACAATAT CCCAGGCCC
Delete N/C-term forward	GTCGCATGGGGAGTCTGTAACTAATTGTTTTGTTATTCATTTA ATG
Delete N/C-term reverse	CATTAAATGAATAACAAAACAATTAGTTACAGACTCCCCATG CGAC

ROC2 Primers	
Delete N-term forward	CCGGGGGGCGCCGCCTGCGCCATCTGCAGGGTC
Delete N-term reverse	GACCCTGCAGATGGCGCAGGCGGCGCCCCCCGG
Delete RING forward	GTGGAGTGCGATACGCAGCAGGACTGGGTG
Delete RING reverse	CACCCAGTCCTGCTGCGTATCGCACTCCAC
Delete C-term forward	CGCCGCCCTCTCTGCTGAGAGTGGTTAGAAG
Delete C-term reverse	CTTCTAACCACTCTCAGCAGAGAGGGCGGCG
Delete N-term/RING forward	CCGGGGGGCGCCGCCCAGCAGGACTGGGTG
Delete N-term/RING reverse	CACCCAGTCCTGCTGGGCGGCGCCCCCCGG
Delete RING/C-term forward	GTGGAGTGCGATACGTGAGAGTGGTTAGAAG
Delete RING/C-term reverse	CTTCTAACCACTCTCACGTATCGCACTCCAC

Yeast two-hybrid assays for confirmation of protein-protein interactions and sequential deletion analyses

First, competent AH109 yeast was prepared using the lithium acetate (LiAc) method. Plasmid DNA (as dictated by the experiment) was then incubated with competent yeast, denatured carrier DNA, and polyethylene glycol (PEG)/LiAc. Yeast was incubated at 30^{o}C for 30 minutes and then DMSO was added and the yeast cells were heat shocked at 42^{o}C for 15 minutes. YPD media (20 g/L peptone, 10 g/L yeast extract, 20 g/L dextrose, Clontech, Mountain View, CA) was then added and cells were incubated at 30^{o}C for 90 minutes to recover. Yeast was pelleted and resuspended in PBS. The yeast transformations were then plated on low stringency SD media plates lacking leucine and trypotophan (SD/-LW) to measure co-transformation efficiency. Yeast transformations were also plated on high stringency SD media

plates lacking adenine, histidine, leucine, and tryptophan (also called quadruple dropout, QDO, plates) to test for interaction between the bait and prey. The plates were then incubated at 30^{o}C for 2-4 days. After incubation, the initial protein-protein interactions were confirmed by the presence of colonies on the QDO plates. As for the sequential deletion analyses, the relative growth of each transformation was quantified by dividing the number of colonies on the high stringency plate by the number of colonies on the low stringency plate. The strength of the interaction in the sequential deletion analyses was then determined by comparing the relative growth for each transformation with the relative growth for the full length proteins and presented as a fold difference of the full length relative growth.

Cell culture

HEK 293T cells were cultured in a 50:50 mix of Dulbecco's Modified Eagle Medium and F-12 (HyClone, Logan, UT) supplemented with 10% fetal bovine serum (FBS). Cells were subcultured regularly, but not used after passage 25.

Plasmid constructs for transfections

nBmp4/HA was prepared by mutating the Bmp4 cDNA in pSP72. The sequencing preceding the alternative start codon was deleted using the primers in Table 2.3 and the QuikChange® II Site-Directed Mutagenesis kit (Stratagene, La Jolla, CA) to prepare an nBmp4 expression plasmid. A C-terminal HA tag was inserted using another round of mutagenesis and the indicated primers in Table 2.3 to prepare the nBmp4/HA in pSP72 expression plasmid. Finally, the nBmp4/HA fragment was subcloned into pcDNA3.1+ for better expression in mammalian cells using the *Hind*III and *Eco*RV.

Table 2.3 Primers used to prepare nBmp4/HA expression plamid. The primers were synthesized at Invitrogen (Carlsbad, CA) and used in QuikChange® II Site-Directed Mutagenesis (Stratagene, La Jolla, CA).

Fdeletesignalpeptide	CTTGTTTTCTGTCAAGACACCATGAGGGACCTTTACCGGC
Rdeletesignalpeptide	CCGGTAAAGGTCCCTCATGGTGTCTTGACAGAAAACAAG
FHACtermInsert	GGTGTGGATGCCGCTATCCTTATGATGTTCCTGATTATGCTTGAGATCAG GCAGTCC
RHACtermInsert	GGACTGCCTGATCTCAAGCATAATCAGGAACATCATAAGGATAGCGGC ATCCACACC

myc/ROC2 was prepared by inserting an N-terminal myc tag in place of the HA tag in HA/SAG (ROC2 variant 1 from Dr. Yi Sun at the University of Michigan, Ann Arbor, MI) using QuikChange® II Site-Directed Mutagenesis (Stratagene, La Jolla, CA) and the primers listed in Table 2.4. Later, ROC1/myc and ROC2/myc were prepared by PCR amplifying the ROC cDNAs from pcDNA3-Myc3-ROC1 (from Dr. Yue Xiong, University of North Carolina, Chapel Hill, NC) and myc/ROC2. The PCR primers used are listed in Table 2.4 and include C-terminal myc tag sequences, BamHI sites on the forward primers and EcoRI sites on the reverse primers, and leading nucleotides to facilitate restriction digestion. The PCR amplicons were subsequently digested with *Bam*HI and *Eco*RI and ligated into pcDNA3.1+ for expression in mammalian cells.

Table 2.4 Primers used to prepare ROC1/myc and ROC2/myc expression plamids. The primers were synthesized at Invitrogen (Carlsbad, CA) and used in either QuikChange® II Site-Directed Mutagenesis (Stratagene, La Jolla, CA) or PCR to prepare ROC1/myc and ROC2/myc.

Myc/ROC2Fmut	GGAATTCGCCACCATGGAACAAAAACTCATCTCAGAAGAGGATCTGGCCG ACGTGGAAGACGG
Myc/ROC2Rmut	CCGTCTTCCACGTCGGCCAGATCCTCTTCTGAGATGAGTTTTTGTTCCATGG TGGCGAATTCC
Roc1/mycF	AAAAAAGGATCCCCAAAATGGCGGCAGCGATGGATG
Roc1/mycR	TTTTTTGAATTCTCACAGATCCTCTTCTGAGATGAGTTTTTGTTCGTGCCCA TACTTTTGGAATTCCCACTC
Roc2/mycF	AAAAAAGGATCCATGGCCGACGTGGAAGACGGAGAG
Roc2/mycR	TTTTTTGAATTCTCACAGATCCTCTTCTGAGATGAGTTTTTGTTCTTTGCCGA TTCTTTGGACCACCCAGTC

Transient transfections

HEK 293T cells were seeded in 6-well plates and grown to a confluence of at least 70%. Cells were then transfected with Lipofectamine™ and PLUS™ Reagent (Invitrogen, Carlsbad,

CA) as follows. 100 µL OPTI-MEM® I (Gibco, Invitrogen, Carlsbad CA) plus 6 µL PLUS™ Reagent were combined for each sample. Then 1 µg nBmp4/HA and 1 µg ROC1/myc, ROC2/myc, or pcDNA3.1+ was added to the diluted PLUS reagent and allowed to form complexes for 15 minutes at room temperature. Meanwhile, 100 µL OPTI-MEM® I plus 4 µL Lipofectamine™ were mixed for each sample. After the 15 minute incubation, the diluted Lipofectamine was added to the DNA/PLUS complexes and incubated for 15 minutes at room temperature. During this second incubation, 1 ml of media was removed from each well. Finally, the DNA/PLUS/Lipofectamine complexes were added dropwise to the cells and mixed gently. Transfected cells were incubated at 37°C with 5% CO_2 for 24 hours and then 1.5 ml 10% FBS media was added to the wells. Transfected cells were allowed to grow for an additional 16-24 hours before being analyzed.

Immunoprecipitation experiments and western blots

Transfected HEK 293T cells were washed once with cold 1x Dulbecco's Phosphate Buffered Saline (PBS, Gibco, Invitrogen, Carlsbad, CA). Cells were then lysed by adding 0.5 ml NP-40 lysis buffer (50 mM Tris-HCl (pH 7.5), 150 mM NaCl, 0.5% NP-40, 50 mM NaF, 1 mM Na_3VO_4, 1 mM DTT, 1x Pierce Protease Inhibitor Cocktail (Fisher Scientific, Pittsburgh, PA), and 1 mM phenylmethanesulfonyl fluoride (PMSF)) and incubating on ice for 20 minutes with occasional rocking. Cells were collected in microcentrifuge tubes then further lysed by rotating at 4°C for 10 minutes. Cell debri was pelleted at 4°C and 14,000 rpm for 10 minutes and the supernatant was transferred to a fresh tube. The protein concentration for each sample was then determined through a Bradford assay. Equal mass samples (200 µg) were prepared and incubated with 3 µL mouse anti-myc (clone 9E10, Enzo Life Sciences) overnight at 4°C. The next day, 25 µL Protein A/G PLUS-Agarose (Santa Cruz Biotechnology® Inc, Santa Cruz, CA) was added to

each sample and incubated for one hour at 4^{o}C with constant rotation. Samples were centrifuged for 2 minutes at 3000 rpm and 4^{o}C and then washed 3 times with 1 ml of cold NP-40 lysis buffer without protease inhibitors. Immunoprecipitates were resuspended in 30 µL 4x sample loading buffer and boiled for 5 minutes.

Immunoprecipitates were separated either using 16.5 % Tricine- or 10 % Tris-Glycine-SDS PAGE and then transferred to nitrocellulose membranes (Biorad, Cat. No. 162-0115, Hercules, CA). Membranes were probed with either rat anti-HA (100 µg/ml, Cat. No. 11867423001, Roche, Indianapolis, IN) or mouse anti-myc (0.7 mg/ml, Cat. No. SA-294 Enzo Life Sciences, Plymouth Meeting, PA) at a 1:2000 dilution overnight at 4^{o}C. Membranes were further probed with horseradish peroxidase (HRP) conjugated secondary antibodies (rabbit anti-mouse (Calbiochem) or goat anti-rat (Santa Cruz Biotechnology® Inc). Finally, membranes were developed using Immobilon^{TM} Western Chemiluminescent HRP Substrate (Millipore, Billerica, MA) and visualized with autoradiography using Blue Basic Autorad Film (ISC Bioexpress, Kaysville, UT).

Results

We have shown that a novel variant of Bmp4 is localized to the nuclei of cells in tissue culture. However, the function of this nuclear variant is still unknown. In order to determine the function of nBmp4, we decided to perform a yeast two-hybrid screen and then use the known functions of the identified binding partners to deduce the function of nBmp4. We prepared a cDNA library from MCF-7 breast cancer cells due to the observed abundance of Bmp4 in the nuclei of these cells. This cDNA library included approximately 4,000,000 clones. We also prepared a bait plasmid that contained the Bmp4 cDNA starting from the alternative start codon (83) fused to the C-terminus of the Gal4 DNA binding domain (Gal4BD/nBmp4). This bait was

tested for autoactivation of the reporter genes in the yeast two-hybrid assay. We found that the His reporter gene had leaky expression. Therefore, to overcome the leaky expression, QDO plates were used to screen the cDNA library for interactions with the bait protein. Gal4BD/nBmp4 was also tested for toxicity and found to be non-toxic. Once the initial testing of the bait protein was completed, a yeast two-hybrid screen was performed using the bait Gal4BD/nBmp4 and the MCF-7 cDNA library.

From the yeast two-hybrid screen, we identified 21 proteins that potentially interact with nBmp4 (Table 2.5). These results were confirmed with subsequent yeast two-hybrid assays between nBmp4 and each potential binding partner and subsequent extraction and verification of the cDNA clone through DNA sequencing. Of the identified binding partners, 2 are involved in translation, 3 are involved in ubiquitination, 3 are involved in oxidation/reduction, 4 are mitochondrial proteins involved in the electron transport chain, and 9 are involved in other processes. Additionally, 7 of the identified proteins are known to be localized to the nucleus, 3 of which are involved in ubiquitination. The two proteins that were encountered most frequently were Regulator of Cullins 1 and 2 (ROC1 and ROC2). It is interesting to note that both ROC1 and ROC2 are classified as the nuclear-localized and ubiquitination-related. ROC proteins are involved in protein degradation through their association with the SCF E3 ubiquitin ligase complex and are also involved in protecting cells from reactive oxygen species (ROS)-induced cell death. Interestingly, we also found ubiquitin in the yeast two-hybrid screen. Due to the prevalence of ubiquitination-related, nuclear-localized potential binding partners, these results suggest that nBmp4 plays a role in protein degradation through ubiquitination.

Table 2.5 Potential nBmp4 binding partners suggest a role in protein degradation, reactive oxygen species modulation, or apoptosis. A yeast two-hybrid screen was performed with a cDNA library from MCF-7 breast cancer cells. The table provides a list of potential binding proteins that have been verified through additional yeast two-hybrid assays. Interestingly, the two most frequently encountered proteins were ROC1 and ROC2, which are involved in protein degradation and protecting cells from reactive oxygen species (ROS)-induced apoptosis.[64]

Interacting Protein	Description	Occurrences
BLCAP	bladder cancer associated protein (3' UTR)	1
BLVRB	biliverdin reductase B (flavin reductase (NADPH))	2
C4orf34	chromosome 4 open reading frame 34	1
CLIC1	chloride intracellular channel 1	1
DDX5	DEAD (Asp-Glu-Ala-Asp) box polypeptide 5	2
EEF1A1	eukaryotic translation elongation factor 1 alpha 1	1
NDUFA3	NADH dehydrogenase (ubiquinone) 1 alpha subcomplex, 3, 9kDa	1
NDUFAB1	NADH dehydrogenase (ubiquinone) 1, alpha/beta subcomplex, 1, 8kDa	1
OCIAD2	OCIA domain containing 2	1
PHF20L1	PHD finger protein 20-like 1	1
PLSCR1	phospholipid scramblase 1	2
POLR2G	polymerase (RNA) II (DNA directed) polypeptide G	2
PRDX4	peroxiredoxin 4	1
RBX1	ring-box 1 (aka ROC1)	7
RNF7	ring finger protein 7 (aka ROC2 and SAG)	4
RPL11	ribosomal protein L11	1
SDHB	succinate dehydrogenase complex, subunit B, iron sulfur (Ip)	1
TXNDC17	thioredoxin domain containing 17	1
UBA52	ubiquitin A-52 residue ribosomal protein fusion product 1	1
UQCRFS1	ubiquinol-cytochrome c reductase, Rieske iron-sulfur polypeptide 1	1
ZBTB8OS	zinc finger and BTB domain containing 8 opposite strand	1

After performing the yeast two-hybrid screen and identifying ROC1 and ROC2 as important nuclear binding partners, we decided to delineate the binding domains utilized in the interactions between nBmp4 and ROC1 and ROC2. In order to determine the domains within nBmp4 that interact with ROC1 and ROC2, we sequentially deleted segments from the N- and C-termini of nBmp4 in the GAL4BD/nBmp4 expression plasmid as shown in Figure 2.2 and again in Figure 2.4. These sequential deletion constructs were analyzed in yeast two-hybrid assays by co-transforming them into yeast along with either GAL4AD/ROC1 or GAL4AD/ROC2. The transformed yeast was then plated onto low stringency plates and high

stringency plates which indicate the efficiency of co-transformation and the presence of an interaction, respectively. The strength of the interaction between the fragment of nBmp4 and either ROC1 or ROC2 was quantified by dividing the number of colonies on the high stringency plate by the number of colonies on the low stringency plate. The strength of interaction for each segment was then compared to the strength of the interaction for full length nBmp4.

The results of the sequential deletion analysis between segments of nBmp4 and full length ROC1 are shown in Figure 2.4B. We found that ROC1 interacts with the N-terminus of nBmp4 as judged by the high relative growth with constructs 6, 7, and 8 and the low relative growth with constructs 1, 2, and 3. Because the interaction was so strong between ROC1 and construct 8 of nBmp4, this suggests that the N-terminal ROC1 binding domain resides in amino acids 1-43 of nBmp4. We also found that ROC1 interacts with the C-terminus of nBmp4 due to the high relative growth when ROC1 is transformed with construct 4. This suggests a C-terminal ROC1 binding domain within amino acids 228 and 326 of nBmp4. Interestingly, the relative growth increased dramatically between constructs 3 and 4 and between constructs 5 and 6 (Figure 2.4B). In both comparisons, the fragment containing amino acids 179-227 of nBmp4 was removed. This suggests that there may be an inhibitory domain within nBmp4 that decreases the interaction between nBmp4 and ROC1 and suggests that the inhibitory domain lies between AA 179 and 227 of nBmp4. Additionally, segments of nBmp4 were prepared that correspond to the propeptide and mature peptide of secretory Bmp4. Both of these segments interacted with ROC1 as strongly as the full length nBmp4.

A similar sequential deletion analysis between fragments of nBmp4 and full length ROC2 was also conducted (see Figure 2.4C). ROC2 interacts with the C-terminus of nBmp4 (amino acids 228-326) as judged by the high relative growth with construct 4 and lower relative growth

with construct 5. The high relative growth between ROC2 and nBmp4 constructs 1, 6, and 7 but low relative growth between ROC2 and nBmp4 constructs 2, 3, and 8 suggests that there is a binding domain located between amino acids 44 and 100 of nBmp4 that interacts with ROC2. There also seems to be a domain of nBmp4 that inhibits the interaction between nBmp4 and ROC2 as judged by the increase in relative growth when amino acids 179-227 are removed (compare the relative growth between constructs 3 and 4 and constructs 5 and 6 in Figure 2.4C). These results suggest that nBmp4 interacts with ROC1 and ROC2 in a similar but not identical manner.

(A)

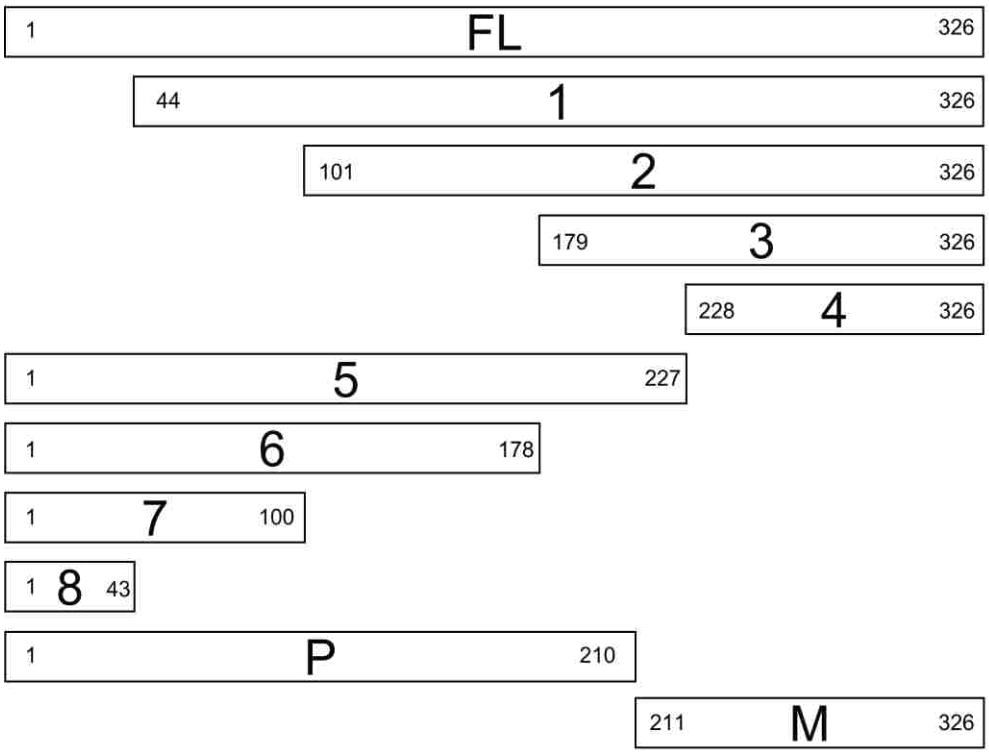

(B)

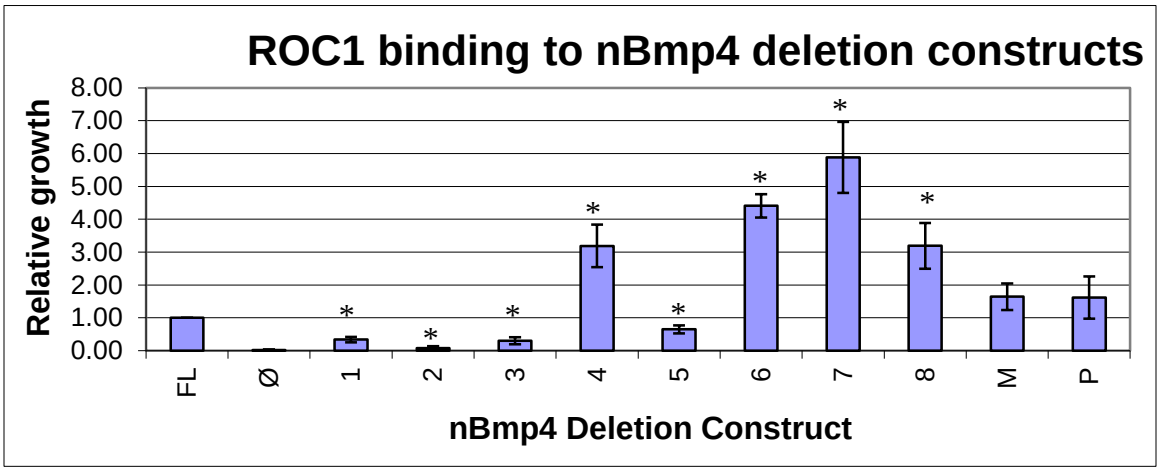

(C)

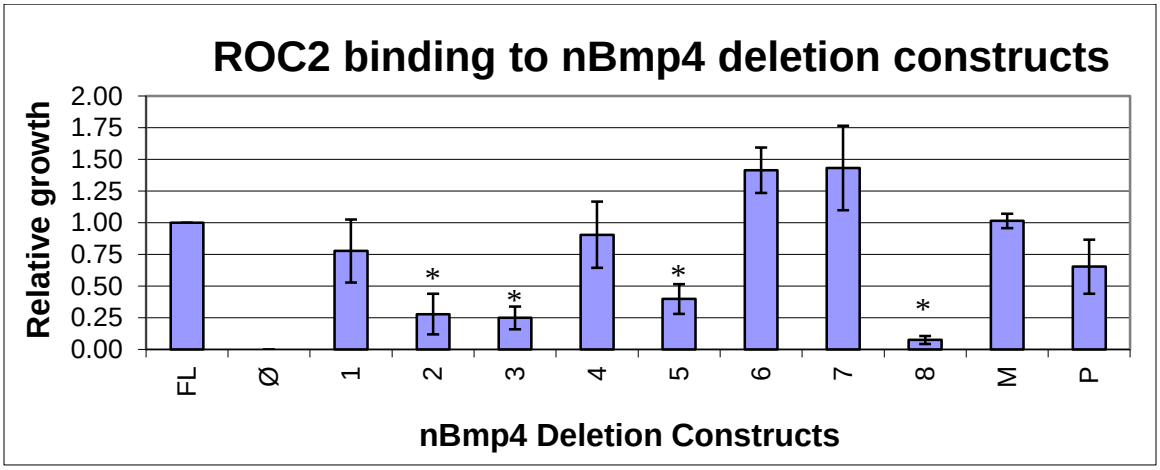

Figure 2.4. nBmp4 interacts with ROC1 and ROC2 through two binding domains and an inhibitory domain. (A) nBmp4 sequential deletion constructs. Segments of the GAL4BD/nBmp4 cDNA expression plasmid were sequentially deleted from the N- and C-termini as shown in order to delineate the domains within nBmp4 that interact with ROC1 and ROC2. Note that the amino acids are numbered starting with the alternative start site as number 1. **(B,C)** Sequential deletion constructs of nBmp4 were used in yeast two-hybrid assays to determine the domains within nBmp4 that interact with ROC1 and ROC2. Note that the ROC1 construct used was an alternative transcript missing exon 4 which results in a partial RING finger and a short alternative C-terminus. GAL4BD/nBmp4 sequential deletion constructs were co-transformed into yeast with GAL4AD/ROC1 or GAL4AD/ROC2. The strength of the interaction between the two proteins was measured by dividing the number of colonies on the high stringency plate by the number of colonies on the low stringency plate. The strength of the interaction for each fragment was then compared to the strength of the interaction for full length nBmp4 to yield a fold difference. **(B)** nBmp4 interacts with ROC1 through an N-terminal binding domain within AA 1-43, a C-terminal binding domain within AA 228-326, and an inhibitory domain between AA 179 and 227. **(C)** nBmp4 interacts with ROC2 through two binding domains: one within AA 44-100 and another within AA 228-326. There is also a domain within AA 179 and 227 of nBmp4 that inhibits the interaction between nbmp4 and ROC2. * : p-value ≤ 0.05.

A second similar question regards the binding domains within ROC1 and ROC2 that interact with nBmp4. It has been shown that the N-terminus of ROC1 interacts with the C-terminus of Cullin 1, while the C-terminal RING domain of ROC1 is sufficient to activate an E2 enzyme.[65] Therefore, in an effort to delineate the functional relationship between nBmp4 and ROC1 or ROC2, we decided to analyze whether nBmp4 interacts with the N-terminal, RING finger, and/or C-terminal domains of ROC1 and ROC2. It is important to note that the ROC1 cDNA clone retrieved from the yeast two-hybrid screen is a transcript variant that is missing exon 4 and results in a truncated RING finger domain and alternative C-terminus. The ROC2 cDNA that was recovered from the MCF-7 cDNA library was the normal ROC2 isoform 1.

Figure 2.5A diagrams the deletion constructs that were prepared from the ROC1 and ROC2 cDNA expression plasmids. These constructs were examined through yeast two-hybrid assays in a manner similar to the nBmp4 sequential deletion analysis experiment. Specifically, ROC1 or ROC2 deletion plasmids were co-transformed into yeast along with full length nBmp4. The transformed yeast was plated onto low stringency and high stringency plates and subsequently scored for growth. As shown in Figure 2.5B, the only ROC1 construct that had a considerable interaction with nBmp4 was the N-terminus. This finding suggests that nBmp4 binds to ROC1 through the same domain that ROC1 binds to the Cullin proteins.

The interactions between the ROC2 deletion constructs and nBmp4 are much more complicated. It was determined that the N-terminus combined with the RING finger interacts moderately with nBmp4 and that the RING finger combined with the C-terminus interacts weakly with nBmp4 (Figure 2.5C). However, nBmp4 did not interact significantly with the isolated N-terminus, RING finger, or C-terminus. This result may suggest that the RING finger is the domain utilized in the interaction, but that the RING finger needs to be combined with

other domains to be functional. Alternatively, this result could indicate that the deletion fragments did not fold properly as they would in the context of the intact protein. These results along with the results from the ROC1 sequential deletion analysis are currently being verified through co-immunoprecipitation experiments using similar constructs.

(A)

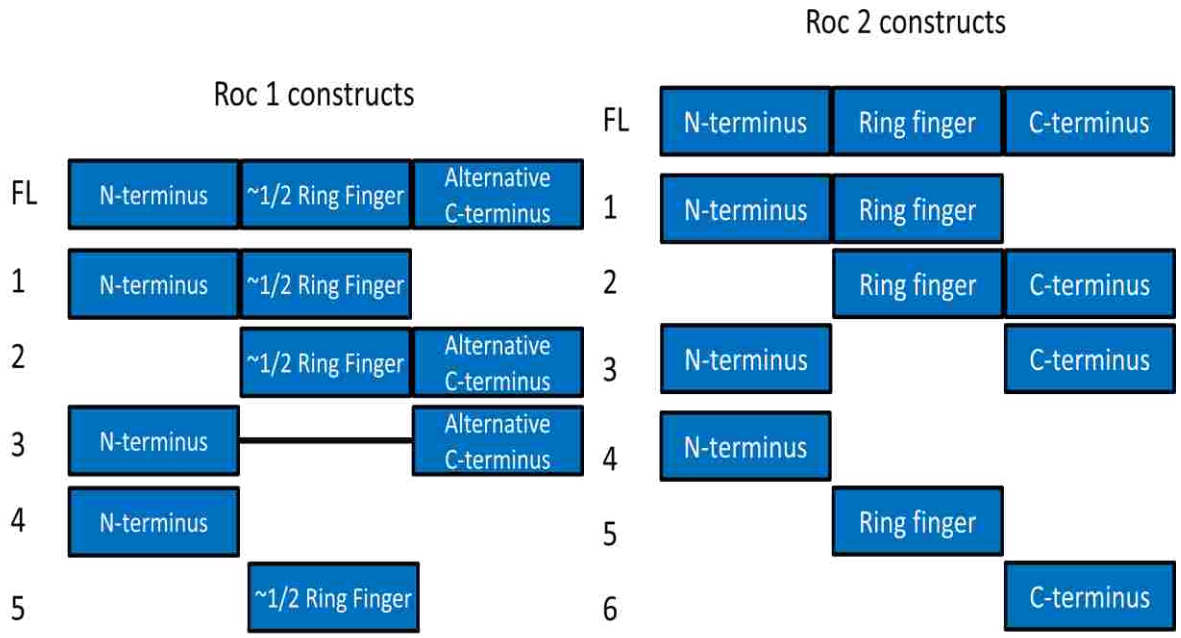

Figure 2.5 ROC1 interacts with nBmp4 through its N-terminal domain and ROC2 interacts with nBmp4 through its RING finger. (A). Deletion constructs of ROC1 and ROC2 were prepared to separate the N-terminus, RING finger, and C-terminus of each protein. As noted earlier, the ROC1 cDNA recovered from the yeast two-hybrid screen is a transcript variant missing exon 4 that results in a partial RING finger and a short alternative C-terminus. **(B,C)** The deletion constructs were used in yeast two-hybrid assays to determine the domains within ROC1 and ROC2 that interact with nBmp4. Full length GAL4BD/nBmp4 was co-transformed separately into yeast with each of the GAL4AD/ROC1 and GAL4AD/ROC2 deletion constructs. The strength of the interaction between the two proteins was measured by dividing the number of colonies on the high stringency plate by the number of colonies on the low stringency plate. The strength of the interaction was then compared to the strength of the interaction for full length ROC1 or ROC2 to yield relative growth. All constructs tested had p-values of < 0.05.

(B)

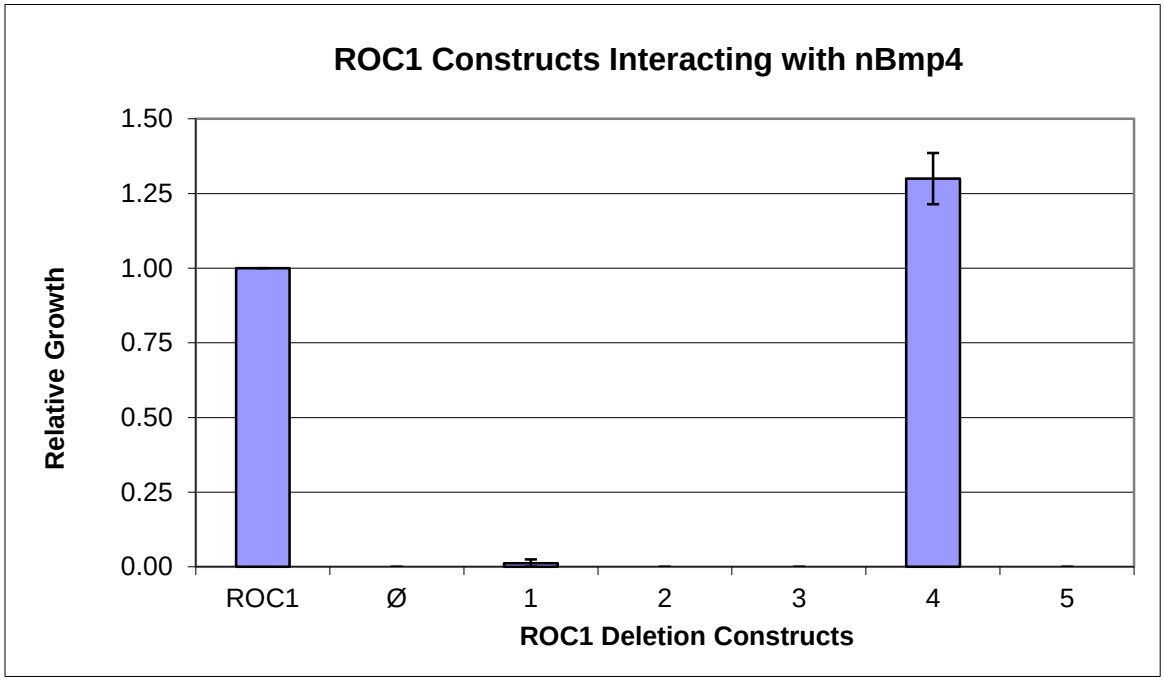
ROC1 Constructs Interacting with nBmp4
Relative Growth
1.50
1.25
1.00
0.75
0.50
0.25
0.00
ROC1
Ø
1
2
3
4
5
ROC1 Deletion Constructs

(C)

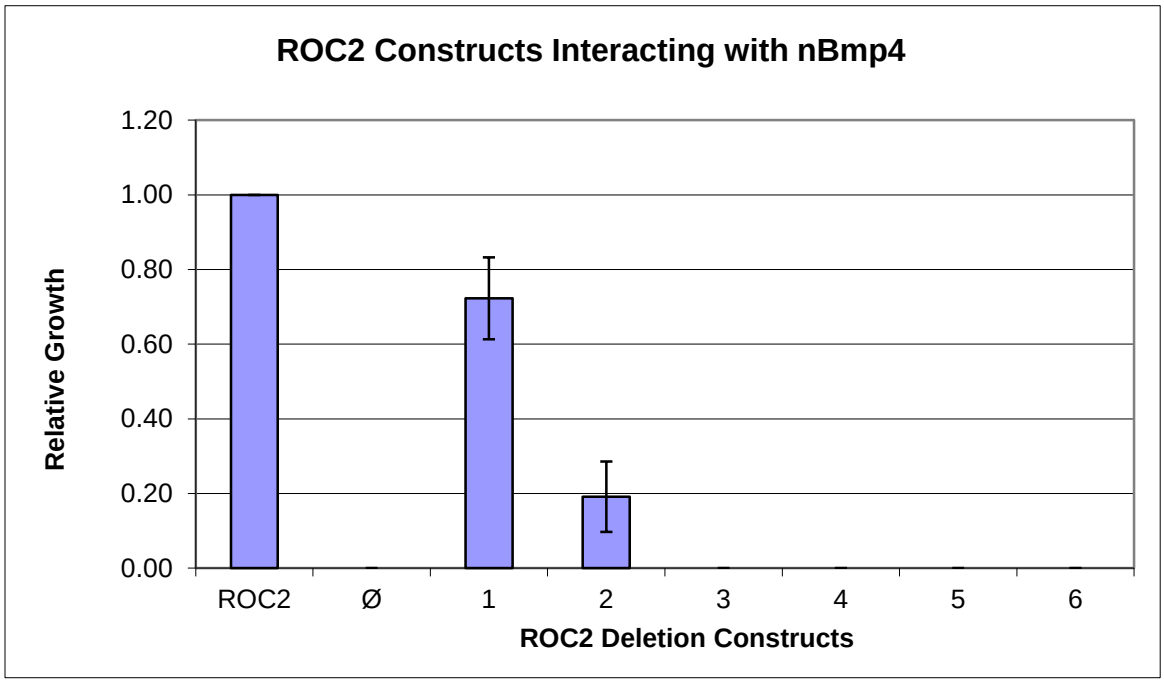
ROC2 Constructs Interacting with nBmp4
Relative Growth
1.20
1.00
0.80
0.60
0.40
0.20
0.00
ROC2
Ø
1
2
3
4
5
6
ROC2 Deletion Constructs

Because ubiquitin is part of the protein degradation pathway and was identified in the yeast two-hybrid screen, it was similarly analyzed in yeast two-hybrid assays to determine the domain within nBmp4 that interacts with ubiquitin. As described above, sequential deletion constructs of nBmp4 (pictured again in Figure 2.6) were co-transformed into yeast along with UBA52, one of the precursor forms of ubiquitin that codes for ubiquitin fused to ribosomal protein L40. It is noteworthy to mention that the UBA52 construct retrieved from the yeast two-hybrid screen was a partial clone that was missing the first 24 amino acids of the 76-amino acid ubiquitin. As shown in Figure 2.6, UBA52 interacts with the N-terminus of nBmp4 (between AA 1 and 43 of nBmp4) as judged by the low relative growth when the N-terminus is deleted (constructs 1 and 2) and the high relative growth when only the N-terminus is present (constructs 7 and 8). UBA52 also interacts with the C-terminal end of nBmp4 between AA 228 and 326, as shown by the high relative growth when only the C-terminus is present (constructs 3 and 4) and the low relative growth when the C-terminus is deleted (constructs 5 and 6). There may also be an inhibitory domain between AA 101 and 179 of nBmp4 as judged by the increase in relative growth when this region is deleted (compare constructs 2 vs. 3 and 6 vs. 7).

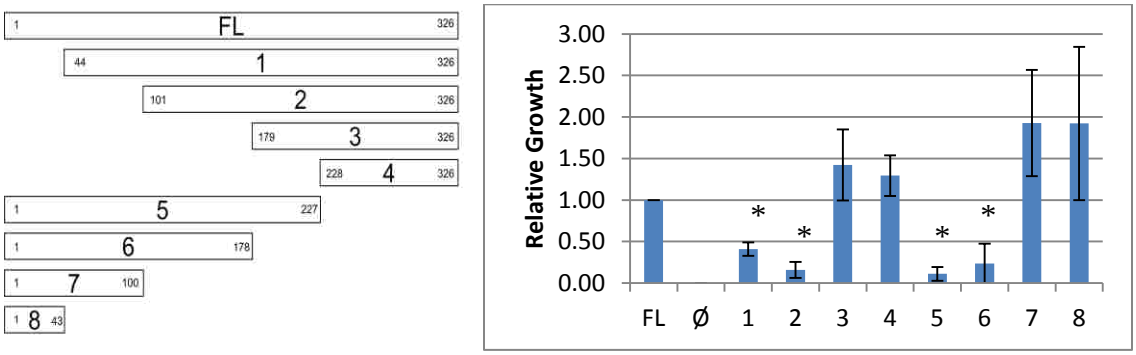

Figure 2.6 nBmp4 interacts with UBA52 through N- and C-terminal binding domains. Sequential deletion constructs of nBmp4 (as shown) were used in yeast two-hybrid assays to determine the domains within nBmp4 that interact with UBA52. GAL4BD/nBmp4 sequential deletion constructs were co-transformed into yeast with a partial GAL4AD/UBA52 construct that contains all but the first 24 AA. The strength of the interaction between the two proteins was measured by dividing the number of colonies on the high stringency plate by the number of colonies on the low stringency plate. The strength of the interaction was then compared to the strength of the interaction for full length nBmp4 to yield relative growth. * : p-value ≤ 0.05.

In an effort to verify the yeast two-hybrid result that nBmp4 interacts with ROC1 and ROC2, co-immunoprecipiation experiments were performed. nBmp4/HA was transiently co-transfected into HEK 293T cells along with pcDNA3.1+, ROC1/myc, or ROC2/myc. After 48 hours, cells were harvested and the lysates were immunoprecipitated with an anti-myc antibody and subsequently western blotted with an anti-HA antibody. As shown in Figure 2.7, nBmp4 does in fact interact with ROC1 and ROC2.

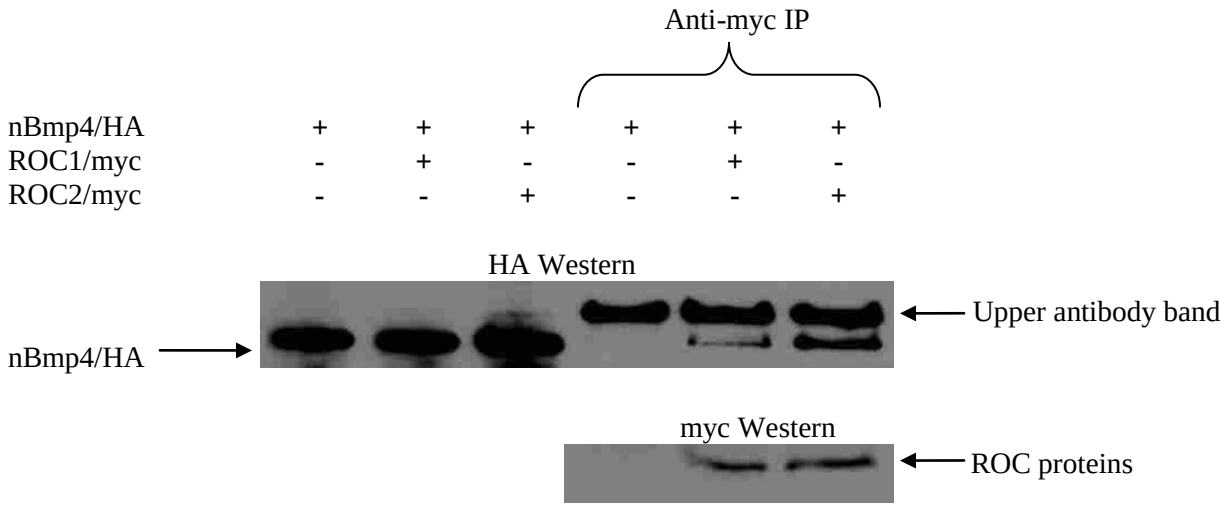

Figure 2.7 nBmp4 interacts with ROC1 and ROC2. HEK 293T cells were transiently co-transfected with nBmp4/HA and either pcDNA3.1+, ROC1/myc, or ROC2/myc. After 40-48 hours, cells were lysed and equal amounts of lysates were immunoprecipitated with an anti-myc antibody. Immunoprecipitates were subsequently immunoblotted with either an anti-HA antibody or an anti-myc antibody.

Discussion

Nuclear variants of BMPs have been identified in tissue culture and have been characterized to arise from translation at alternative start codons which allows a bipartite nuclear localization signals to direct translocation of the nuclear BMPs to the nucleus. The function of these variants is currently undergoing intense research. In an effort to determine the function of the nuclear variant of Bmp4, a yeast two-hybrid screen was performed using a cDNA library derived from MCF-7 breast cancer cells. Of the 21 identified binding partners, 7 are known to be

localized to the nucleus. Because we are studying a nuclear protein, we decided to analyze these proteins further. Of the potential binding partners that are known to be localized to the nucleus, 3 are involved in ubiquitination. The identified proteins that were categorized as nuclear localized and involved in ubiquitination were Regulator of Cullins 1 and 2 (ROC1 and ROC2) and ubiquitin itself. It is also important to note that ROC1 and ROC2 were the two most frequently encountered clones from the yeast two-hybrid screen. From this analysis of the results of the yeast two-hybrid screen, we hypothesize that nBmp4 is involved in ubiquitination in the nucleus.

In order to further characterize the binding domains within nBmp4 that interact with ROC1, and ROC2, we performed sequential deletion analyses in which segments of the N-terminus and C-terminus were sequentially removed and the strength of the interaction between the remaining nBmp4 fragment and ROC1 or ROC2 was quantified. From this analysis, we found that there are two domains within nBmp4 that interact with ROC1 and ROC2, namely one N-terminal binding domain (within the first 43 amino acids for ROC1 and between amino acids 44 and 100 for ROC2) of nBmp4 and one C-terminal binding domain within amino acids 228 and 326 of nBmp4. We also did the complementary experiment in which the domains of ROC1 and ROC2 were sequentially deleted and the strength of the interactions between the ROC fragments and nBmp4 were quantified. The results of these experiments suggest that nBmp4 interacts with the N-terminus of ROC1 and with the RING finger of ROC2. It is known that ROC1 interacts with Cullin1 through its N-terminus.[65] Therefore, the interaction of nBmp4 with the N-terminus of ROC1 suggests that nBmp4 may be binding in a similar manner and may inhibit the binding of Cullin1 to ROC1. Similarly, the RING finger of ROC2 interacts with the E2 enzyme that transports ubiquitin to the E3 ubiquitin ligase and promotes ubiquitination of the target protein.[65] The interaction of nBmp4 with the RING finger domain of ROC2 suggests that

nBmp4 may be binding in a similar manner and may inhibit the ability of the E2 enzyme to interact with ROC2.

The interacting domains within the ROC proteins suggest that nBmp4 may either be interfering with the ability of the SCF E3 ligase to form a complex and function properly or may function as a part of the ubiquitin ligase complex. It is important to note that it is still uncertain whether all of the protein fragments folded correctly during the sequential deletion analyses. Additionally, the identification of different nBmp4 binding domains within ROC1 and ROC2 could be due to the fact that the cDNA construct of ROC1 from the yeast two-hybrid screen was a partial cDNA. Therefore, the ROC sequential deletion analyses are currently being verified in cells through transfection and co-immunoprecipitation experiments to confirm the domains within the ROC proteins that interact with nBmp4.

As previously described, putative interactions identified through the yeast two-hybrid technique must be validated through other techniques including co-immunoprecipitation in cells. Accordingly, we performed co-immunoprecipiation experiments and verified the interaction between full length nBmp4 and both full length ROC proteins.

In conclusion, nBmp4 binding partners have been identified that suggest a function for nBmp4 in the ubiquitination pathway. The interactions between nBmp4 and the ROC proteins suggest that nBmp4 interacts with the SCF E3 ubiquitin ligase complex and either increases or decreases the activity of the complex. Further experiments will explore the functional relationship between nBmp4 and the ubiquitination pathway.

Chapter 3: nBmp4 interacts with SCF E3 ubiquitin ligase components and affects the cell cycle

Summary

We have previously verified the interaction between nBmp4 and ROC proteins. However, it is uncertain whether nBmp4 interacts with other proteins that function in conjunction with the ROC proteins. Due to the role that ROC proteins play as components of the SCF E3 ubiquitin ligase, we decided to analyze the interactions between nBmp4 and the other subunits of the SCF E3 ubiquitin ligase complexes. The results of this chapter show that nBmp4 interacts with five different Cullin proteins and two different F-box proteins. These interactions suggest that nBmp4 may play a role in cell cycle regulation through its association with the E3 ligase complex. Indeed, we further show that nBmp4 does in fact affect the cell cycle. Finally, we show that nBmp4 is actively poly-ubiquitinated. Overall, the results of this chapter suggest that nBmp4 plays a role in cell cycle regulation through its association with SCF E3 ubiquitin ligase components in the nucleus.

Introduction

Two of the verified nBmp4 binding partners are regulator of cullins 1 and 2 (ROC1 and ROC2), which are members of the RING Finger gene family.[64] ROC1 and ROC2 are expressed ubiquitously in the heart, skeletal muscles, and testis.[64] ROC2 is localized to the cytoplasm and to the nucleus.[66, 67] The ROC proteins have two very interesting functions: they play a role in protein degradation and they play a role in protecting cells from ROS-induced apoptosis.[64] ROC1 and ROC2 are involved in protein degradation due to their E3 ubiquitin ligase activity[68, 69].

The ubiquitin-proteasome system is vital in virtually all biological processes.[70] The degradation of proteins through this system involves two important steps: first, the successive

attachment of a chain of ubiquitin tags and second, the degradation of the protein by the 26S proteasome.[71, 72] The reaction entailing the attachment of a chain of ubiquitin proteins onto a substrate protein is performed via an organized pathway that involves three types of enzymes: ubiquitin activating (E1), ubiquitin conjugating (E2), and ubiquitin ligase (E3) enzymes.[72] First, an E1 enzyme activates ubiquitin, a conserved 76 amino acid protein that is derived from the UBA52, UBB, or UBC genes, by binding to it through a high-energy thiolester bond.[72] The activated ubiquitin is then transferred to one of the more than twenty identified E2 ubiquitin-conjugating enzymes.[73] Finally, E3 ubiquitin ligases, which interact with both the E2 enzymes and the target proteins, bring activated ubiquitin into close proximity with the target protein and mediate ligation of ubiquitin to the target protein[64]. The ubiquitin moiety is linked to the target protein through an isopeptide bond between the C-terminal glycine in ubiquitin and a lysine residue in the target protein.[72] The process of attaching ubiquitin moieties is repeated several times by linking a new ubiquitin moiety onto the previously bound ubiqutitin to create a polyubiquitin chain. The polyubiquitinated protein is then recognized by the 26S proteasome and degraded.

There are two major types of E3 ubiquitin ligases: HECT domain and RING finger domain containing ligases. One major difference between the two ligases is that HECT domain E3 ligases bind directly to the ubiquitin while RING finger E3 ligases use their zinc-binding domains to recruit E2 enzymes and direct the E2 enzymes to the target substrate without ever binding directly to the ubiquitin.[72] As mentioned in chapter 1, HECT domain E3 ligases Smurf1 and Smurf2 are involved in the degradation of Smad proteins.

A well studied RING finger E3 ubiquitin ligase family is the SCF (Skp1/Cullin/F-box) E3 ubiquitin ligase family, in which ROC proteins bind between the Cullin and the E2 enzyme

and are essential for ligase function. SCF E3 ubiquitin ligases function in signal transduction as well as regulating G1 cell cycle control.[65, 68, 74-76] SCF E3 ubiquitin ligases are comprised of 4 main subunits: ROC, Cullin, Skp1, and F-box proteins. Although there are many different SCF complexes, the arrangement between subunits is conserved. ROC proteins interact through their RING fingers to E2 enzymes and through their N-terminal ends to the C-terminal end of Cullin proteins.[65, 68, 77] Cullins, in turn, bind through their N-termini to Skp1 or other adapter proteins.[77] Skp1 then associates with the F-box motif within F-box proteins.[78] Finally, the F-box proteins recruit the substrates through specific protein-protein interaction domains, including WD-40 repeats or leucine-rich repeats.[78] β-TrCP is a well studied F-box protein with WD-40 repeats and Skp2 is a well studied F-box containing leucine-rich repeats. Because F-box proteins contain protein-protein interaction domains that are specific for the substrate, F-box proteins are vitally important in the recognition and specificity of the SCF complex. The SCF complex assembly is depicted in Figure 3.1. There are hundreds of E3 ubiquitin ligase complexes due to multiple Cullin, Skp1, F-box, and ROC family members interacting in various combinations which allows for specificity in target protein degradation.[72]

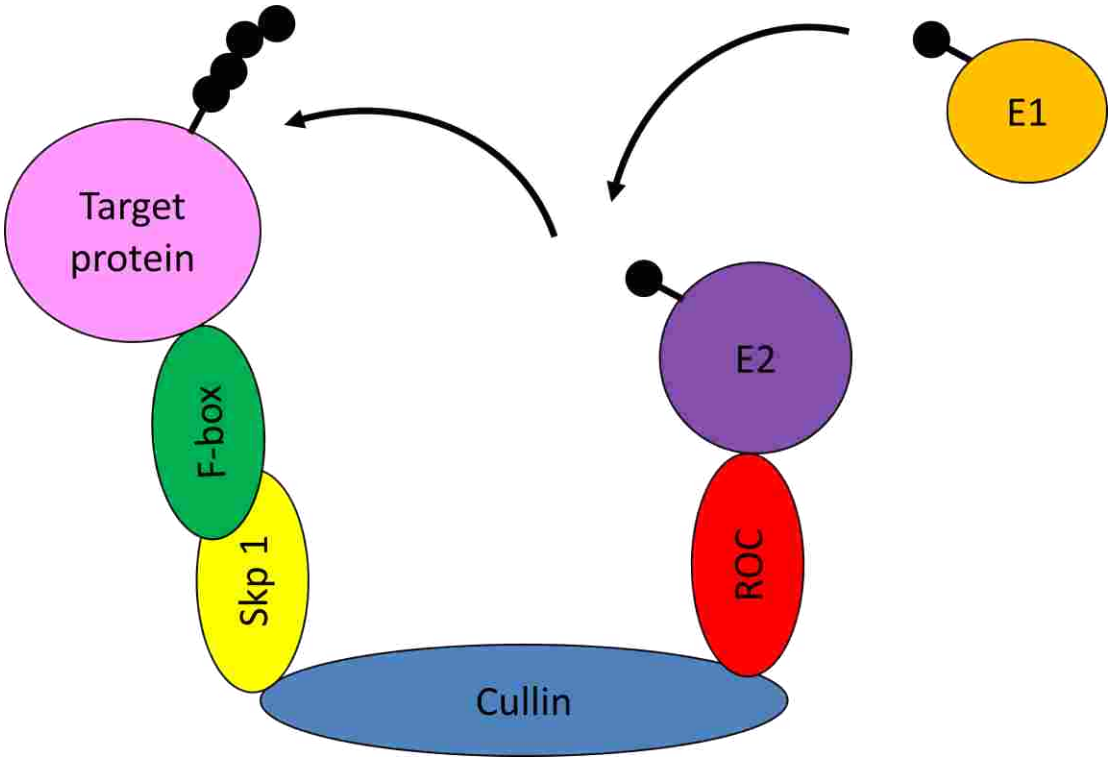

Figure 3.1 Schematic representation of SCF E3 ubiquitin ligase. The SCF ubiquitin ligase is comprised of 4 main proteins: Skp1, Cullin, F-box, and ROC proteins. In the process of ubiquitination, an E1 ubiquitin activating enzyme transfers ubiquitin to an E2 enzyme. The E2 associates with the SCF E3 ubiquitin ligase complex, which allows the target protein to come in close proximity with the E2 enzyme. The ubiquitin is then transferred to the target protein. This process happens several times in order to yield a poly-ubiquitinated target protein. The poly-ubiquitinated protein is then degraded by the 26S proteasome.

A well known example of an SCF E3 ubiquitin ligase is $SCF^{\beta\text{-}TrCP}$ (where the F-box protein is written in the superscript) which targets IκBα, Smad3, Smad4.[79-82] Another well known E3 ligase is SCF^{Skp2}. SCF^{Skp2} plays an important role in cell cycle control by targeting the CDK inhibitors p27, $p21^{Cip1}$, $p57^{Kip2}$, the tumor suppressor p130, the transcription factor E2F-1 that drives gene expression at the G1/S transition,[83] and Myc for degradation.[72] SCF^{Skp2} also targets hOrc1, a protein involved in the origin recognition complex, for degradation which keeps DNA replication to once per cell cycle.[84] Finally, a third well known SCF complex, SCF^{Fbw7}, degrades targets such as cyclin E, Notch, and Myc.[72] There are also other RING finger ligases such as EC_2S^{VHL}, and BC_3B^{MEL26} that contain Cullin 2 and Cullin 3 and target HIF-1α and MEI-

1, respectively. Additionally, there is an E3 ubiquitin ligase comprised of DDB1-CUL4A-ROC1 that targets CDT1 for ubiquitination in response to DNA damage.[85] Clearly, SCF ubiquitin ligases are involved in a plethora of cellular events.

ROC1 and ROC2 are imperative to the functionality of the SCF complex due to their role in linking the E2 ubiquitin conjugating enzyme to the E3 ubiquitin ligase that is holstering the target protein (see Figure 3.1). ROC1 was discovered as a component of E3 ubiquitin ligases while ROC2 was initially discovered as a gene that was sensitive to apoptosis.[66, 68, 75, 76, 86] There are two basic domains in ROC proteins: the N-terminal domain and the RING finger. The RING finger of ROC1 is required for ubiquitin ligation activity.[87] ROC proteins interact with Cullins through their N-termini.[65] ROC1 interacts similarly with Cul1, Cul2, Cul3, Cul4A, and Cul5 while ROC2 binds preferentially to Cul5, moderately with Cul1 and Cul2, and minimally with Cul3 and Cul4A.[65, 88] Therefore, ROC1 and ROC2 can be used by the cell in many different SCF ubiquitin ligase complexes.

Both ROC1 and ROC2 are zinc RING finger proteins that bind to two atoms of zinc in a cross-braced structure.[64] ROC proteins are evolutionarily conserved and are expressed in similar patterns throughout human tissues, with their highest expression in the heart, skeletal muscle, and testis.[64, 66, 69] ROC proteins are highly involved in cell proliferation and cell death. ROC1 is an essential gene in mouse embryogenesis, the targeted loss of which results in embryonic lethality at embryonic day 7.5.[89] This lethality is caused by an accumulation of p27, reduced proliferation, and "prolonged G1 arrest".[89] Interestingly, the removal of ROC1 through siRNA also leads to cell death, but through a different pathway. This cell death is triggered by the induction of G2-M arrest, followed by senescence and apoptosis. These, in turn, were triggered by the accumulation of 14-3-3σ and the reduction of Bcl-2, Mcl-1 and survivin.[89] Inactivation of

ROC1 also results in cell cycle arrest at G1/S due to the stabilization of SCF^{Cdc4} substrates Sic1 (p27) and Cln2 (cyclin).[76]

ROC2 is also involved in cell proliferation and cell death. ROC2 induces cell proliferation under serum starvation, which appears to be associated with ROC2's role in promoting p27 degradation.[90] Alternatively, the removal of ROC2 from yeast results in cell death that was accompanied by cell enlargement.[64, 88] The enlargement was due to an induction of G1/S and G2/M checkpoint control genes, indicating that ROC2 is involved in control of cell cycle progression.

As mentioned earlier, ROC1 and ROC2 protect cells from reactive oxygen species (ROS)-induced apoptosis.[64, 91] This protection against apoptosis has been linked to two different processes. In one pathway, ROC2 is able to protect cells from ROS-induced apoptosis due to its radical scavenging activity.[88, 92] However, another mechanism by which the ROC proteins protect cells against apoptosis is through their role in the $SCF^{\beta\text{-}TrCP}$ complex targeting pro-capase-3 for degradation.[93] Because ROC proteins promote the degradation of pro-caspase-3, they reduce its basal level thereby decreasing the availability of this important protein in the caspase cascade.[93]

There are at least 8 known mammalian Cullin proteins: CUL1, CUL2, CUL3, CUL4A, CUL4B, CUL5, CUL7, and CUL9. Interestingly, CUL1, mCUL2, CUL4A and CUL5 have been found to be predominantly localized to the nucleus.[94] The nuclear localization of CUL1 is facilitated by its interaction with ROC1 and leads to the modification of CUL1 by Nedd8 which resides mainly in the nucleus.[94, 95] The conjugation of Nedd8 to CUL1 is required for efficient ubiquitin ligase activity of the CUL1-ROC1 complex.

The different Cullin proteins assemble in diverse complexes to promote degradation of different protein substrates. For instance, CUL2 along with Elongins B and C (instead of Skp1) and Roc1 interact with mammalian mediator subunit mMED8 to form a functional ubiquitin ligase, which suggests a recruitment of ubiquitin ligase complexes to the transcription machinery.[96] Another SCF complex is comprised of the *Arabidopsis thaliana* protein AtDET1 along with DDB1, CUL4A, and ROC1 to promote the ubiquitination of c-Jun.[97] The CUL4-DDB-ROC1 complex is also involved in ubiquitinating histones H3 and H4, which facilitates the recruitment of DNA repair proteins to areas of DNA damage.[98]

Skp1 is an important adaptor protein that links the Cullin subunit to the different F-box proteins. As mentioned above, Skp1 interacts with F-box proteins through their F-box domains. Skp1 is essential for both G1/S and G2/M phase transitions.[78] There are also other adaptor proteins involved in SCF E3 ubiquitin ligases. For instance, Elongins B and C can interact with Cullin 2 to form a functional E3 ubiquitin ligase and DDB1 can interact with Cul4A.

As mentioned above, F-box proteins provide specificity in target protein recognition. Through specific protein-protein interactions, the F-box proteins allow the SCF E3 ligases to regulate different cellular process. For example, there are three F-box proteins that are important in cell cycle regulation, namely Skp2, β-TrCP, and Fbw7.[99] Skp2 is involved in the cell cycle through its well known role in degrading p27. β-TrCP is also highly involved in regulating the cell cycle, in part by regulating the abundance of Cdc25A, which activates cyclin dependent kinases.[100] Fbw7 is involved in cell cycle control due to its role in ubiquitinating Cyclin E.[101] Notably, Fbw7 isoforms α and γ were found to be localized to the nucleus.[102] It is interesting to note that SCF^{Skp2} complexes mediate negative regulators of the cell cycle (i.e. p27, p21, p57, and p130) while SCF^{Fbw7} complexes mediate the degradation of positive cell cycle regulators (i.e.

Cyclin E, c-Jun, and c-myc).[103] As discussed by Onoyama et al., when cells are reentering the cell cycle, they degrade the negative cell cycle regulators through SCF^{Skp2}-dependent degradation.[103]

p27 plays an important role in regulation of the cell cycle. The degradation of p27 is vital for entry into the S-phase.[72] p27 inhibits the cell cycle by inhibiting cyclinA-Cdk2 and cyclinE-Cdk2, both of which are complexes needed for cell cycle progression into the S phase.[104] p27 is normally localized to the nucleus and is activated by anti-mitogenic signals.[105] However, following growth signals, p27 is degraded[106-108], the bulk of which is degraded in the nucleus.[109] p27 has been shown to be degraded by an SCF E3 ubiquitin ligase including Roc2 and Skp2, and also by the RING-H2-type ubiquitin ligase Pirh2.[110, 111] Roc1 has also been found to be important in the degradation of p27.[89] Because Roc1 and Roc2 are involved in the degradation of p27, the loss of Roc proteins leads to an accumulation of p27 and a decrease in cell proliferation. Interestingly, there are conflicting results as to whether the major role of the SCF^{Skp2} ligase in promoting the degradation of p27 occurs during the G1/S transition or during the G2/M transition. Two different reports indicate that Skp2 expression is upregulated and peaks during the S phase of the cell cycle.[112, 113]

The activity of SCF ligases is subject to regulatory events. SCF complexes are positively regulated by the addition of Nedd8 to the Cullin subunit. When Nedd8 is conjugated to Cul1, the ability of the Cul1-ROC1 complex to promote ubiquitination is increased.[77] Additionally, SCF complexes are negatively regulated by Cand1. Cand1 binds to un-neddylated Cullin1-Roc1 complexes and inhibits their association with Skp1.[72] However, when Cullin1 is bound to Nedd8, the Skp1-Cullin1-Roc1 complex is stabilized.[114] Additionally, ROC1, ROC2, and Skp2 have

been found to be degraded in ubiquitin-proteasome dependent manners.[67, 113, 115] All of these events can be used to regulate the activity of SCF E3 ubiquitin ligases.

Clearly, SCF E3 ubiquitin ligase complexes play an important role in maintaining cellular homeostasis. Additionally, the presence of ROC proteins and Cullins in the nucleus suggests that nBmp4 may interact with these proteins therein. Therefore, the interaction between nBmp4 and ROC proteins is important and suggests that nBmp4 may also play a role in protein degradation and cell cycle control.

Experimental Procedures

Cell culture

HEK 293T cells were cultured in a 50:50 mix of Dulbecco's Modified Eagle Medium and F-12 (HyClone) supplemented with 10% FBS. Cells were subcultured regularly, but not used after passage 25.

Plasmid constructs

The five myc/Cullin constructs, namely pcDNA3-Myc3-hCul1, pcDNA3-myc3-Cul2, pcDNA3-Myc-hCul3, pcDNA3-myc3-hCul4A, and pcDNA3-Myc-hCul5, along with pcDNA3-Myc3-ROC1 and pcDNA3-HA-hCul1 were generously provided by Dr. Yue Xiong at the University of North Carolina (Chapel Hill, NC). The plasmids Flag-β-TrCP1 and Skp1/HA were generously provided by Dr. Yi Sun at the University of Michigan (Ann Arbor, MI). The Flag-ubiquitin plasmid was generously provided by Dr. Yoko Kimura at the Tokyo Metropolitan Institute of Medical Science (Tokyo, Japan).

The nBmp4/HA expression plasmid was previously described. nBmp4/myc was prepared by adding a C-terminal myc tag in place of the C-terminal HA tag from the nBmp4/HA

expression plasmid. The first two primers in Table 3.1 were used in QuikChange II Site-Directed Mutagenesis Kit (Stratagene, La Jolla, CA) according to the manufacturer's protocol. First, one myc tag was added. Later, the QuikChange II Site-Directed Mutagenesis Kit (Stratagene, La Jolla, CA) was used again with the 3rd and 4th primers in Table 3.1 to insert 4 more myc tags for better identification of the fusion protein using anti-myc antibodies.

Table 3.1 Primers used to prepare nBmp4/myc. The primers were synthesized at Invitrogen (Carlsbad, CA). The first two primers were used in QuikChange II Site-Directed Mutagenesis Kit (Stratagene, La Jolla, CA) according to the manufacturer's protocol to insert the primary myc tag in place of the HA tag in the nBmp4/HA expression plasmid. Later, QuikChange II Site-Directed Mutagenesis Kit (Stratagene, La Jolla, CA) was used again with the last two primers to insert 4 more myc tags in tandem.

FmycinsertCterm	GGTGTGGATGCCGCGAACAAAAACTCATCTCAGAAGAGGATCTGT GAGATCAGGCAGTCC
RmycinsertCterm	GGACTGCCTGATCTCACAGATCCTCTTCTGAGATGAGTTTTTGTTCG CGGCATCCACACC
FBmp4doublemycCt	GGTGTGGATGCCGCGAACAAAAACTCATCTCAGAAGAGGATCTGG AACAAAAACTCATCTCAG
RBmp4doublemycCt	CTGAGATGAGTTTTTGTTCCAGATCCTCTTCTGAGATGAGTTTTTGT TCGCGGCATCCACACC

The myc/Skp2 expression plasmid was prepared by PCR amplifying the Skp2 variant 1 from mRNA extracted from MCF-7 cells using the following primers: 5' ACCATGGAACAAAAACTCATCTCAGAAGAGGATCTGATGCACAGGAAGCACCTCCA GGAG 3' and 5' AAAGAAGAGACACCATCCTGCAATAAATACTTCA 3'. The PCR amplicon was subcloned into pcDNA3.1+.

The nBmp4-IRES-GFP and IRES-GFP fragments were subcloned from pBigT-nBmp4-IRES-GFP and pBigT-IresGFP, respectively, into pcDNA3.1+ using NotI and NheI. All expression plasmids were verified by DNA sequencing at the BYU Sequencing Center.

Transient transfections

HEK 293T cells were seeded in 6-well plates and grown to a confluence of at least 70%. Cells were then transfected with Lipofectamine™ and PLUS™ Reagent (Invitrogen, Carlsbad,

CA) as follows. 100 µL OPTI-MEM® I (Gibco) plus 6 µL PLUS™ Reagent were combined for each sample. Then 1 µg of each plasmid DNA (as dictated by the experiment, except 0.5 µg of each plasmid was used in the competitive binding experiment) was added to the diluted PLUS reagent and allowed to form complexes for 15 minutes at room temperature. Meanwhile, 100 µL OPTI-MEM® I plus 4 µL Lipofectamine™ were mixed for each sample. After the incubation, diluted Lipofectamine was added to the DNA/PLUS complexes and incubated for 15 minutes at room temperature. During this incubation, 1 ml of media was removed from each well to leave approximately 1 ml media. Finally, the DNA/PLUS/Lipofectamine complexes were added dropwise to the cells and mixed gently. Transfected cells were incubated at 37°C with 5% CO_2 for 24 hours and then 1.5 ml 10% FBS media was added to the wells. Transfected cells were allowed to grow for a total of 40-48 hours before being analyzed.

Immunoprecipitation experiments

Transfected HEK 293T cells were washed once with cold 1x Dulbecco's Phosphate Buffered Saline (PBS, Gibco). Cells were then lysed by adding 0.5 ml NP-40 lysis buffer (50 mM Tris-HCl (pH 7.5), 150 mM NaCl, 0.5% NP-40, 50 mM NaF, 1 mM Na_3VO_4, 1 mM DTT, 1x protease inhibitor cocktail (Thermo Scientific), and 1 mM phenylmethanesulfonyl fluoride (PMSF)) and incubating on ice for 20 minutes with occasional shaking. Cells were then further lysed by rotating at 4°C for 10 minutes. Cell debris was pelleted at 4°C and 14,000 rpm for 10 minutes. The supernatant was then transferred to a fresh tube and the protein concentration was determined through a Bradford assay. Equal mass samples (200-650 µg) were prepared and incubated with 3-5 µL mouse anti-myc (0.7 mg/ml, Enzo Life Sciences, Plymouth Meeting, PA, Cat No. SA-294), 5 µL rat anti-HA (100 µg/ml, Roche, Indianapolis, IN, Cat. No. 11867423001), or 1 µL mouse anti-FLAG (3.8 mg/ml, Sigma Aldrich, St. Louis, MO, Cat. No.

F3165) overnight at 4°C. The next day, 25 µL Protein A/G PLUS-Agarose (Santa Cruz Biotechnology® Inc, Santa Cruz, CA) was added to each sample and incubated for an additional hour at 4°C. Samples were centrifuged for 2 minutes at 3000 rpm and 4°C and then washed 3 times with cold NP-40 lysis buffer without protease inhibitors. Immunoprecipitates were resuspended in 30 µL 4x sample loading buffer and boiled for 5 minutes.

Western blots

Immunoprecipitates and/or lysates were separated using either 16.5 % Tricine- or 10 % Tris-Glycine-SDS PAGE and then transferred to nitrocellulose membranes. Membranes were probed with either rat anti-HA (1:2000, Roche) or mouse anti-myc (1:2000, Enzo Life Sciences) overnight at 4°C. Membranes were further probed with rabbit anti-mouse horseradish peroxidase (HRP) conjugated secondary antibodies (Calbiochem, EMD Chemicals, Gibbstown, NJ) or goat anti-rat HRP conjugated secondary antibodies (Santa Cruz Biotechnology® Inc, Santa Cruz, CA). Finally, membranes were developed using Immobilon™ Western Chemiluminescent HRP Substrate (Millipore, Billerica, MA) and visualized with autoradiography using Blue Basic Autorad Film (ISC Bioexpress, Kaysville, UT). Western blots were quantified using AlphaEaseFC™ Software (Alpha Innotech, Cell Biosciences, Inc., Santa Clara, CA).

Cell cycle analysis

325,000 HEK 293T cells were seeded into 6 well plates in order to be 30-40% confluent the following day. Cells were separately transiently transfected with nBmp4-IRES-GFP, IRES-GFP, or pcDNA3.1+ according to the transient transfection protocol outlined above. Non-transfected cells were also grown as a control. 48 hours after transfection, cells were trypsinized and resuspended in 2 ml 10% FBS media. Cells were then subject to the GFP-Certified™ Nuclear-ID™ Red Cell Cycle Analysis Kit (Enzo Life Sciences, Plymouth Meeting, PA).

Briefly, samples were centrifuged at 400 x g for 5 minutes at room temperature and then the supernatant was discarded. The samples were resuspended in 2 ml cold 1x PBS, centrifuged again, and resuspended in 1 ml cold 1x PBS. Then 0.5 ml of each sample was transferred to a separate 5 ml falcon tube and 2 µL Nuclear-ID^{TM} Red Cell Cycle Detection Reagent was mixed in gently. Samples were incubated at 37^{o}C for 30 minutes in the dark and then analyzed via flow cytometry using an excitation wavelength of 488 nm. Non-transfected cells without Nuclear-ID^{TM} Red were used as a negative control and non-transfected cells with Nuclear-ID^{TM} Red were used as a positive control for the Nuclear-ID^{TM} Red. IRES-GFP transfected cells without Nuclear-ID^{TM} Red were used as a positive control for GFP. Cell cycle data was analyzed using ModFit LT (Verity Software House, Topsham, ME).

Cell Synchronization

In order to synchronize cells for cell cycle analysis, cells were transiently transfected at 20-40% confluence with nBmp4-IRES-GFP, IRES-GFP, or pcDNA3.1+ according to the transient transfection protocol outlined above with some exceptions. At 24 hours, instead of adding 2 ml 10% FBS media, cells were washed twice with 2 ml 1x PBS and then incubated in 2 ml serum free medium. After an additional 24 hours, cells were washed twice with 2 ml 1x PBS and 2 ml 10% FBS media was added to each well. Four hours after the addition of FBS, cells were trypsinized and resuspended in 2 ml 10% FBS media and then analyzed using the GFP-Certified^{TM} Nuclear-ID^{TM} Red Cell Cycle Analysis Kit (Enzo Life Sciences, Plymouth Meeting, PA) as detailed above. Again, non-transfected cells were used as a control.

Ubiquitination studies

In order to analyze the ubiquitination patterns of nBmp4, cells were transiently transfected with Flag-ubiquitin and either nBmp4/HA or empty vector. 36 hours later, 10 µM

MG132 was added to inhibit proteasome activity. After an additional 12 hours, cells were lysed and equal amounts of cellular lysates were incubated with anti-Flag antibodies (Sigma Aldrich Cat. No. F3165). Immunoprecipitates were subsequently analyzed by western blotting with anti-HA antibodies in order to identify any characteristic ubiquitin laddering of nBmp4/HA.

Results

Due to the verified interactions of nBmp4 with ROC1 and ROC2 and the well studied interactions between ROC proteins and other subunits of SCF E3 ubiquitin ligase complexes, we decided to delineate the interactions of nBmp4 with other SCF E3 ubiquitin ligase components. We started by testing the interaction of nBmp4 with the component closest to the ROC proteins in the SCF E3 ubiquitin ligase, the Cullin protein. As mentioned earlier, there are at least 8 different mammalian Cullin proteins. We analyzed the interactions between nBmp4 and 5 of these Cullins, namely Cullin1, Cullin2, Cullin3, Cullin4A, and Cullin5. As shown in Figure 3.2, nBmp4 co-immunoprecipitated with all five Cullins examined.

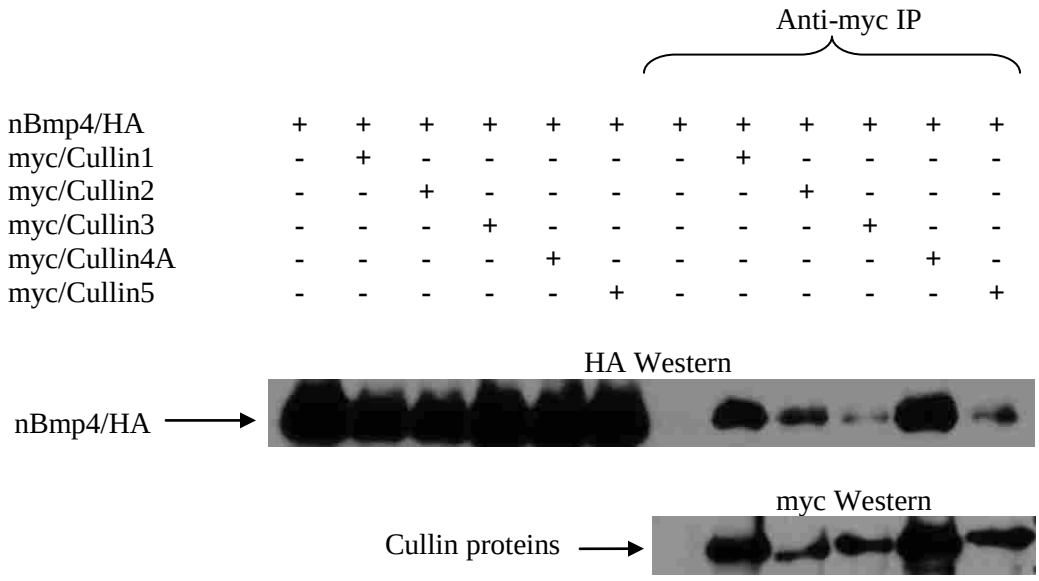

Figure 3.2 nBmp4 interacts with Cullin1, Cullin2, Cullin3, Cullin4A and Cullin5. HEK 293T cells were transiently co-transfected with the indicated plasmids. After 40-48 hours, cells were lysed and equal amounts of lysates were immunoprecipitated with anti-myc antibodies. Immunoprecipitates were subsequently immunoblotted with either anti-HA or anti-myc antibodies.

Continuing around the SCF ubiquitin ligase, we next went on to determine if nBmp4 interacts with Skp1. As described earlier, Skp1 is a protein that links the Cullin subunit to the F-box subunit in the SCF complex. As shown in Figure 3.3, nBmp4 does not interact with Skp1.

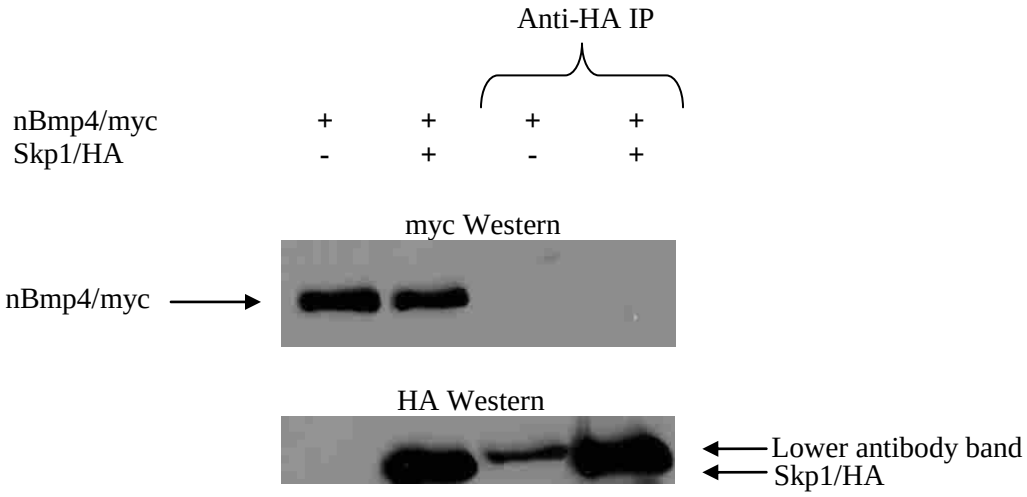

Figure 3.3 nBmp4 does not interact with Skp1. HEK 293T cells were transiently co-transfected with the indicated plasmids. After 40-48 hours, cells were lysed and equal amounts of lysates were immunoprecipitated with anti-HA antibodies. Immunoprecipitates were subsequently immunoblotted with either anti-HA or anti-myc antibodies.

Finally, the component of the SCF E3 ubiquitin ligase that is furthest away from the ROC proteins is the F-box protein. We decided to analyze the interactions between nBmp4 and two different F-box proteins, namely Skp2 and β-TrCP1. As shown in Figure 3.4, nBmp4 does, in fact, interact with both of these F-box proteins.

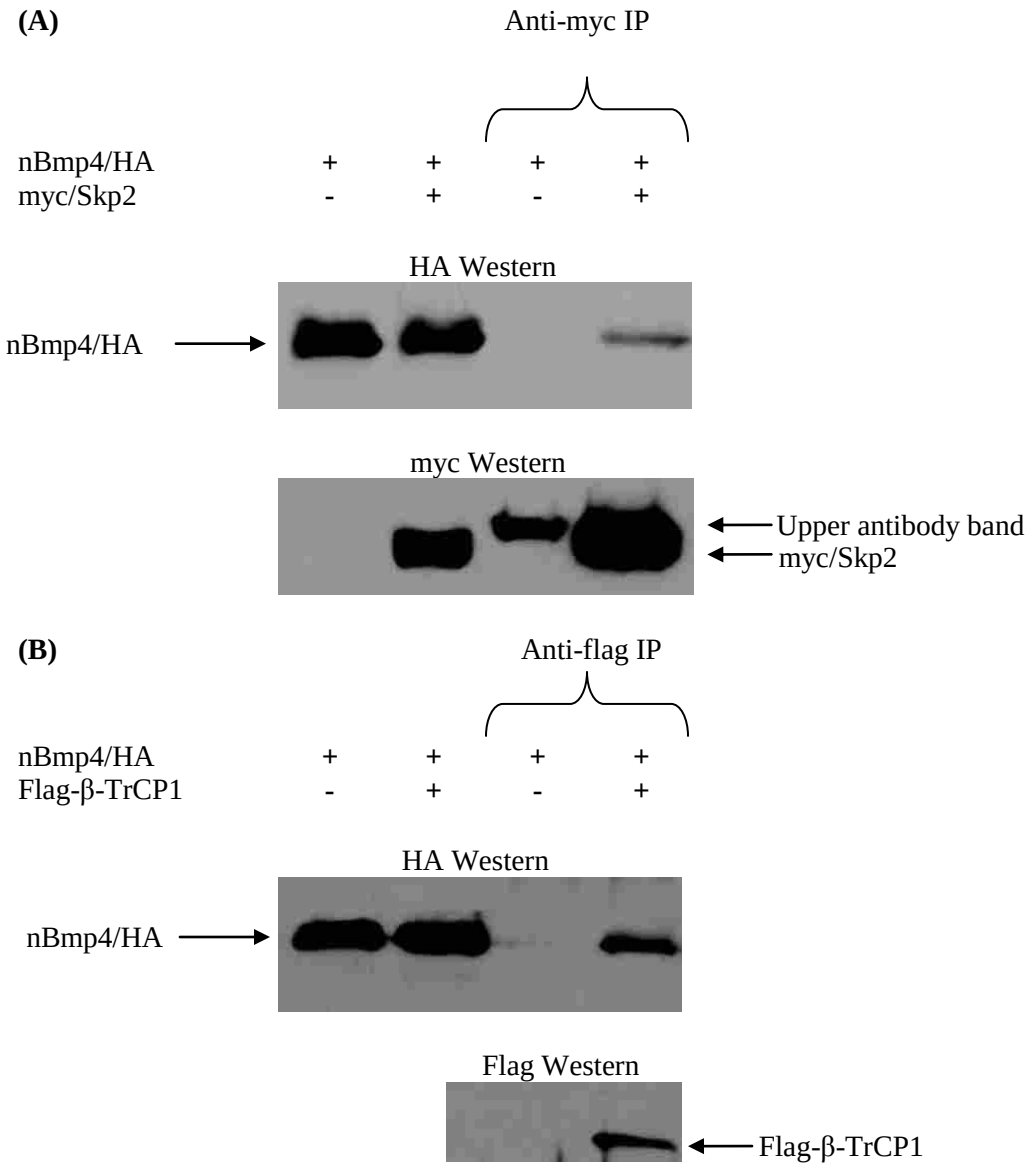

Figure 3.4 nBmp4 interacts with F-box proteins Skp2 and β-TrCP1. HEK 293T cells were transiently co-transfected with the indicated plasmids. After 40-48 hours, cells were lysed and equal amounts of lysates were immunoprecipitated with either anti-myc or anti-flag antibodies as indicated. Immunoprecipitates were subsequently immunoblotted with either anti-HA, anti-flag or anti-myc antibodies.

Thus far, we have identified interactions between nBmp4 and the ROC, Cullin, and F-box subunits of the SCF E3 ubiquitin ligase. Due to the finding that nBmp4 interacts with ROC1 through its N-terminus (see Figure 2.4B) which is the domain through which Cullin1 interacts with ROC1, we went on to determine if nBmp4 is competitively binding to ROC1 in order to inhibit the interaction between ROC1 and Cullin1. To analyze the competitive binding between nBmp4 and Cullin1 to ROC1, we expressed ROC1 with either nBmp4, Cullin1, or both nBmp4 and Cullin1. We then immunoprecipitated ROC1 and analyzed the co-immunoprecipitation levels of nBmp4 and Cullin1. From this experiment, we did not find any competitive binding between Cullin1 and nBmp4 for ROC1. As shown in Figure 3.5, similar levels of Cullin1 and nBmp4 interact with ROC1 when expressed individually or in combination.

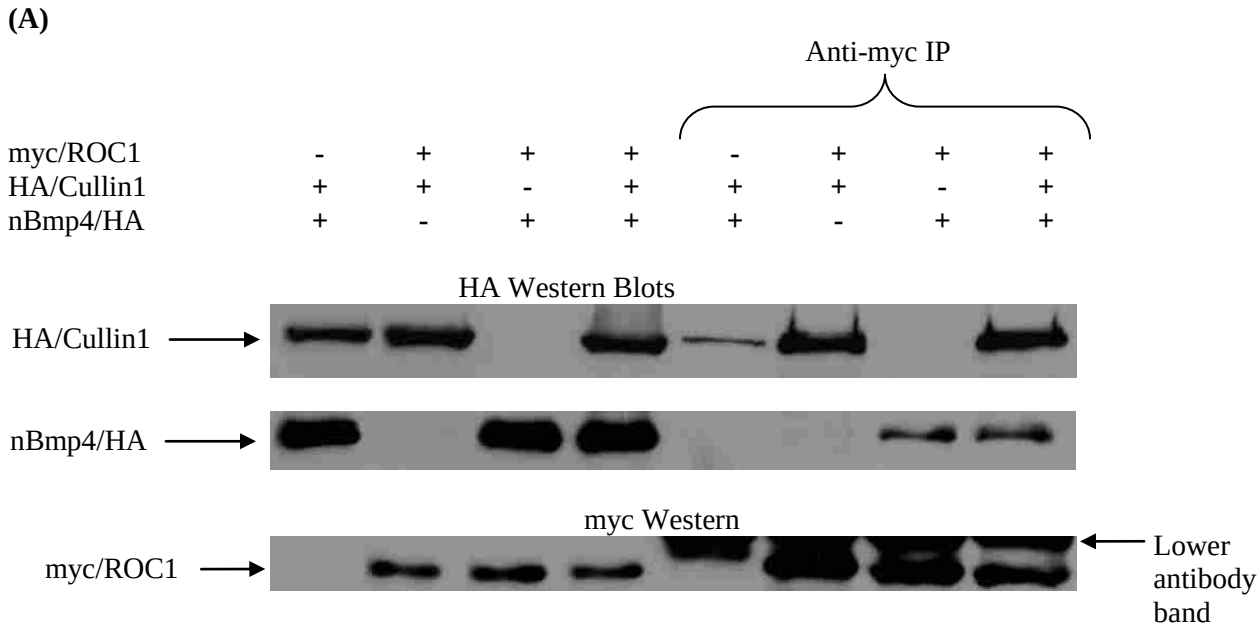

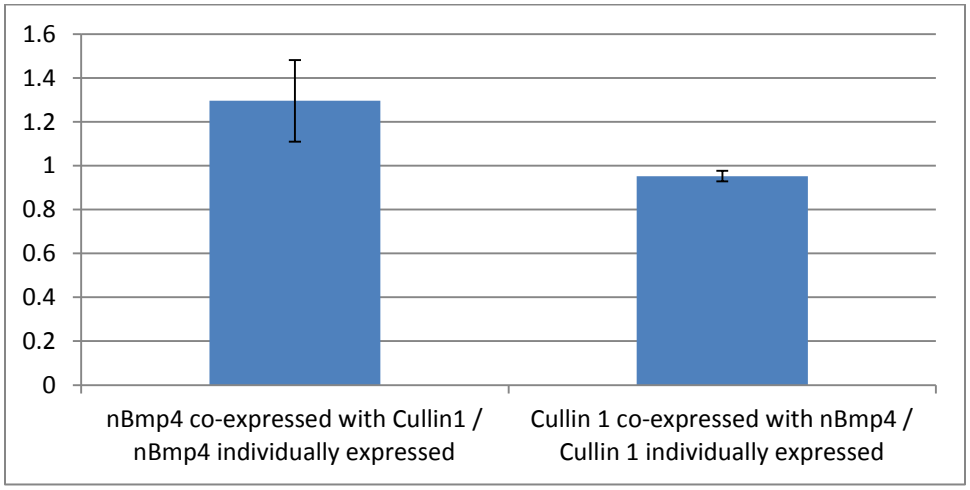

Figure 3.5 nBmp4 and Cullin1 do not competitively bind to ROC1. (A) HEK 293T cells were transiently co-transfected with the indicated plasmids. After 40-48 hours, cells were lysed and equal amounts of lysates were immunoprecipitated with anti-myc antibodies. Immunoprecipitates were subsequently immunoblotted with anti-HA antibodies to determine the levels of Cullin1 and nBmp4 binding to ROC1. Additionally, immunoprecipitates were immunoblotted with anti-myc antibodies to verify similar expression and immunoprecipitation levels of ROC1. The blots shown are representative from several repeats. (B) The histogram represents the ratio of nBmp4 co-immunoprecipitating with ROC1 when expressed alone divided by nBmp4 co-immunoprecipitation levels when co-expressed with Cullin1. It also represents the ratio of Cullin1 immunoprecipating with ROC1 when expressed alone divided by Cullin1 co-immunoprecipitation levels when expressed with nBmp4. The quantification represents three repeats of the competitive binding experiment.

Thus far, we have confirmed the yeast two-hybrid result that nBmp4 interacts with ROC1 and ROC2 and determined that nBmp4 interacts with several other subunits in the SCF E3 ubiquitin ligase complex. Because SCF ligases are highly involved in the controlling the cell cycle, one way to determine if nBmp4 is affecting the activity of the SCF complexes is to analyze the effect of nBmp4 on the cell cycle. Therefore, we hypothesized that the over-expression of nBmp4 would affect the cell cycle. To test this hypothesis, HEK 293T cells were seeded at a low confluence (30-40%) in order to examine the cells during active growth. The cells were transfected with nBmp4-IRES-GFP, IRES-GFP, or pcDNA3.1+, and then analyzed for their cell cycle progression. The inclusion of GFP allowed us to narrow our analysis to the cells that were specifically expressing GFP. As shown in Figure 3.6A, there was no difference in the percent of cells in G1 phase between cells that were expressing nBmp4-IRES-GFP and cells that were expressing IRES-GFP (p-value 0.207). However, there was a statistically significant difference in the percent of cells in G2 phase between nBmp4 expressing cells and the negative control (p-value 0.023). This suggests that nBmp4 causes cells to accumulate in G0/G1.

In order to better analyze the cell cycle, we decided to analyze the cells following synchronization via serum starvation and reinstitution of serum. When the cells were synchronized, the results confirm that nBmp4 does, in fact, affect the cell cycle (Figure 3.6B). Cells expressing nBmp4 were found more in the G0/G1 phase (p-value 0.026), and less in the G2 phase (p-value 0.028). This again suggests that nBmp4 causes cells to accumulate in G0/G1.

(A)

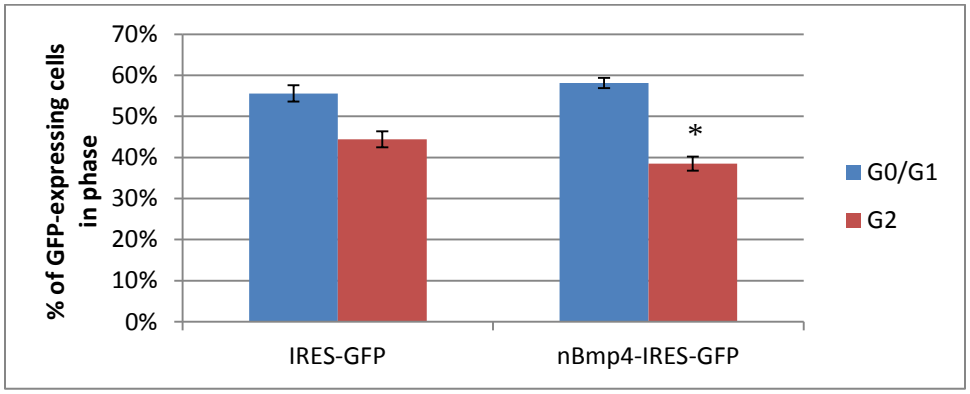

(B)

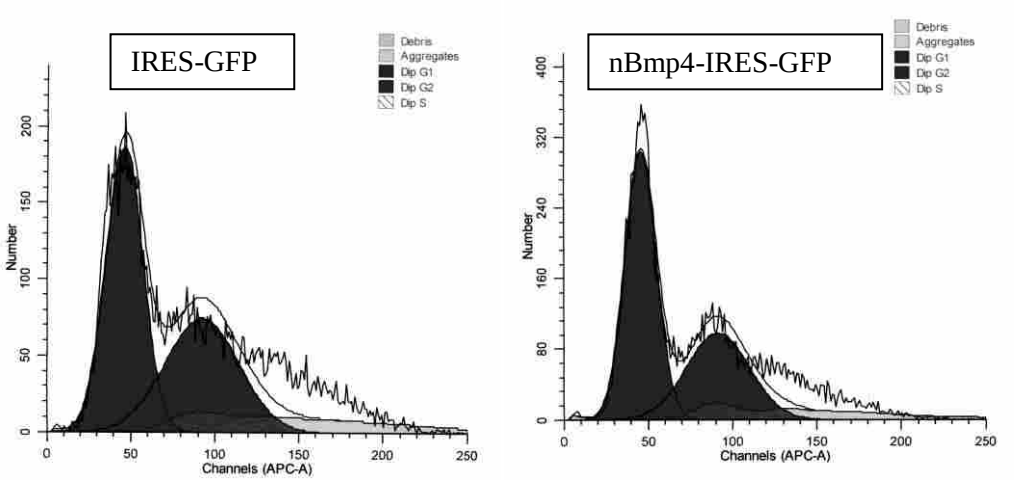

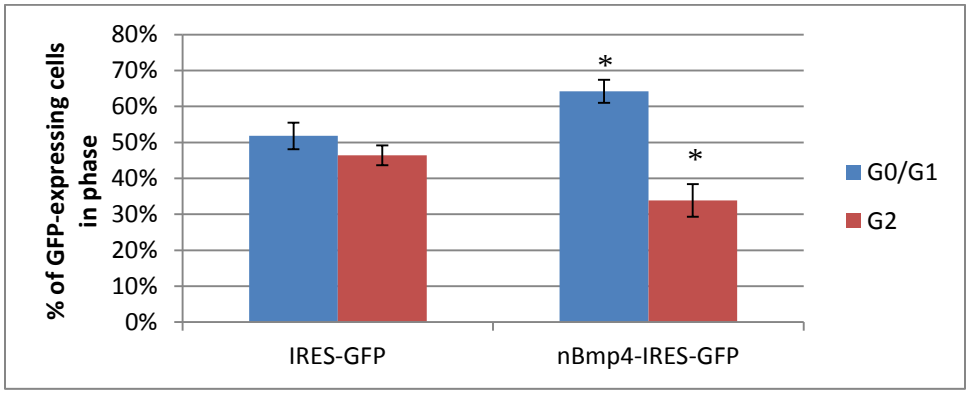

Figure 3.6. nBmp4 affects the cell cycle by causing accumulation in G0/G1. Cell cycle analysis was performed using the GFP-Certified™ Nuclear-ID™ Red Cell Cycle Analysis Kit (Enzo Life Sciences) following transient transfection of HEK293T cells with nBmp4-IRES-GFP, IRES-GFP, or pcDNA3.1+. (A) Results from non-synchronized cells. (B) Results following cell synchronization. The analysis of cell cycle progression was only conducted on GFP-expressing cells in order to narrow the analysis to the successfully transfected cells. * indicates p-value < 0.05 using the paired Student's t-test with 2 tails.

In light of the fact that nBmp4 interacts with SCF E3 ubiquitin ligase components, it is important to determine if nBmp4 itself is being ubiquitinated. Therefore, we transfected cells with FLAG-ubiquitin and either pcDNA3.1+ or nBmp4/HA and then added a proteasome inhibitor (MG132) after 36 hours. After 12 additional hours, cells were lysed and immunoprecipitated with anti-FLAG and then the immunoprecipitates were immunoblotted for anti-HA to see if nBmp4 is being ubiquitinated. In fact, nBmp4 is being actively poly-ubiquitinated in cell culture as demonstrated in Figure 3.7.

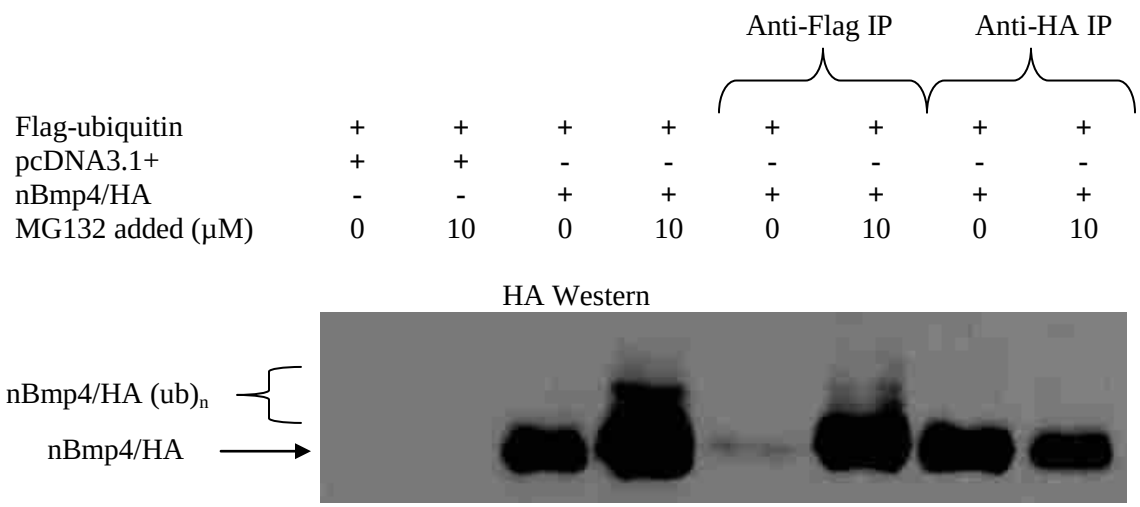

Figure 3.7 nBmp4 is actively poly-ubiquitinated. HEK 293T cells were transiently co-transfected with Flag-ubiquitin and either nBmp4/HA or pcDNA3.1+. After 36 hours, either 0 or 10 μM MG132 was added to the cells. After an additional 12 hours, cells were lysed and equal amounts of lysates were immunoprecipitated with anti-Flag antibodies (in order to concentrate the ubiquitinated proteins) or anti-HA antibodies. Immunoprecipitates were subsequently immunoblotted with anti-HA antibodies to determine if nBmp4/HA was among the ubiquitinated proteins.

Discussion

We have previously described the interaction between nBmp4 and the ROC proteins. As ROC proteins are components of SCF E3 ubiquitin ligases, we analyzed the interactions between nBmp4 and the other subunits in the SCF E3 ubiquitin ligase complex. In summary, we have shown that nBmp4 interacts with 2 different ROC proteins, 5 different Cullin proteins, and 2 different F-box proteins. We were unable to identify an interaction between nBmp4 and Skp1. However, the lack of interaction with Skp1 is not unprecedented. Roc1, when first identified, was found to individually bind to Cdc4 (F-box protein), Cdc53 (Cullin), and Cdc34 (an E2 enzyme), but not to Skp1. Although ROC1 was not found to individually bind to Skp1, Skp1 did interact with ROC1 when Cullin and F-box were also present.[76] Therefore, our inability to verify an interaction between nBmp4 and Skp1 is not too surprising. Future experiments will be performed to determine if Skp1 interacts with nBmp4 when the other SCF components are present. Together, the identified interactions of nBmp4 with ROC proteins, Cullins, and F-box proteins suggest that nBmp4 plays a role through its association with the SCF E3 ubiquitin ligase.

The identification of the interaction between nBmp4 and SCF E3 ubiquitin ligase components could suggest a functional role for nBmp4 in protein degradation and, thereby, cell cycle control. However, one important question lies in whether or not nBmp4 and the identified interacting proteins can exist in the same organelle. nBmp4 has been shown to be a nuclear variant of the secreted protein Bmp4. Therefore, the existence of a nuclear SCF E3 ligase is vitally important in order to extrapolate a function from the identified interactions. As discussed earlier, ROC proteins have been found to localize to the nucleus and Cullin1, Cullin2, Cullin4A, and Cullin5 have been found predominantly in the nucleus, as well as the modifier, Nedd8. It has

also been noted that the E2 enzyme Cdc34 is localized to the nucleus.[94] It has been shown that all components of the ubiquitin proteasome system that are necessary for degradation reside in the nucleus.[116] Additionally, it has been shown that there are nuclear proteins that are substrates for degradation and that proteasome-dependent proteolysis actually occurs in distinct foci in the nucleus.[117, 118] Therefore, there is substantial evidence that the ubiquitin proteasome system is functional within the nucleus. The results from this chapter therefore suggest a role for nBmp4 through its interaction with SCF E3 ubiquitin ligase complexes that reside in the nucleus.

Due to the finding that nBmp4 interacts with the N-terminus of ROC1, which is the domain with which Cullin1 interacts, we next analyzed whether nBmp4 and Cullin1 competitively bind to ROC1. As shown in Figure 3.5, the combined presence of both nBmp4 and Cullin1 does not inhibit the binding of either protein to ROC1. Therefore, nBmp4 and Cullin1 do not compete for binding to ROC1. Further studies could be performed to delineate the different binding domains within the N-terminus of ROC1 that interact with either nBmp4 or Cullin1.

SCF ligases are known for their major role in regulating the cell cycle. Specifically, they function in regulating both the G1/S transition and the G2/M transition by promoting the degradation of cell cycle regulators. Therefore, as the functional role of the interaction between nBmp4 and SCF components has not been elucidated, we hypothesized that nBmp4 also plays a role in cell cycle control. Our results show that nBmp4 does, indeed, affect the cell cycle. When nBmp4 is over-expressed, fewer cells are able to exit G0/G1. As discussed, SCF^{Skp2} complexes mediate negative regulators of the cell cycle while SCF^{Fbw7} complexes mediate the degradation of positive cell cycle regulators.[103] When cells are reentering the cell cycle, they must degrade the negative cell cycle regulators through SCF^{Skp2}-dependent degradation.[103] Because we

identified a defect in G0/G1 exit, this suggests that nBmp4 is inhibiting SCF^{Skp2}-dependent degradation. The SCF^{Skp2} complex targets many proteins for degradation, including p21, p27, p57, p130 and E2F-1. It may be that nBmp4 functions through inhibiting the degradation of these proteins and thereby decreases the ability of cells to progress out of G0 or G1. The further analysis of cell cycle regulatory protein levels will aid in determining how nBmp4 is inhibiting the progression of the cell cycle.

We have also determined that nBmp4 is being actively poly-ubiquitinated in cell culture. This result does not necessarily indicate that nBmp4 does not play a role in protein degradation. As shown by Ohta et al. and He et al., ROC1 and ROC2 are also degraded in a proteasome-dependent manner.[67, 115] Additionally, the interaction between nBmp4 and F-box proteins does not necessarily indicate the use of those F-box proteins to degrade nBmp4 due to the fact that Roc1 also interacts directly with F-box proteins.[74, 76, 86] Instead, the interaction of nBmp4 and SCF E3 ligase components may suggest a functional role for nBmp4 in protein degradation and regulation of the cell cycle.

Chapter 4: Tissue specific nBmp4 over-expression mouse

Summary

As discussed in the previous chapters, there is an important nuclear variant of the secreted growth factor Bmp4. The function of nBmp4 has been characterized in tissue culture to be involved in cell cycle progression and apoptosis, and is associated with protein degradation machinery. In an effort to delineate the function of nBmp4 *in vivo*, we decided to generate a mouse model in which nBmp4 is over-expressed in a tissue specific manner. Due to the finding that zebrafish have heart defects when the translation of nBmp4 is blocked, the presence of ROC proteins in heart and skeletal muscle tissues, and the role that the ubiquitin proteasome system plays in cardiovascular development, we decided to specifically over-express nBmp4 in heart tissue. The analysis of this mouse model will greatly aid in understanding the role of endogenous nBmp4.

Introduction

Gene targeting is a very useful technique that has grown dramatically since its inception. Through the use of gene targeting, mutations may be introduced into stem cells through homologous recombination.[119] These stem cells are then screened for correct recombination events. The successfully targeted stem cells are then injected into blastocysts with the aim that the mutated cells become integrated into the germ line of the chimeric mice.[120] Through this technique, any gene of interest may be mutated and the effects of the mutation may be thereby studied through the mutant mice.

The conventional method for gene targeting in mice results in every cell of the mouse having the same mutation. While this technique is important, the conventional method of mutating gene expression does not allow for the specific study of gene function in a particular

cell type or during adulthood if the gene is necessary during development.[121] A flexible, inducible technology is needed in order to specify the tissue of interest or the stage of development that is under investigation. Several new systems have been invented whereby the expression or perturbation of a gene of interest may be specifically regulated. One such system to regulate the tissue specificity is called the Cre-Lox system.[122, 123] In this system, the Cre recombinase is used to remove DNA that is flanked by LoxP sites (also referred to as floxed DNA). This Cre recombinase-induced removal of DNA can be exploited to inactivate a gene of interest by removing part of the coding sequence. Alternatively, the Cre recombinase-induced removal of DNA can result in the activation of DNA if the floxed DNA inhibits the expression of the gene of interest. The Cre-Lox system is highly used and can be used in a tissue specific manner.[124] Namely, mice that have been genetically engineered to contain floxed DNA can be mated with tissue-specific Cre recombinase-expressing mice and their progeny will have recombination of the floxed site only in the tissue of interest. It may also be important to regulate the timing of the removal of floxed DNA. This may be accomplished through tamoxifen-inducible Cre-recombinase expression. In these tamoxifen-inducible mice, the Cre-recombinase is fused to the ligand binding domain of a mutated estrogen receptor. The fusion protein is maintained in the cytoplasm by heat shock proteins until the administration of tamoxifen liberates the Cre recombinase.[121, 125] Many strains of mice have been created that have tissue-specific Cre recombinase expression under tamoxifen regulation.

The Cre-recombinase mediated removal of floxed DNA is not always perfect. Therefore, methods have been devised to identify the tissues in which the recombination has been successful. For instance, Mao et. al. designed a mouse in which enhanced green fluorescent protein (EGFP) is encoded downstream of a transcriptional stop site that is flanked with LoxP

sites.[126] The successful removal of the stop site allows for transcription of EGFP. This method allows for simple identification of cells in which successful recombination mediated by the Cre recombinase has occurred.

Finally, when the over-expression of a gene is under investigation, it is desirable to insert the gene of interest into a locus that is constitutively active and available for recombination mediated by the Cre recombinase. The ROSA26 locus has been found to be constitutively active and is a desirable locus for gene targeting.[127, 128]

In an effort to determine the *in vivo* function of nBmp4, we set out to make an nBmp4 over-expression mouse. It has been shown that Bmp4 knockout mice are embryonic lethal[16, 20, 21] and nBmp2 knockout mice have a discrete phenotype (unpublished observations in the Bridgewater lab). Therefore, we decided to prepare a mouse strain that specifically over-expresses nBmp4 in a tissue specific manner and then to analyze the particular tissue. Through the aid of Dr. Jeffery Barrow, we were provided the ability to use the method described above in which a gene of interest is inserted downstream of a floxed transcriptional stop site. The gene of interest is followed by an internal ribosomal entry site (IRES) and GFP which allows easy detection of tissues that are expressing the gene of interest. This construct is homologously recombined into the constitutively active ROSA26 locus. Because the gene of interest is downstream of a transcriptional stop site, it will not be expressed in the mutant mice. However, when the mutant mice are mated with Cre recombinase expressing mice, the transcriptional stop site will be removed through specific recombination of the floxed site. This will allow expression of the gene of interest and the associated GFP.

Several observations suggest that nBmp4 plays a role in heart development. First, BMPs are known to have dynamic expression patterns throughout the heart during development, as

judged by in situ hybridizatoin.[129] Additionally, Jaime Mayo, a previous PhD student in Dr. Laura Bridgewater's lab, performed experiments in zebrafish in which morpholinos were used to block translation from the alternative start codon of Bmp4. Although the zebrafish were minimally analyzed, it was noted that the mutant zebrafish had severe heart problems. The identification of the interaction between nBmp4 and the ROC proteins and the abundance of ROC proteins in heart and skeletal muscle also suggests that nBmp4 plays a role in the heart.[64] Finally, it has been noted that the ubiquitin proteasome system is involved in cardiac disease and vascular development.[130] For instance, the F-box protein FBW7 and Cullin 7 are required for cardiovascular development. It has also been shown that an F-box protein called atrogin-1 inhibits calcineurin dependent-cardiac hypertrophy by targeting calcineurin for degradation.[131] These many lines of evidence suggest that nBmp4 may play a special role in heart tissue. Therefore, we decided to design a mouse that specifically over-expresses nBmp4 in the heart tissue.

Experimental Procedures

Vector preparation

In order to prepare DNA to electroporate into stem cells, nBmp4 was cut out of the pcDNA4/TO vector using the SalI and ClaI restriction sites. The plasmid pBigT-IresGFP was digested with the same two enzymes. pBigT-IresGFP includes a transcriptional stop site that is surrounded by LoxP sites followed by an internal ribosomal entry site (IRES) and GFP. This allows specific expression of the gene of interest. When Cre is present, the gene of interest is activated and the expression of the gene of interest will always be accompanied by the expression of GFP in the same cells. However, the gene of interest will not be fused to GFP which could potentially interfere with the function of the gene of interest. The nBmp4 fragment

was ligated into pBigT-IresGFP using a 3:1 insert:vector ratio to make pBigT-nBmp4-IRES-GFP. As described above, the ROSA26 locus is always activated. To exploit this phenomenon, the nBmp4-IRES-GFP fragment was cut out of pBigT-nBmp4-IRES-GFP using the PacI and AscI restriction endonucleases. The pBC_R26_mCherry vector was also digested with PacI and AscI to remove mCherry. pBC_R26_mCherry contains ROSA26 5' and 3' homologous ends which facilitate homologous recombination into the endogenous ROSA26 locus. nBmp4-IRES-GFP was then ligated using a 1:1 insert:vector ratio into pBC_R26 in place of the mCherry gene to create nBmp4-IRES-GFP-ROSA26. Finally, a maxi prep of nBmp4-IRES-GFP-ROSA26 was prepared and linearized with XhoI in preparation to be electroporated into stem cells.

Electroporation and selection

The electroporation of nBmp4-IRES-GFP-ROSA26 into 129×C57BL/6 F_1 embryonic stem cells was conducted in Dr. Jeffery Barrow's lab. Briefly, cells were washed, trypsinized, counted, and adjusted to 13 million cells/0.8 ml (in 1x PBS). 30 µg linearized DNA (nBmp4-IRES-GFP-ROSA26) is then mixed well with the thirteen million cells in a 4 mm cuvette. Once the sample resistance is below 13 Ω, the sample was electroporated with the following settings: 220 V, 500 µF, and a resistance of ∞. The cells were placed on ice for 20 minutes, mixed with ES media, and plated onto Mitomycin C-treated neomycin resistant mouse embryonic fibroblasts (NeoMEFs). A negative control of stem cells without DNA was also electroporated. This negative control was used to determine when the non-targeted cells were sufficiently cleared during the selection process.

The cells were grown in ES medium + G418 (ES medium consists of 15% FBS, 1% MEM Non-Essential Amino Acids Solution 10 mM [Invitrogen, Carlsbad, CA], 1% Nucleotides, 1% β-mercaptoethanol, 1% PSG [Penicillin-Streptomycin-Glutamine], 0.1% LIF [Leukemia

Inhibitory Factor], ~81% DMEM without HEPES, and 200μg/ml G418) for approximately 5-7 days until the negative control cells had all been cleared. Individual colonies were then isolated by picking them individually, transferred to a 48-well plate, and incubated in trypsin at 37^{o}C for 10 minutes to promote dispersion of the cells in the colony. ES medium + G418 was then added to inactivate the trypsin and cells were allowed to grow until near complete confluence. Meanwhile, the media was changed every other day. Once most of the colonies in the 48-well plate were near confluence, the cells were trypsinized and divided into two plates: one to be frozen for future use in aggregations and the other for DNA isolation and identification of correct homologous recombination events.

Southern blotting

The cells in the replica plate used for DNA isolation were grown to maximum confluence. The cells were then washed twice with 1x PBS and lysed overnight in cell lysis buffer with proteinase K (10 mM Tris (pH 7.5),10 mM EDTA (pH8.0), 10 mM NaCl, 0.5% SDS, 1 mg/ml Proteinase K) at 37^{o}C, 5.0% CO_2 in a humidified chamber. The cell lysate was then transferred to a microcentrifuge for further DNA purification.

The genomic DNA was purified using the phenol/chloroform method. First, samples were mixed with an equal volume of phenol:chloroform:isoamyl (25:24:1) and centrifuged for 5 minutes at room temperature. The aqueous phase (upper layer) was then mixed with an equal volume of chloroform:isoamyl (24:1) and centrifuged for 5 minutes at room temperature. DNA in the aqueous phase (upper layer) was then precipitated by adding $MgCl_2$ (10 mM final concentration), NaCl (200 mM final concentration), and 2.5 volumes of 100% ethanol. The samples were incubated at -80^{o}C for at least 20 minutes and then centrifuged for 20 minutes at 4^{o}C, 14,000 rpm. Pellets were washed with 80% ethanol. Samples were immediately

resuspended in 27 µL TE buffer (10 mM Tris pH 8.0, 1mM EDTA) and incubated overnight at 37^{o}C.

Successfully targeted stem cells have a new *Eco*RV site inserted into the Rosa26 locus. This will produce a 4.1 kb band instead of the 11.5 kb band for wild type after digesting chromosomal DNA with *Eco*RV. Accordingly, 25 µL DNA was digested in Buffer R with BSA and 20 units of *Eco*RV (Fermentas, Glen Burnie, MD) at 37^{o}C overnight. Samples were then separated on a 0.8% agarose/TAE gel at 75 V for 3-4 hours or at 23 V overnight. The gel was subsequently denatured for 1 hour in denaturing solution (3 M NaCl, 0.4 M NaOH) and then equilibrated in transfer buffer (3 M NaCl, 8 mM NaOH) for 1 minute. The DNA in the gel was then transferred onto a nylon transfer membrane (Nytran N, Whatman, Piscataway, NJ) using the downward alkaline capillary transfer method and the transfer buffer described above. In the downward alkaline capillary transfer method, a stack of dry paper towels is placed in the bottom of a 9 x 13 baking dish, and then 2 pieces of filter paper were soaked in transfer buffer and placed on top of the paper towels making sure to eliminate any bubbles. The nylon membrane was wetted in the transfer buffer and placed on top of the filter paper, followed by the gel, again making sure that there were no bubbles that would inhibit efficient transfer of the DNA to the membrane. Two more pieces of filter paper were wetted and placed on top of the gel followed by sponges that were saturated in transfer buffer. Parafilm was stretched around the gel to separate the paper towels from the sponge. This was done in order to ensure that the transfer would not "short circuit." This set up is illustrated in Figure 4.1. The DNA was allowed to transfer for 2 hours to overnight at room temperature.

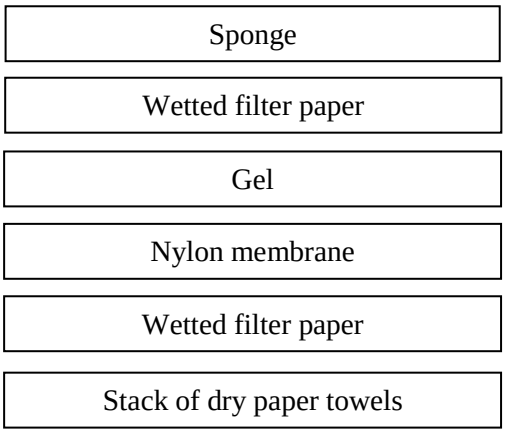

Figure 4.1 Downward alkaline capillary transfer method. Schematic of transfer apparatus set up in order to transfer DNA from a gel to a Nylon membrane during the Southern blotting technique.

After sufficient time (2 hours or overnight), the membrane was neutralized in neutralization buffer (0.2 M Sodium phosphate buffer pH 6.5, approximately ½ sodium phosphate monobasic and ½ sodium phosphate dibasic) for 10 minutes at room temperature without shaking. The membrane was then dried at 80^{o}C for 2 hours to bake the DNA onto the membrane. The membrane was either stored at 4^{o}C between two pieces of filter paper in a dry plastic bag until ready for use or incubated with prewarmed Hybrisol I (Millipore, Billerica, MA) for 1-2 hours at 42^{o}C.

The DNA probe was prepared from a 5' ROSA26 probe plasmid from Dr. Mario Capecchi's lab. The 5' ROSA26 probe was isolated from the plasmid by digesting with *Hind*III and *Eco*RI, run on a 0.8-1% agarose/TAE gel, and purified using the QIAquick® Gel Extraction Kit (Qiagen, Valencia, CA). The purified 5' ROSA26 probe was then radioactively labeled with α ^{32}P dCTP using the NEBlot kit (New England Biolabs, Ipswich, MA) according to the manufacturer's instructions. Briefly, 25 ng probe was incubated with octadeoxyribonucleotides in 10x labeling buffer, dATP, dTTP, dGTP, α^{32}P dCTP (50 µCi), and Klenow Fragment for 1 hour at 37^{o}C. The elongation reaction was terminated by adding 2 µL 0.5 M EDTA (pH 8.0).

The probe was then purified away from any unincorporated radioisotope using illustra™ NICK™ Columns (GE Healthcare, Piscataway, NJ) according to the manufacturer's protocol. Once the probe was purified, the radioactivity was measured using 2 µL probe and 5 ml scintillation fluid. The probe was then boiled for 5 minutes and cooled on ice for 5 minutes before being added to the tube containing the prewarmed Hybrisol I and membrane. (The ideal strength of the probe was >5 x 10^6 cpm/ml Hybrisol I.) The membrane was then incubated with the probe at 42°C overnight with rotation to sufficiently disperse the probe.

The next day, the membrane was washed two times at room temperature for 15 minutes each in 2x SSC, 0.1% SDS (20x SSC: 300 mM trisodium citrate, 3 M NaCl, pH 7.0). The membrane was then washed one or two times with 0.2x SSC, 0.1% SDS at 42°C for 15 minutes each. The membrane was then rinsed with water, dried at room temperature for 5 minutes, wrapped in plastic wrap, and taped into a cassette. Film was added to the cassette and was allowed to develop at 80°C for 1-5 days. The film was then developed. Alternatively, the membrane was dried at room temperature for 35 minutes, wrapped in plastic wrap, taped into a cassette (Amersham Biosciences, Piscataway, NJ) and then exposed to a phosphor-imaging screen overnight at room temperature. The next day, the phosphor-imaging screen was scanned using a Storm 860 PhosphorImager.

Long Range PCR

In addition to Southern blots, correct homologous recombination in stem cell populations was also verified by long range PCR conducted at the University of Utah (Salt Lake City, UT) in Dr. Mario Capecchi's laboratory through the aid of Dr. Sen Wu and Yuanyuan Wu. In order to verify correct integration at the 5' end, PCR was performed using the specified primers in Table 4.1. The temperature cycle used was 98°C for 2 minutes followed by 35 cycles of 98°C for 20

seconds, 60°C for 20 seconds, and 72°C for 1 minute. The cycles were followed by a 7 minute extension time at 72°C. In the case of correct integration, the expected band is 1.2 kb.

The 3' integration site was also analyzed via long range PCR. First, the genomic DNA was diluted 1:10 in lysis buffer (25 mM NaOH, 0.2 mM $Na_2EDTAx2H_2O$) and boiled for 15 to 20 minutes. PCR was then performed with 2 µL diluted DNA, the primers indicated in Table 4.1, and the Roche Expand Long Template PCR Kit. The temperature cycle was as follows: 92°C for 2 minutes followed by 10 cycles of 92°C for 10 seconds, 58.5°C for 30 seconds, and 68°C for 5 minutes. This was followed by 20 cycles of 92°C for 15 seconds, 58.5°C for 30 seconds, and 68°C for 5 minutes and 20 seconds. Finally, there was an extension of 68°C for 7 minutes. Correct integration of the insert into the ROSA26 locus will yield a product of 4.6 kb when analyzing the 3' integration site.

Table 4.1 Primers used for Long Range PCR analysis of ROSA26 integration. PCR was performed in Dr. Mario Capecchi's lab to analyze correct recombination of the nBmp4-IRES-GFP-ROSA26 insert at both the 3' and 5' ends of the ROSA26 homologous arms (University of Utah, Salt Lake City, Utah).

WS140 (for 5' PCR)	CCTAAAGAAGAGGCTGTGCTTTGG
WS141 (for 5' PCR)	CATCAAGGAAACCCTGGACTACTG
WS681BigT3'f2 (for 3' PCR)	TATGGCTTCTGAGGCGGAAAGA
WS678Rosa3_r1 (for 3' PCR)	GTGCAGTGTTGAGGGCAATCTG

ES cell preparation

The stem cell preparation was performed in the Barrow lab by Jubal Stewart. In short, stem cells from a colony that has had nBmp4-IRES-GFP-ROSA26 correctly recombined into the endogenous ROSA26 locus are thawed three days prior to morulae aggregation. The cells are thawed onto 35-mm dishes and grown for two days in ES medium (15% FBS, 1% NEAA, 1% Nucleotides, 1% β-mercaptoethanol, 1% PSG [Penicillin-Streptomycin-Glutamine], 0.1% LIF [Leukemia Inhibitory Factor], and ~81% DMEM without HEPES) at 37°C with 5% CO_2 in a humidified chamber. After two days, the cells are washed twice with 1x PBS and then

trypsinized for five minutes at 37°C, 5% CO_2. The trypsin is inactivated by the addition of MEF medium (10% FBS, 1% NEAA, 1% Nucleotides, 1% β-mercaptoethanol, 1% PSG [Penicillin-Streptomycin-Glutamine], 0.1% LIF [Leukemia Inhibitory Factor], and ~81% DMEM without HEPES) or ES medium, triturated, and centrifuged for five minutes to pellet the cells. The pellets are then resuspended in fresh ES medium. Cells are thoroughly triturated and divided into two new 35-mm dishes, one dish with 1/3 of the cells and the other dish with 2/3 of the cells. The cells are then allowed to grow for one more day at 37°C.

The day of morulae aggregation, stem cells were washed twice with 1x PBS and trypsinized long enough to release the ES cell colonies. The trypsin was then inactivated with ES medium and cells were triturated to release them from the dish and then transferred to a conical vile for transportation.

Morulae aggregation and implantation

The morulae aggregation was also performed by the Barrow lab. To be extrememly brief, female CD-1 strain mice were induced to superovulate and subsequently mated with CD-1 male mice. Female mice that were found to have seminal residues were then euthanized two days after identification of the plug and the oviducts and upper third of the uteri were surgically removed and placed in M2 medium (M2 medium without HEPES and without penicillin, Sigma Aldrich, St. Louis, MO). The oviducts and uteri were then cleaned and the embryos were flushed out of the infindibulum of the oviduct into the M2 medium. The embryos were then collecting using mouth pipettes into a drop (~80 µL) of M2 medium.

The zona pellucida surrounding each embryo (morula) was then removed by incubating the embryos in acidic Tyrode's Solution (EmbryoMax® Acidic Tyrode's Solution, Millipore, Billerica, MA) until the zonae pellucidae were no longer visible under the light microscope. The

de-zoned embryos were then moved to M2 medium to remove an excess Tyrode's Solution and then moved to individual divots in droplets of M16 medium (M16 medium without sodium bicarbonate, Sigma Aldrich, St. Louis, MO) that are covered with light mineral oil.

Finally, 5-12 ES colonies are washed in M16 medium and transferred to individual divots containing the morulae. The cells are allowed to aggregate while being incubated at 37^{o}C, 5% CO_2 20-24 hours in a humidified chamber in preparation of being injected into Swiss Webster (SW) mice. The female SW mice are prepared for injections by mating with vasectimized SW males. Only the mice that have seminal residues two days previous to the time of injections are used (which mimicks the stage of the embryos harvested from the CD-1 mice). After the 20-24 hour incubation, the embryos are implanted into SW female mice that have been mated as described. Pups are usually born about 16.5 days later and are analyzed for chimeric content. Because the CD-1 embryos are homozygous recessive, the black fur originating from the 129×C57BL/6 F_1 embryonic stem cells is evident. The chimeric mice must then be mated with CD-1 mice to determine if the mutant gene was integrated into the germ line. Once mutant mice are produced, they will be mated with tissue-specific Cre recombinase expressing mice in order to analyze tissue specific over expression of nBmp4.

Results

We have shown that nBmp4 is important in cell death and in cell cycle progression. However, both of these effects were analyzed in tissue culture. In order to analyze the function of nBmp4 *in vivo,* we decided to make a mouse model in which nBmp4 is over-expressed in a tissue-specific manner. Due to the observations that ROC1 and ROC2 are expressed highly in the heart, that the ubiquitin proteasome system plays a role in cardiac development and disease, and

that nBmp4 mutant zebrafish have heart defects, we propose to analyze nBmp4 specifically in heart tissue.

nBmp4 was first ligated into the pBigT-IresGFP vector. This construct allows the tissues expressing nBmp4 to be distinguished readily because of the parallel expression of both nBmp4 and GFP. The pBigT-IresGFP construct also contains a transcriptional stop site (4 polyA) that is enclosed in LoxP sites just upstream of nBmp4-IRES-GFP. Therefore, nBmp4 will not be expressed until the tissue comes in contact with the Cre recombinase, in which case nBmp4 and GFP will be expressed. Finally, the LoxP-stop-LoxP-nBmp4-IRES-GFP DNA was transferred to a vector containing ROSA26 homologous arms. The nBmp4-IRES-GFP-ROSA26 DNA was then linearized and electroporated into G4 embryonic stem cells. Once the stem cells were selected in G418 for 5-7 days and the negative control was sufficiently cleared, the remaining colonies were isolated and screened by Southern blots to determine if any stem cell colonies had correct recombination of nBmp4-IRES-GFP-ROSA26 into the endogenous ROSA26 locus. Correct recombination was determined by identifying a 4.1 kb band after an EcoRV digest as opposed to the wild type 11.5 kb band. From the first electroporation performed, colony 7A2 was found to have recombined correctly into the endogenous ROSA26 locus as shown by the Southern blot in Figure 4.2. From the second electroporation performed, colonies A1, A2, and A5 were found to have recombined correctly into the endogenous ROSA26 locus as determined by the long range PCR results obtained by the Capecchi lab that are shown in Figure 4.3.

Colony 7A2 from the first electroporation was grown up and aggregated with morulae in order to create chimeric mice. As of now, a male with approximately 50% chimerism has been born, but the presence of the mutant ROSA26 locus in the germ line has yet to be determined. Once the mutant mice have been successfully identified and propagated, they will be mated with

mice that have a tamoxifen-inducible Cre recombinase specifically in the heart tissue (either B6.Cg-Tg(Myh6-cre/Esr1)1Jmk/J (stock number 005657) or B6;129-Tg(Myh6-cre/Esr1)1Jmk/J (stock number 005650) from The Jackson Laboratory, Bar Harbor, ME). The resulting mice will then have an over abundance of nBmp4 in their hearts. It may also be of use to mate these mice with mice expressing Cre recombinase in the skeletal muscle and cardiac muscle (B6.FVB(129S4)-Tg(Ckmm-cre)5Khn/J (stock number 006475) from The Jackson Laboratory, Bar Harbor, ME) due to the muscle defects that are being discovered in nBmp2 knockout mice.

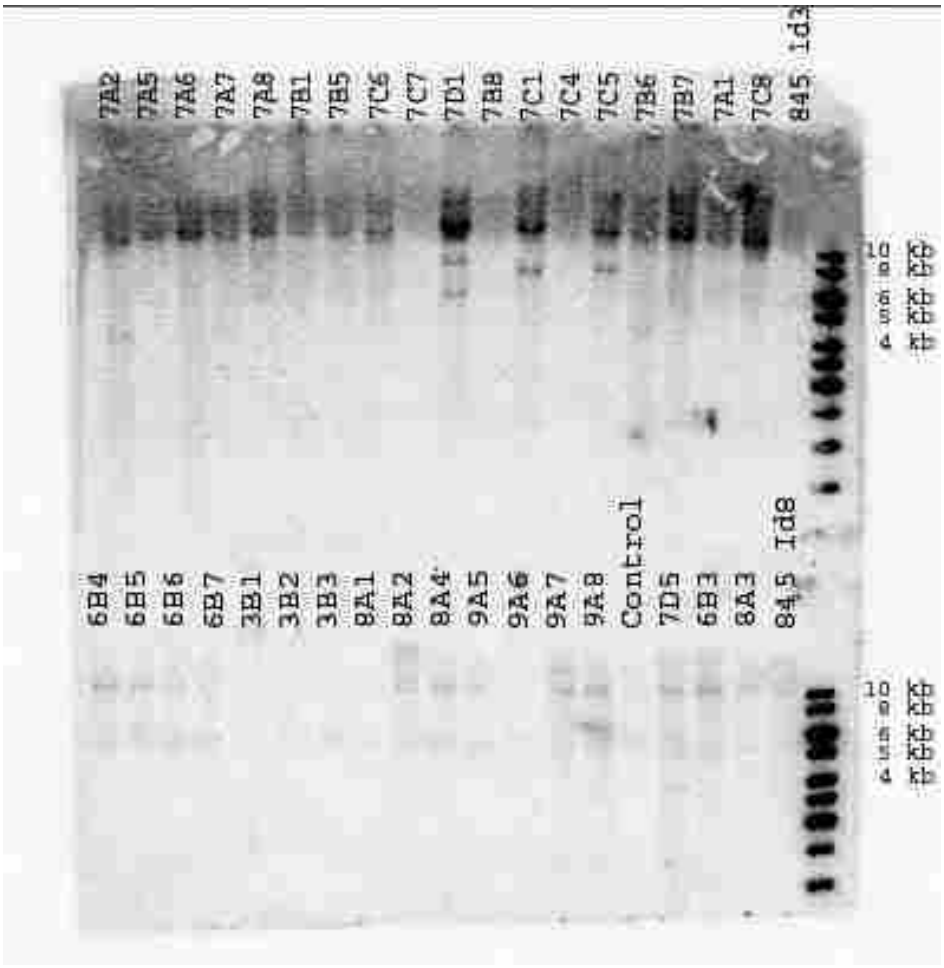

Figure 4.2 Sample 7A2 has nBmp4-IRES-GFP correctly recombined into the ROSA26 locus.
Southern blots were performed on several stem cell colonies in order to determine which colony, if any, had nBmp4-IRES-GFP correctly integrated into the ROSA26 locus. The wild-type band is located at 11.5 kb and the mutant band is located at 4.1 kb.

(A)

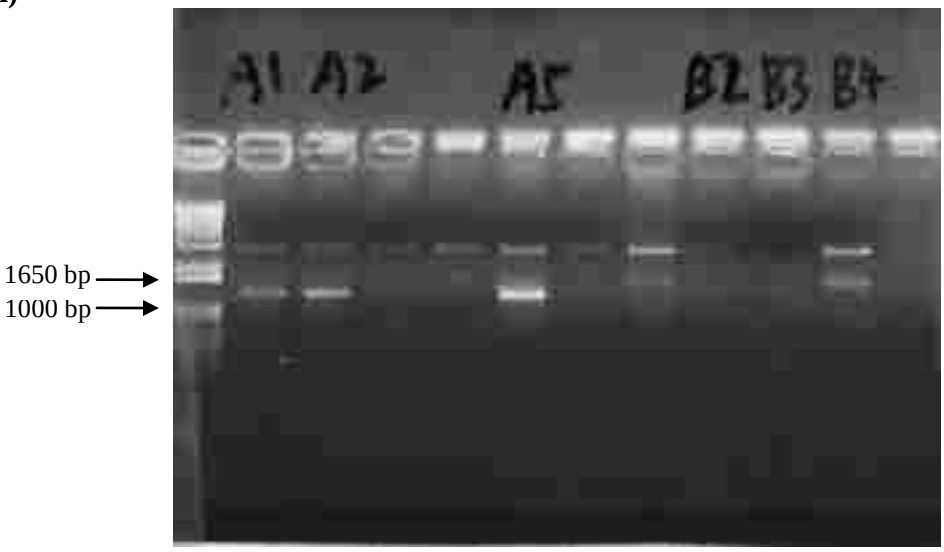

(B)

Figure 4.3 Samples A1, A2, and A5 have nBmp4-IRES-GFP correctly recombined into the ROSA26 locus. Long range PCR was performed by Yuan Wu in Mario Capecchi's lab at the University of Utah (Salt Lake City, UT). **(A)** Results from PCR analyzing the 5' integration site of ten samples indicate that samples A1, A2, and A5 have nBmp4-IRES-GFP recombined correctly into the ROSA26 locus, as judged by the band at 1.2 kb. **(B)** Results from PCR analyzing the 5' integration site confirm that samples A1, A2, and A5 have recombined correctly into the endogenous ROSA26 locus, as judged by the band at 4.6 kb. The DNA ladder used in both gels is the 1 Kb Plus DNA Ladder (Invitrogen, Carlsbad, CA).

Discussion

Although the nBmp4 mutant mice have yet to come to fruition, this project is of vital importance. As demonstrated throughout this paper, nBmp4 is an important nuclear variant of the secreted growth factor Bmp4. It has been shown that nBmp4 plays a role in apoptosis, cell cycle progression, and interacts with protein degradation machinery. Additionally, it has been noted that nBmp4 mutant zebrafish have heart defects and SCF E3 ubiquitin ligase components are required for cardiovascular development. Therefore, analyzing the effects of nBmp4 in the hearts of these mutant mice will be of utmost importance in the path to determine the *in vivo* function of nBmp4.

Conclusion

In conclusion, we have reported evidence for a nuclear variant of the growth factor Bmp4. The nuclear variant is translated from an alternative start codon that is located downstream from the signal peptide sequence. This translational start site allows the protein to be made without a signal peptide and is, therefore, translated in the cytoplasm. A bipartite nuclear localization signal is then able to transport nBmp4 to the nucleus. Nuclear variants of BMPs have never before been identified or characterized. Therefore, it is of upmost importance to determine what processes these nuclear variants are involved in. The nuclear BMPs may be responsible for some of the many functions that have been attributed to the secreted growth factors.

We have performed a yeast two-hybrid screen to identify proteins that interact with nBmp4 in order to delineate the function of nBmp4. From the yeast two-hybrid screen, we identified 21 potential binding partners. Three of these binding partners are localized to the nucleus and are involved in the ubiquitin-proteasome system, namely Regulator of Cullins 1 and 2 (ROC1 and ROC2) and ubiquitin. Through a series of sequential deletion analyses, we have determined that nBmp4 interacts with ROC1 and ROC2 through its N- and C-terminal binding domains. We have also determined that ROC1 interacts with nBmp4 through its N-terminus and that ROC2 interacts with nBmp4 through its RING finger. However, there is still uncertainty as to whether all of the constructs expressed the protein fragments similarly and whether the fragments folded correctly. The results of the ROC sequential deletion analyses are, therefore, being repeated in tissue culture.

The interaction of nBmp4 with ROC proteins suggested a role for nBmp4 in the ubiquitin-proteasome system. ROC proteins are components of SCF E3 ubiquitin ligases and, as

such, they help to identify and tag target proteins for degradation. This role of the ROC proteins prompted us to determine if nBmp4 interacts with other subunits of the SCF E3 ubiquitin ligase. The SCF E3 ubiquitin ligases are composed Skp1, Cullin, and F-box proteins along with ROC proteins. We have shown that nBmp4 interacts with 5 different Cullin proteins and 2 different F-box proteins. nBmp4 did not interact with Skp1, as judged by co-immunoprecipitation experiments. However, when ROC1 was first identified, it was not shown to interact with Skp1 individually either. The interaction between nBmp4 and Skp1 could be further analyzed following the over-expression of all subunits in the SCF E3 ubiquitin ligase to determine if the abundance of other subunits augments the binding between nBmp4 and Skp1.

SCF E3 ubiquitin ligases are well known for their role in cell cycle regulation. Different E3 ubiquitin ligases are required for the degradation of cell cycle regulatory proteins that control either the G1/S transition or the G2/M transition. Due to the known role of the SCF E3 ubiquitin ligases and the interaction between nBmp4 and the SCF subunits, we decided to analyze the effect that nBmp4 has on the cell cycle. Indeed, we found that nBmp4 does affect the cell cycle. When nBmp4 is over-expressed, cells are accumulated in G0/G1. These results, together with the confirmed interaction of nBmp4 with SCF E3 ubiquitin ligase components, suggested that nBmp4 functions through its association with the ubiquitin-proteasome system. The results also suggested that nBmp4 inhibits the SCF E3 ubiquitin ligase from ubiquitinating cell cycle regulatory proteins that function to inhibit cell cycle progression.

It is important to note that SCF E3 ubiquitin ligases reside in the nucleus. As mentioned, ROC1 and ROC2 have been found to localize to the nucleus, as well as Skp2. Others have shown that all of the proteins needed for the ubiquitin-proteasome system reside within the nucleus. Therefore, the results of this research provide evidence that nBmp4 functions within the nucleus

through its association with the SCF E3 ubiquitin ligase. Future research will determine which cell cycle regulatory proteins are being protected from degradation to yield the inhibited cell cycle progression phenotype manifested when nBmp4 is over-expressed

Finally, an nBmp4 over-expression mouse is being generated in which nBmp4 will only be over-expressed when the tissue comes in contact with the Cre-recombinase. Due to the localization of ROC proteins to heart and skeletal muscle, the heart defect in nBmp4 morphant zebrafish, and the requirement for E3 ubiquitin ligases in cardiovascular development, we decided to analyze the over-expression of nBmp4 in heart tissue. The analysis of these mice will greatly aid in determining the function of nBmp4 *in vivo.*

Appendix: Additional Preliminary Data

Introduction

Due to the interaction between nBmp4 and the SCF E3 ubiquitin ligase complex and the active polyubiquitination of nBmp4, it is unclear whether the interaction between nBmp4 and the SCF complex is involved in the functionality of nBmp4 or if the interaction is solely facilitating the ubiquitination of nBmp4. Therefore, we decided to analyze a mutant form of nBmp4 that should not interact with the SCF E3 ligase and determine if it has an effect on the cell cycle and is actively ubiquitinated. This mutant should aid in distinguishing between the different reasons for the interaction between nBmp4 and the SCF E3 ligase complex.

Experimental Procedures

Plasmid constructs

The nBmp4/GFP construct was prepared by deleting the first 82 amino acids from the Bmp4/GFP construct using the QuikChange II Site-Directed Mutagenesis Kit (Stratagene, La Jolla, CA) according to the manufacturer's protocol and the primers shown in Table A.1. Similarly, the nBmp4mut/GFP construct was prepared by deleting the first 182 amino acids with the exception of the initiating methionine from the Bmp4/GFP construct using mutagenesis and the primers in Table A.1.

The nBmp4mut/HA and nBmp4mut-IRES-GFP constructs were prepared by deleting the sequence coding for the first 100 amino acids (except the starting methionine) of nBmp4 from the nBmp4/HA and nBmp4-IRES-GFP constructs, respectively, using the QuikChange II Site-Directed Mutagenesis Kit (Stratagene, La Jolla, CA) according to the manufacturer's protocol

and the primers in Table A.1. All expression plasmids were verified by sequencing at the BYU Sequencing Center.

Table A.1 Primers used to prepare nBmp4/GFP and nBmp4mut plasmids. The primers were synthesized at Invitrogen (Carlsbad, CA). The primers were used in QuikChange II Site-Directed Mutagenesis Kit (Stratagene, La Jolla, CA) according to the manufacturer's protocol to delete the first 100 amino acids of nBmp4 except the initiating methionine.

nBmp4/GFP Forward	GTTTTCTGTCAAGACACCATGAGGGACCTTTACCGGC
nBmp4/GFP Reverse	GCCGGTAAAGGTCCCTCATGGTGTCTTGACAGAAAAC
nBmp4mut Forward	GTTTTCTGTCAAGACACCATGGAGGTTATGAAGCCCCCAGC
nBmp4mut Reverse	GCTGGGGGCTTCATAACCTCCATGGTGTCTTGACAGAAAAC

Fixation of cells and fluorescence microscopy

Cells were washed three times with 2 ml 1x PBS per well. Cells were then fixed by incubating with 4% PFA in PBS for 30 minutes at room temperature with rotation. The fixative was then removed and the cells were washed three additional times with 1x PBS. To visualize the nuclei, the cells were incubated with DAPI (1:100, Invitrogen, Carlsbad, CA) for 10 minutes at room temperature in the dark. Finally, the cells were washed with 1x PBS three more times and then visualized using an Olympus IX70 fluorescent microscope. Pictures were taken using MagnaFIRE SP. DAPI was observed using an excitation wavelength of 350 nm and GFP was visualized using an excitation wavelength of 488 nm.

Other methods

Cell culture, transient transfections, immunoprecipitation experiments, western blots, synchronization and cell cycle, and ubiquitination studies were all performed as described in Chapter 3 using the appropriate plasmid constructs.

Results

In order to distinguish between the possibilities that the interaction between nBmp4 and the SCF ligase was functional or if the interaction was simply facilitating nBmp4 degradation, a

mutant nBmp4 was prepared in which the first 100 amino acids were deleted (named nBmp4mut) and tested for its ability to affect the cell cycle and be actively poly-ubiquitinated. This mutant nBmp4 construct was previously tested through yeast two-hybrid assays and found to interact weakly with ROC1 and ROC2 (see Figure 2.4). To confirm these results, co-immunoprecipitation experiments were performed. Though expression levels were low, the results suggest that nBmp4mut does not interact with ROC1 or ROC2 (Figure A.1A). Additionally, nBmp4mut does not interact with Cullin1 (Figure A.1B). Therefore, it was determined that this mutant form of nBmp4 does not interact with the SCF E3 ligase.

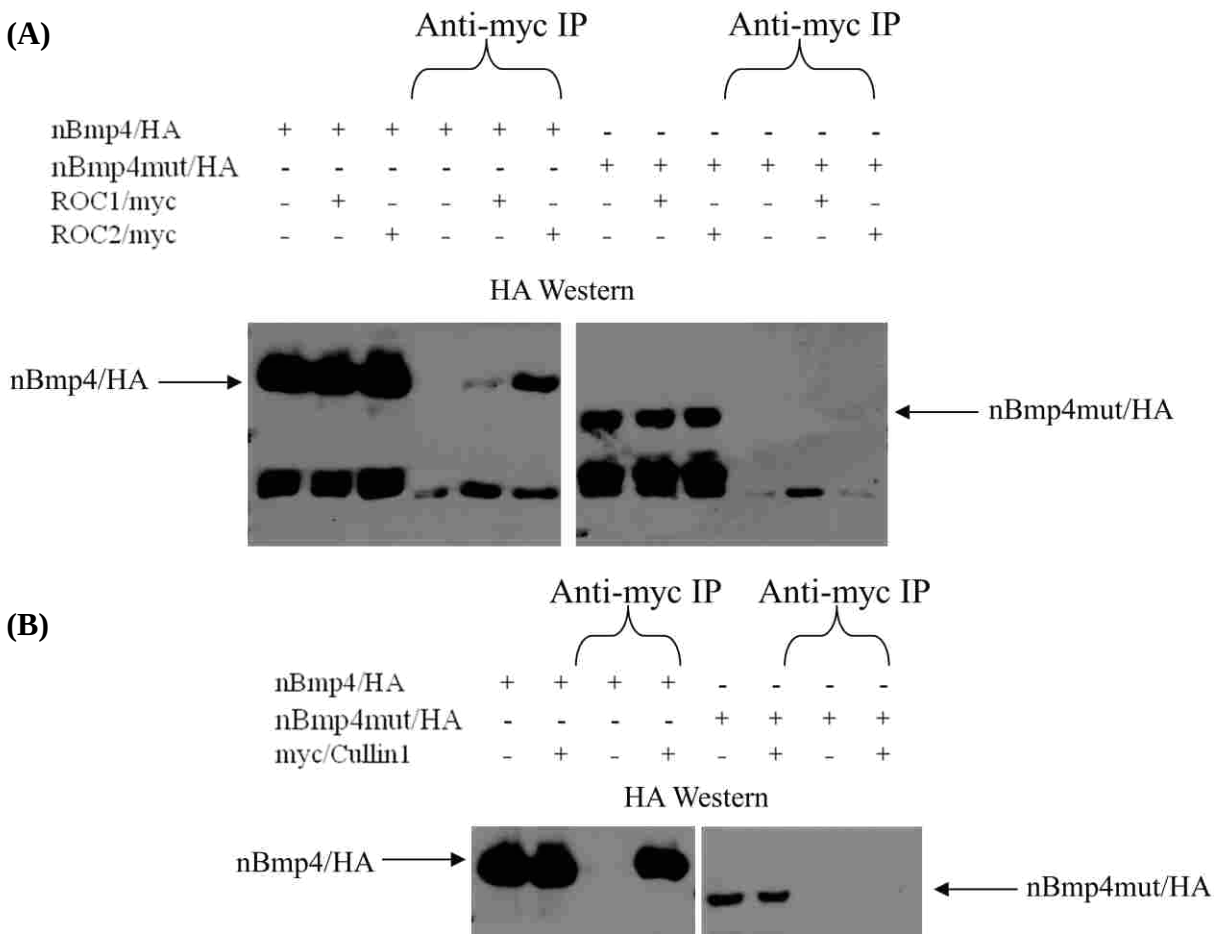

Figure A.1 nBmp4mut does not interact with SCF ligase. HEK 293T cells were transiently co-transfected with the indicated plasmids. After 40-48 hours, cells were lysed and equal amounts of lysates were immunoprecipitated with anti-myc antibodies. Immunoprecipitates were subsequently immunoblotted with anti-HA antibodies.

Next, the nBmp4 mutant was analyzed for localization patterns. As shown in Figure A.2, nBmp4mut is localized to the nucleus of cells as judged by transfection of an nBmp4mut/GFP construct into HEK 293T cells.

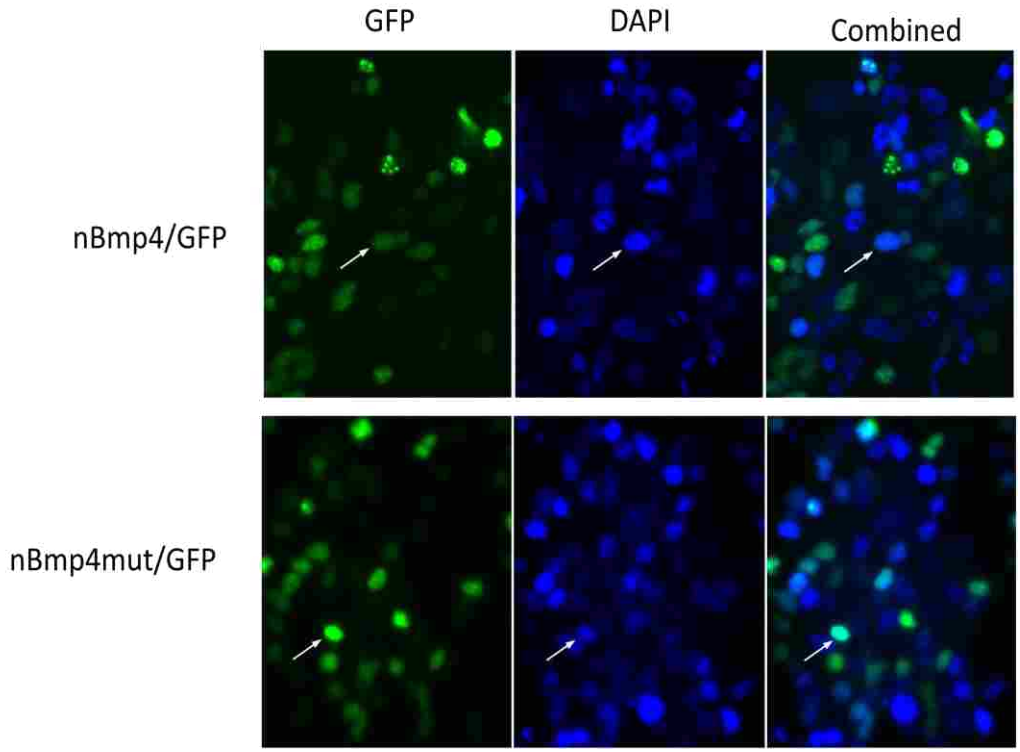

Figure A.2 nBmp4mut is localized to the nucleus of cultured cells. HEK 293T cells were transiently transfected with the indicated plasmids. After approximately 47 hours, cells were fixed and stained with DAPI. Cells were visualized using an Olymus IX70 fluorescent microscope. DAPI was visualized using an excitation wavelength of 350 nm and GFP was visualized using an excitation wavelength of 488 nm.

The ubiquitination patterns of nBmp4mut were also examined. Interestingly, the ubiquitination of nBmp4mut is significantly decreased as compared to wild type nBmp4 (Figure A.3).

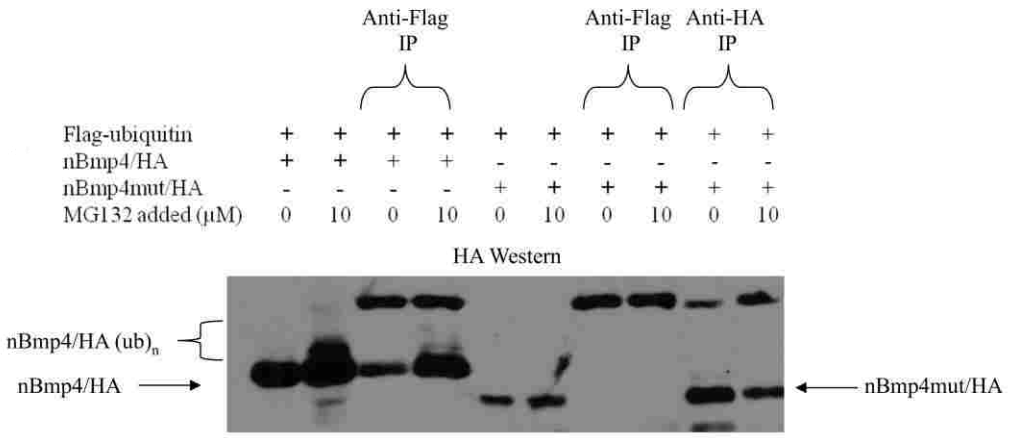

Figure A.3 nBmp4mut is not actively poly-ubiquitinated. HEK 293T cells were transiently co-transfected with Flag-ubiquitin and either nBmp4/HA, or nBmp4mut/HA. After 36 hours, either 0 or 10 μM MG132 was added to the cells. After an additional 12 hours, cells were lysed and equal amounts of lysates were immunoprecipitated with anti-Flag antibodies (in order to concentrate the ubiquitinated proteins) or anti-HA antibodies. Immunoprecipitates were subsequently immunoblotted with anti-HA antibodies to determine if nBmp4/HA was among the ubiquitinated proteins.

Finally, nBmp4mut was analyzed for its effect on the cell cycle. It was determined that nBmp4mut does, in fact, affect the cell cycle in a similar manner to nBmp4 (Figure A.4).

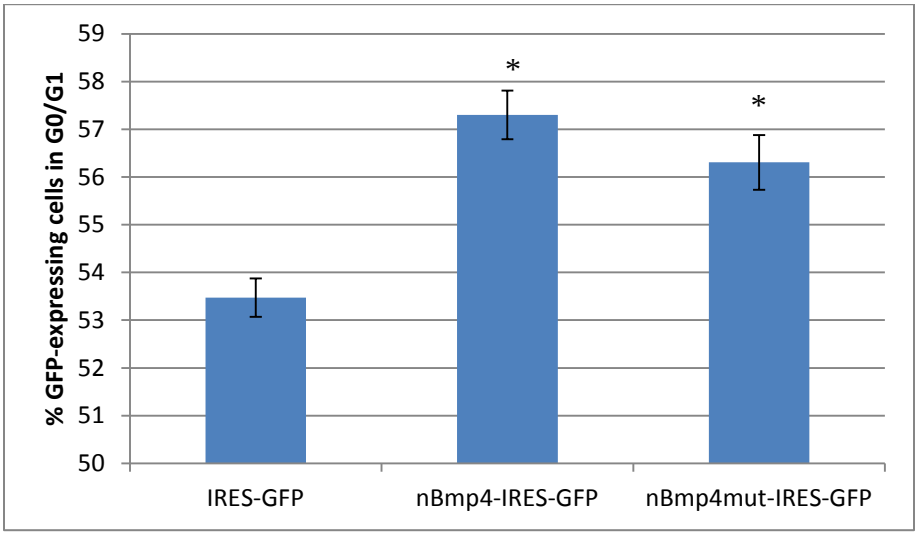

Figure A.4 nBmp4mut also affects the cell cycle by causing accumulation in G0/G1. Cell cycle analysis was performed following cell synchronization using the GFP-Certified™ Nuclear-ID™ Red Cell Cycle Analysis Kit (Enzo Life Sciences) following transient transfection of HEK293T cells with nBmp4-IRES-GFP, nBmp4mut-IRES-GFP, or IRES-GFP. The analysis of cell cycle progression was only conducted on GFP-expressing cells in order to narrow the analysis to the successfully transfected cells. * indicates p-value < 0.05 using the paired Student's t-test with 2 tails.

Discussion

In order to distinguish between the possibilities that the interaction between the SCF E3 ubiquitin ligase complex and nBmp4 is functional solely to degrade nBmp4 or if the interaction suggests that nBmp4 plays a role in protein degradation, a mutant nBmp4 was produced (nBmp4mut). nBmp4mut is a truncated mutant of nBmp4 that is missing the first 100 amino acids. Through a series of experiments, we were able to show that the interaction between nBmp4mut and the SCF E3 ubiquitin ligase was significantly reduced, if not completely abolish. We have also shown that nBmp4mut is localized to the nuclei of cultured cells. Interestingly, the ubiquitination of nBmp4mut is severely decreased or completely eliminated. This suggests that the interaction between nBmp4 and the SCF E3 ubiquitin ligase is functional to promote the

ubiquitination of nBmp4. Finally, we have shown that nBmp4mut affects the cell cycle in a similar manner to nBmp4. Because the interaction with the SCF ligase has been reduced, this suggests that the ability of nBmp4 to affect the cell cycle may be independent from the interaction between nBmp4 and the SCF E3 ubiquitin ligase. In conclusion, nBmp4 functions through promoting cells to accumulate in G0/G1 and is tagged for degradation by the SCF E3 ubiquitin ligase. These are depicted as independent events in Figure A.5. The mechanism by which nBmp4 promotes G0/G1 accumulation will be further analyzed in future studies.

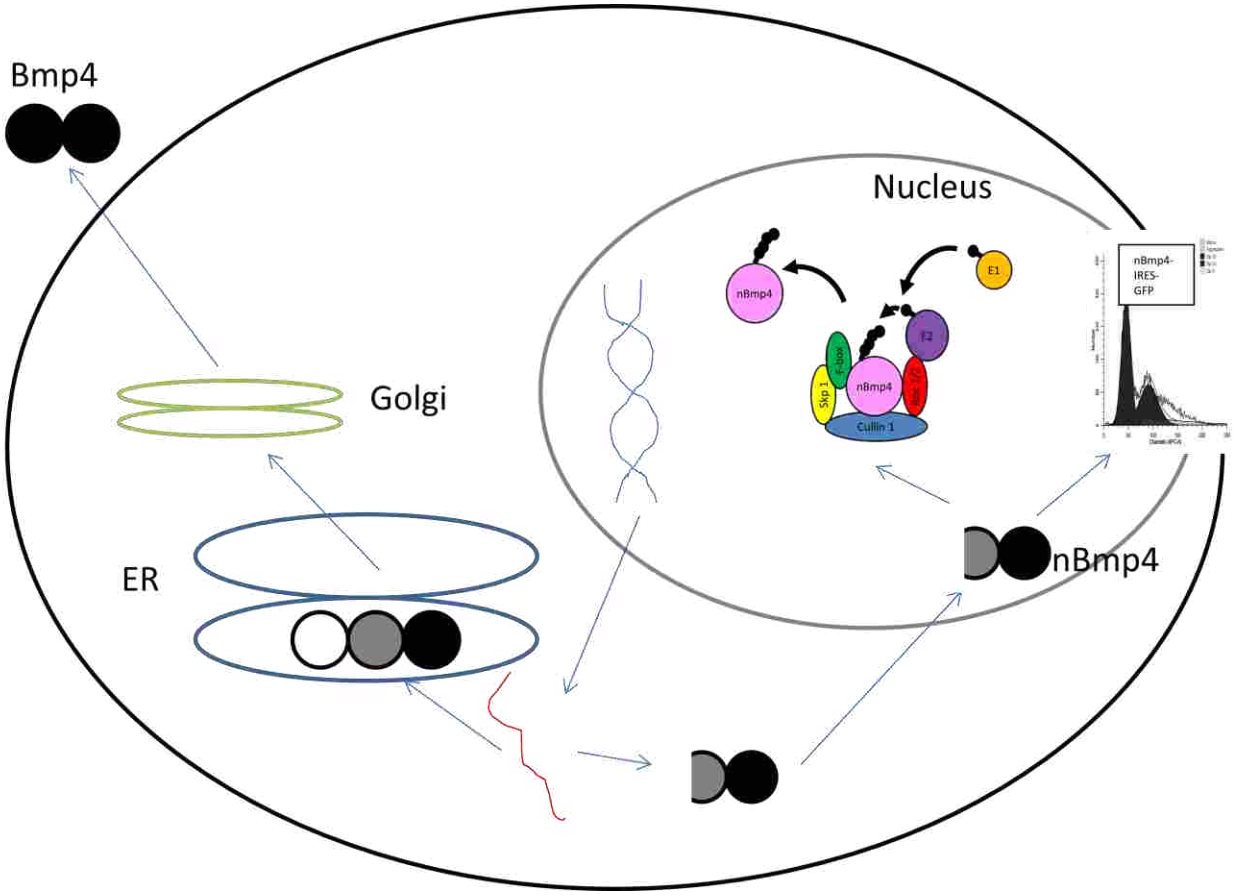

Figure A.5 nBmp4 schematic. nBmp4 is translated from an alternative downstream start codon and then localized to the nucleus through a bipartite nuclear localization signal. In the nucleus, nBmp4 functions to promote accumulation in G0/G1. The degradation of nBmp4 is facilitated by the SCF E3 ubiquitin ligase.

References

1. Madoz-Gurpide J, Lopez-Serra P, Martinez-Torrecuadrada JL *et al.* Proteomics-based validation of genomic data: applications in colorectal cancer diagnosis. Mol Cell Proteomics 2006; **5** (8):1471-1483.
2. Felin JE, Mayo JL, Loos TJ *et al.* Nuclear variants of bone morphogenetic proteins. BMC Cell Biol; **11**:20.
3. Gerhart J. 1998 Warkany lecture: signaling pathways in development. Teratology 1999; **60** (4):226-239.
4. Wozney JM. The bone morphogenetic protein family and osteogenesis. Mol Reprod Dev 1992; **32** (2):160-167.
5. Cui Y, Jean F, Thomas G, Christian JL. BMP-4 is proteolytically activated by furin and/or PC6 during vertebrate embryonic development. Embo J 1998; **17** (16):4735-4743.
6. Chen D, Zhao M, Harris SE, Mi Z. Signal transduction and biological functions of bone morphogenetic proteins. Front Biosci 2004; **9**:349-358.
7. Larsson J, Karlsson S. The role of Smad signaling in hematopoiesis. Oncogene 2005; **24** (37):5676-5692.
8. Zeng S, Chen J, Shen H. Controlling of bone morphogenetic protein signaling. Cell Signal; **22** (6):888-893.
9. Derynck R, Zhang YE. Smad-dependent and Smad-independent pathways in TGF-beta family signalling. Nature 2003; **425** (6958):577-584.
10. Inoue Y, Imamura T. Regulation of TGF-beta family signaling by E3 ubiquitin ligases. Cancer Sci 2008; **99** (11):2107-2112.
11. Wozney JM, Rosen V, Celeste AJ *et al.* Novel regulators of bone formation: molecular clones and activities. Science 1988; **242** (4885):1528-1534.
12. Fiedler J, Roderer G, Gunther KP, Brenner RE. BMP-2, BMP-4, and PDGF-bb stimulate chemotactic migration of primary human mesenchymal progenitor cells. J Cell Biochem 2002; **87** (3):305-312.
13. Hammonds RG, Jr., Schwall R, Dudley A *et al.* Bone-inducing activity of mature BMP-2b produced from a hybrid BMP-2a/2b precursor. Molecular endocrinology (Baltimore, Md 1991; **5** (1):149-155.
14. Zakin L, De Robertis EM. Inactivation of mouse Twisted gastrulation reveals its role in promoting Bmp4 activity during forebrain development. Development 2004; **131** (2):413-424.
15. Thompson DL, Gerlach-Bank LM, Barald KF, Koenig RJ. Retinoic acid repression of bone morphogenetic protein 4 in inner ear development. Mol Cell Biol 2003; **23** (7):2277-2286.
16. Winnier G, Blessing M, Labosky PA, Hogan BL. Bone morphogenetic protein-4 is required for mesoderm formation and patterning in the mouse. Genes Dev 1995; **9** (17):2105-2116.
17. Fang J, Zhu YY, Smiley E *et al.* Stimulation of new bone formation by direct transfer of osteogenic plasmid genes. Proc Natl Acad Sci U S A 1996; **93** (12):5753-5758.
18. Chocron S, Verhoeven MC, Rentzsch F, Hammerschmidt M, Bakkers J. Zebrafish Bmp4 regulates left-right asymmetry at two distinct developmental time points. Dev Biol 2007; **305** (2):577-588.
19. Ying QL, Nichols J, Chambers I, Smith A. BMP induction of Id proteins suppresses differentiation and sustains embryonic stem cell self-renewal in collaboration with STAT3. 2003:281 - 292.

20. Furuta Y, Hogan BL. BMP4 is essential for lens induction in the mouse embryo. Genes Dev 1998; **12** (23):3764-3775.
21. Lawson KA, Dunn NR, Roelen BA *et al.* Bmp4 is required for the generation of primordial germ cells in the mouse embryo. Genes Dev 1999; **13** (4):424-436.
22. Piccirillo SG, Reynolds BA, Zanetti N *et al.* Bone morphogenetic proteins inhibit the tumorigenic potential of human brain tumour-initiating cells. Nature 2006; **444** (7120):761-765.
23. Buckley S, Shi W, Driscoll B *et al.* BMP4 signaling induces senescence and modulates the oncogenic phenotype of A549 lung adenocarcinoma cells. Am J Physiol Lung Cell Mol Physiol 2004; **286** (1):L81-86.
24. Bastida MF, Delgado MD, Wang B *et al.* Levels of Gli3 repressor correlate with Bmp4 expression and apoptosis during limb development. Dev Dyn 2004; **231** (1):148-160.
25. Van den Wijngaard A, Pijpers MA, Joosten PH *et al.* Functional characterization of two promoters in the human bone morphogenetic protein-4 gene. J Bone Miner Res 1999; **14** (8):1432-1441.
26. Rothhammer T, Poser I, Soncin F *et al.* Bone morphogenic proteins are overexpressed in malignant melanoma and promote cell invasion and migration. Cancer research 2005; **65** (2):448-456.
27. Theriault BL, Shepherd TG, Mujoomdar ML, Nachtigal MW. BMP4 induces EMT and Rho GTPase activation in human ovarian cancer cells. Carcinogenesis 2007; **28** (6):1153-1162.
28. Shepherd TG, Nachtigal MW. Identification of a putative autocrine bone morphogenetic protein-signaling pathway in human ovarian surface epithelium and ovarian cancer cells. Endocrinology 2003; **144** (8):3306-3314.
29. Kim JS, Crooks H, Dracheva T *et al.* Oncogenic beta-catenin is required for bone morphogenetic protein 4 expression in human cancer cells. Cancer research 2002; **62** (10):2744-2748.
30. Nishanian TG, Kim JS, Foxworth A, Waldman T. Suppression of tumorigenesis and activation of Wnt signaling by bone morphogenetic protein 4 in human cancer cells. Cancer Biol Ther 2004; **3** (7):667-675.
31. Felin JE, Mayo JL, Sudweeks TJ *et al.* BMP family proteins in the nucleus.
32. Lange A, Mills RE, Lange CJ *et al.* Classical nuclear localization signals: definition, function, and interaction with importin alpha. J Biol Chem 2007; **282** (8):5101-5105.
33. Kalderon D, Richardson WD, Markham AF, Smith AE. Sequence requirements for nuclear location of simian virus 40 large-T antigen. Nature 1984; **311** (5981):33-38.
34. Robbins J, Dilworth SM, Laskey RA, Dingwall C. Two interdependent basic domains in nucleoplasmin nuclear targeting sequence: identification of a class of bipartite nuclear targeting sequence. Cell 1991; **64** (3):615-623.
35. Gorlich D, Kostka S, Kraft R *et al.* Two different subunits of importin cooperate to recognize nuclear localization signals and bind them to the nuclear envelope. Curr Biol 1995; **5** (4):383-392.
36. Sorokin AV, Kim ER, Ovchinnikov LP. Nucleocytoplasmic transport of proteins. Biochemistry (Mosc) 2007; **72** (13):1439-1457.
37. Quimby BB, Dasso M. The small GTPase Ran: interpreting the signs. Curr Opin Cell Biol 2003; **15** (3):338-344.
38. Becker J, Melchior F, Gerke V *et al.* RNA1 encodes a GTPase-activating protein specific for Gsp1p, the Ran/TC4 homologue of Saccharomyces cerevisiae. J Biol Chem 1995; **270** (20):11860-11865.

39. Bischoff FR, Ponstingl H. Catalysis of guanine nucleotide exchange on Ran by the mitotic regulator RCC1. Nature 1991; **354** (6348):80-82.
40. Corbett AH, Koepp DM, Schlenstedt G *et al.* Rna1p, a Ran/TC4 GTPase activating protein, is required for nuclear import. J Cell Biol 1995; **130** (5):1017-1026.
41. Klebe C, Prinz H, Wittinghofer A, Goody RS. The kinetic mechanism of Ran--nucleotide exchange catalyzed by RCC1. Biochemistry 1995; **34** (39):12543-12552.
42. Damelin M, Silver PA, Corbett AH. Nuclear protein transport. Methods Enzymol 2002; **351**:587-607.
43. PSORT II Prediction. Available from: http://psort.nibb.ac.jp/form2.html.
44. Pedersen AG, Nielsen H. Neural network prediction of translation initiation sites in eukaryotes: perspectives for EST and genome analysis. Proc Int Conf Intell Syst Mol Biol 1997; **5**:226-233.
45. Oida S, Iimura T, Maruoka Y, Takeda K, Sasaki S. Cloning and sequence of bone morphogenetic protein 4 (BMP-4) from a human placental cDNA library. DNA Seq 1995; **5** (5):273-275.
46. Yeung PL, Zhang A, Chen JD. Nuclear localization of coactivator RAC3 is mediated by a bipartite NLS and importin alpha3. Biochem Biophys Res Commun 2006; **348** (1):13-24.
47. Patterson JB, Samuel CE. Expression and regulation by interferon of a double-stranded-RNA-specific adenosine deaminase from human cells: evidence for two forms of the deaminase. Mol Cell Biol 1995; **15** (10):5376-5388.
48. Le Quesne JP, Stoneley M, Fraser GA, Willis AE. Derivation of a structural model for the c-myc IRES. J Mol Biol 2001; **310** (1):111-126.
49. Hann SR, King MW, Bentley DL, Anderson CW, Eisenman RN. A non-AUG translational initiation in c-myc exon 1 generates an N-terminally distinct protein whose synthesis is disrupted in Burkitt's lymphomas. Cell 1988; **52** (2):185-195.
50. Blackwood EM, Lugo TG, Kretzner L *et al.* Functional analysis of the AUG- and CUG-initiated forms of the c-Myc protein. Mol Biol Cell 1994; **5** (5):597-609.
51. Hann SR, Dixit M, Sears RC, Sealy L. The alternatively initiated c-Myc proteins differentially regulate transcription through a noncanonical DNA-binding site. Genes Dev 1994; **8** (20):2441-2452.
52. Stoneley M, Subkhankulova T, Le Quesne JP *et al.* Analysis of the c-myc IRES; a potential role for cell-type specific trans-acting factors and the nuclear compartment. Nucleic acids research 2000; **28** (3):687-694.
53. Florkiewicz RZ, Sommer A. Human basic fibroblast growth factor gene encodes four polypeptides: three initiate translation from non-AUG codons. Proc Natl Acad Sci U S A 1989; **86** (11):3978-3981.
54. Prats H, Kaghad M, Prats AC *et al.* High molecular mass forms of basic fibroblast growth factor are initiated by alternative CUG codons. Proc Natl Acad Sci U S A 1989; **86** (6):1836-1840.
55. Renko M, Quarto N, Morimoto T, Rifkin DB. Nuclear and cytoplasmic localization of different basic fibroblast growth factor species. J Cell Physiol 1990; **144** (1):108-114.
56. Bugler B, Amalric F, Prats H. Alternative initiation of translation determines cytoplasmic or nuclear localization of basic fibroblast growth factor. Mol Cell Biol 1991; **11** (1):573-577.
57. Acland P, Dixon M, Peters G, Dickson C. Subcellular fate of the int-2 oncoprotein is determined by choice of initiation codon. Nature 1990; **343** (6259):662-665.

58. Nguyen M, He B, Karaplis A. Nuclear forms of parathyroid hormone-related peptide are translated from non-AUG start sites downstream from the initiator methionine. Endocrinology 2001; **142** (2):694-703.
59. Lam MH, Hu W, Xiao CY, Gillespie MT, Jans DA. Molecular dissection of the importin beta1-recognized nuclear targeting signal of parathyroid hormone-related protein. Biochem Biophys Res Commun 2001; **282** (2):629-634.
60. Mukherjee S, Bal S, Saha P. Protein interaction maps using yeast two-hybrid assay. Current Science 2001; **81** (5):458-464.
61. Chien CT, Bartel PL, Sternglanz R, Fields S. The two-hybrid system: a method to identify and clone genes for proteins that interact with a protein of interest. Proc Natl Acad Sci U S A 1991; **88** (21):9578-9582.
62. Fields S, Song O. A novel genetic system to detect protein-protein interactions. Nature 1989; **340** (6230):245-246.
63. Estojak J, Brent R, Golemis EA. Correlation of two-hybrid affinity data with in vitro measurements. Mol Cell Biol 1995; **15** (10):5820-5829.
64. Sun Y, Tan M, Duan H, Swaroop M. SAG/ROC/Rbx/Hrt, a zinc RING finger gene family: molecular cloning, biochemical properties, and biological functions. Antioxidants & redox signaling 2001; **3** (4):635-650.
65. Furukawa M, Ohta T, Xiong Y. Activation of UBC5 ubiquitin-conjugating enzyme by the RING finger of ROC1 and assembly of active ubiquitin ligases by all cullins. J Biol Chem 2002; **277** (18):15758-15765.
66. Duan H, Wang Y, Aviram M *et al.* SAG, a novel zinc RING finger protein that protects cells from apoptosis induced by redox agents. Mol Cell Biol 1999; **19** (4):3145-3155.
67. He H, Tan M, Pamarthy D *et al.* CK2 phosphorylation of SAG at Thr10 regulates SAG stability, but not its E3 ligase activity. Mol Cell Biochem 2007; **295** (1-2):179-188.
68. Ohta T, Michel JJ, Schottelius AJ, Xiong Y. ROC1, a homolog of APC11, represents a family of cullin partners with an associated ubiquitin ligase activity. Molecular cell 1999; **3** (4):535-541.
69. Swaroop M, Gosink M, Sun Y. SAG/ROC2/Rbx2/Hrt2, a component of SCF E3 ubiquitin ligase: genomic structure, a splicing variant, and two family pseudogenes. DNA and cell biology 2001; **20** (7):425-434.
70. Hershko A, Ciechanover A. The ubiquitin system. Annu Rev Biochem 1998; **67**:425-479.
71. Pickart CM. Mechanisms underlying ubiquitination. Annu Rev Biochem 2001; **70**:503-533.
72. Willems AR, Schwab M, Tyers M. A hitchhiker's guide to the cullin ubiquitin ligases: SCF and its kin. Biochimica et biophysica acta 2004; **1695** (1-3):133-170.
73. Di Fiore PP, Polo S, Hofmann K. When ubiquitin meets ubiquitin receptors: a signalling connection. Nature reviews 2003; **4** (6):491-497.
74. Skowyra D, Koepp DM, Kamura T *et al.* Reconstitution of G1 cyclin ubiquitination with complexes containing SCFGrr1 and Rbx1. Science 1999; **284** (5414):662-665.
75. Tan P, Fuchs SY, Chen A *et al.* Recruitment of a ROC1-CUL1 ubiquitin ligase by Skp1 and HOS to catalyze the ubiquitination of I kappa B alpha. Molecular cell 1999; **3** (4):527-533.
76. Seol JH, Feldman RM, Zachariae W *et al.* Cdc53/cullin and the essential Hrt1 RING-H2 subunit of SCF define a ubiquitin ligase module that activates the E2 enzyme Cdc34. Genes Dev 1999; **13** (12):1614-1626.

77. Wu K, Fuchs SY, Chen A *et al.* The SCF(HOS/beta-TRCP)-ROC1 E3 ubiquitin ligase utilizes two distinct domains within CUL1 for substrate targeting and ubiquitin ligation. Mol Cell Biol 2000; **20** (4):1382-1393.
78. Bai C, Sen P, Hofmann K *et al.* SKP1 connects cell cycle regulators to the ubiquitin proteolysis machinery through a novel motif, the F-box. Cell 1996; **86** (2):263-274.
79. Hatakeyama S, Kitagawa M, Nakayama K *et al.* Ubiquitin-dependent degradation of IkappaBalpha is mediated by a ubiquitin ligase Skp1/Cul 1/F-box protein FWD1. Proc Natl Acad Sci U S A 1999; **96** (7):3859-3863.
80. Wan M, Tang Y, Tytler EM *et al.* Smad4 protein stability is regulated by ubiquitin ligase SCF beta-TrCP1. J Biol Chem 2004; **279** (15):14484-14487.
81. Fukuchi M, Imamura T, Chiba T *et al.* Ligand-dependent degradation of Smad3 by a ubiquitin ligase complex of ROC1 and associated proteins. Mol Biol Cell 2001; **12** (5):1431-1443.
82. Maniatis T. A ubiquitin ligase complex essential for the NF-kappaB, Wnt/Wingless, and Hedgehog signaling pathways. Genes Dev 1999; **13** (5):505-510.
83. Trimarchi JM, Lees JA. Sibling rivalry in the E2F family. Nature reviews 2002; **3** (1):11-20.
84. Mendez J, Zou-Yang XH, Kim SY *et al.* Human origin recognition complex large subunit is degraded by ubiquitin-mediated proteolysis after initiation of DNA replication. Molecular cell 2002; **9** (3):481-491.
85. Hu J, McCall CM, Ohta T, Xiong Y. Targeted ubiquitination of CDT1 by the DDB1-CUL4A-ROC1 ligase in response to DNA damage. Nat Cell Biol 2004; **6** (10):1003-1009.
86. Kamura T, Koepp DM, Conrad MN *et al.* Rbx1, a component of the VHL tumor suppressor complex and SCF ubiquitin ligase. Science 1999; **284** (5414):657-661.
87. Chen A, Wu K, Fuchs SY *et al.* The conserved RING-H2 finger of ROC1 is required for ubiquitin ligation. J Biol Chem 2000; **275** (20):15432-15439.
88. Swaroop M, Wang Y, Miller P *et al.* Yeast homolog of human SAG/ROC2/Rbx2/Hrt2 is essential for cell growth, but not for germination: chip profiling implicates its role in cell cycle regulation. Oncogene 2000; **19** (24):2855-2866.
89. Jia L, Sun Y. RBX1/ROC1-SCF E3 ubiquitin ligase is required for mouse embryogenesis and cancer cell survival. Cell Div 2009; **4**:16.
90. Duan H, Tsvetkov LM, Liu Y *et al.* Promotion of S-phase entry and cell growth under serum starvation by SAG/ROC2/Rbx2/Hrt2, an E3 ubiquitin ligase component: association with inhibition of p27 accumulation. Mol Carcinog 2001; **30** (1):37-46.
91. Yang ES, Park JW. Regulation of nitric oxide-induced apoptosis by sensitive to apoptosis gene protein. Free Radic Res 2006; **40** (3):279-284.
92. Swaroop M, Bian J, Aviram M *et al.* Expression, purification, and biochemical characterization of SAG, a ring finger redox-sensitive protein. Free radical biology & medicine 1999; **27** (1-2):193-202.
93. Tan M, Gallegos JR, Gu Q *et al.* SAG/ROC-SCF beta-TrCP E3 ubiquitin ligase promotes pro-caspase-3 degradation as a mechanism of apoptosis protection. Neoplasia 2006; **8** (12):1042-1054.
94. Furukawa M, Zhang Y, McCarville J, Ohta T, Xiong Y. The CUL1 C-terminal sequence and ROC1 are required for efficient nuclear accumulation, NEDD8 modification, and ubiquitin ligase activity of CUL1. Mol Cell Biol 2000; **20** (21):8185-8197.

95. Kamitani T, Kito K, Nguyen HP, Yeh ETH. Characterization of NEDD8, a developmentally down-regulated ubiquitin-like protein. Journal of Biological Chemistry 1997; **272** (45):28557-28562.
96. Brower CS, Sato S, Tomomori-Sato C *et al.* Mammalian mediator subunit mMED8 is an Elongin BC-interacting protein that can assemble with Cul2 and Rbx1 to reconstitute a ubiquitin ligase. Proc Natl Acad Sci U S A 2002; **99** (16):10353-10358.
97. Wertz IE, O'Rourke KM, Zhang Z *et al.* Human De-etiolated-1 regulates c-Jun by assembling a CUL4A ubiquitin ligase. Science 2004; **303** (5662):1371-1374.
98. Wang H, Zhai L, Xu J *et al.* Histone H3 and H4 ubiquitylation by the CUL4-DDB-ROC1 ubiquitin ligase facilitates cellular response to DNA damage. Molecular cell 2006; **22** (3):383-394.
99. Ho MS, Tsai PI, Chien CT. F-box proteins: the key to protein degradation. J Biomed Sci 2006; **13** (2):181-191.
100. Busino L, Donzelli M, Chiesa M *et al.* Degradation of Cdc25A by beta-TrCP during S phase and in response to DNA damage. Nature 2003; **426** (6962):87-91.
101. Koepp DM, Schaefer LK, Ye X *et al.* Phosphorylation-dependent ubiquitination of cyclin E by the SCFFbw7 ubiquitin ligase. Science 2001; **294** (5540):173-177.
102. Welcker M, Orian A, Grim JE, Eisenman RN, Clurman BE. A nucleolar isoform of the Fbw7 ubiquitin ligase regulates c-Myc and cell size. Curr Biol 2004; **14** (20):1852-1857.
103. Onoyama I, Nakayama KI. Fbxw7 in cell cycle exit and stem cell maintenance: insight from gene-targeted mice. Cell Cycle 2008; **7** (21):3307-3313.
104. Pagano M. Cell cycle regulation by the ubiquitin pathway. FASEB J 1997; **11** (13):1067-1075.
105. Blain SW, Massague J. Breast cancer banishes p27 from nucleus. Nat Med 2002; **8** (10):1076-1078.
106. Hengst L, Reed SI. Translational control of p27Kip1 accumulation during the cell cycle. Science 1996; **271** (5257):1861-1864.
107. Hershko A. Roles of ubiquitin-mediated proteolysis in cell cycle control. Curr Opin Cell Biol 1997; **9** (6):788-799.
108. Pagano M, Tam SW, Theodoras AM *et al.* Role of the ubiquitin-proteasome pathway in regulating abundance of the cyclin-dependent kinase inhibitor p27. Science 1995; **269** (5224):682-685.
109. Rodier G, Montagnoli A, Di Marcotullio L *et al.* p27 cytoplasmic localization is regulated by phosphorylation on Ser10 and is not a prerequisite for its proteolysis. Embo J 2001; **20** (23):6672-6682.
110. Carrano AC, Eytan E, Hershko A, Pagano M. SKP2 is required for ubiquitin-mediated degradation of the CDK inhibitor p27. Nat Cell Biol 1999; **1** (4):193-199.
111. Hattori T, Isobe T, Abe K *et al.* Pirh2 promotes ubiquitin-dependent degradation of the cyclin-dependent kinase inhibitor p27Kip1. Cancer research 2007; **67** (22):10789-10795.
112. Nakayama KI, Nakayama K. Regulation of the cell cycle by SCF-type ubiquitin ligases. Semin Cell Dev Biol 2005; **16** (3):323-333.
113. Kipreos ET, Pagano M. The F-box protein family. Genome Biol 2000; **1** (5):REVIEWS3002.
114. Liu J, Furukawa M, Matsumoto T, Xiong Y. NEDD8 modification of CUL1 dissociates p120(CAND1), an inhibitor of CUL1-SKP1 binding and SCF ligases. Molecular cell 2002; **10** (6):1511-1518.

115. Ohta T, Michel JJ, Xiong Y. Association with cullin partners protects ROC proteins from proteasome-dependent degradation. Oncogene 1999; **18** (48):6758-6766.
116. Pines J, Lindon C. Proteolysis: anytime, any place, anywhere? Nature Cell Biology 2005; **7** (8):731-735.
117. Lee DH, Goldberg AL. Proteasome inhibitors: valuable new tools for cell biologists. Trends in Cell Biology 1998; **8** (10):397-403.
118. Rockel TD, Stuhlmann D, von Mikecz A. Proteasomes degrade proteins in focal subdomains of the human cell nucleus. J Cell Sci 2005; **118** (Pt 22):5231-5242.
119. Jonkers J, Berns A. Conditional mouse models of sporadic cancer. Nat Rev Cancer 2002; **2** (4):251-265.
120. Robertson E, Bradley A, Kuehn M, Evans M. Germ-line transmission of genes introduced into cultured pluripotential cells by retroviral vector. Nature 1986; **323** (6087):445-448.
121. Ryding AD, Sharp MG, Mullins JJ. Conditional transgenic technologies. J Endocrinol 2001; **171** (1):1-14.
122. Rajewsky K, Gu H, Kuhn R *et al.* Conditional gene targeting. J Clin Invest 1996; **98** (3):600-603.
123. Rossant J, McMahon A. "Cre"-ating mouse mutants-a meeting review on conditional mouse genetics. Genes Dev 1999; **13** (2):142-145.
124. Lewandoski M. Conditional control of gene expression in the mouse. Nat Rev Genet 2001; **2** (10):743-755.
125. Metzger D, Clifford J, Chiba H, Chambon P. Conditional site-specific recombination in mammalian cells using a ligand-dependent chimeric Cre recombinase. Proc Natl Acad Sci U S A 1995; **92** (15):6991-6995.
126. Mao X, Fujiwara Y, Chapdelaine A, Yang H, Orkin SH. Activation of EGFP expression by Cre-mediated excision in a new ROSA26 reporter mouse strain. Blood 2001; **97** (1):324-326.
127. Soriano P. Generalized lacZ expression with the ROSA26 Cre reporter strain. Nat Genet 1999; **21** (1):70-71.
128. Zambrowicz BP, Imamoto A, Fiering S *et al.* Disruption of overlapping transcripts in the ROSA beta geo 26 gene trap strain leads to widespread expression of beta-galactosidase in mouse embryos and hematopoietic cells. Proc Natl Acad Sci U S A 1997; **94** (8):3789-3794.
129. Somi S, Buffing AA, Moorman AF, Van Den Hoff MJ. Dynamic patterns of expression of BMP isoforms 2, 4, 5, 6, and 7 during chicken heart development. Anat Rec A Discov Mol Cell Evol Biol 2004; **279** (1):636-651.
130. Willis MS, Townley-Tilson WH, Kang EY, Homeister JW, Patterson C. Sent to destroy: the ubiquitin proteasome system regulates cell signaling and protein quality control in cardiovascular development and disease. Circ Res; **106** (3):463-478.
131. Li HH, Kedar V, Zhang C *et al.* Atrogin-1/muscle atrophy F-box inhibits calcineurin-dependent cardiac hypertrophy by participating in an SCF ubiquitin ligase complex. J Clin Invest 2004; **114** (8):1058-1071.